HOMININ TECHNOLOGICAL BEHAVIOR DURING THE LATER MIDDLE PLEISTOCENE IN THE GADEMOTTA FORMATION, MAIN ETHIOPIAN RIFT

BY

YONATAN SAHLE CHEMERE

A DISSERTATION PRESENTED TO
THE UNIVERSITY OF CAPE TOWN
FOR THE DEGREE OF
DOCTOR OF PHILOSOPHY
IN
ARCHAEOLOGY

CAPE TOWN

MAY 2013

HOMININ TECHNOLOGICAL BEHAVIOR DURING THE LATER MIDDLE-PLEISTOCENE IN THE GADEMOTTA FORMATION, MAIN ETHIOPIAN RIFT

BY

YONATAN SAHLE CHEMERE

A Dissertation presented to
the University of Cape Town
for the Degree of
Doctor of Philosophy
in
Archaeology

Written under the supervision of
Dr. David R. Braun and Prof. Judith C. Sealy

Cape Town
May 2013

HOMININ TECHNOLOGICAL BEHAVIOR DURING THE LATER MIDDLE PLEISTOCENE IN THE GADEMOTTA FORMATION, MAIN ETHIOPIAN RIFT

YONATAN SAHLE CHEMERE

ABSTRACT

The evidence now strongly supports an African origin of the first *Homo sapiens*. Currently, the best-known fossil evidence for the earliest *H. sapiens* derives from the Omo Kibish and Herto sites in Ethiopia, and dates to *ca.* 200-150 thousand years ago (ka). However, very few archaeological data spanning the critical period across our species' evolutionary origin are known from securely dated contexts on the continent.

Through renewed excavations and analysis of newly-recovered as well as previously excavated lithic assemblages from the Gademotta Formation, this dissertation investigates the technological behavior and broader evolutionary context across the time period when the first *H. sapiens* emerged in the wider rift valley in Ethiopia.

Results from new geochronological analyses establish the age of the lowermost cultural horizon at Gademotta as 279 ± 2 ka, making it the oldest precisely dated Middle Stone Age (MSA) site. Lithic analysis reveals that Middle Pleistocene hominin populations at Gademotta incorporated into their technological repertoire the earliest stone-tipped projectile weapons as early as >279 ka. Comparisons of technological behavior of later Middle Pleistocene with earlier Upper Pleistocene hominin populations in the Ethiopian rift valley indicate that they possessed substantially comparable capacities for behavioral variability. Data from the present study strongly support the existence of relatively stable adaptations across the period when *H. sapiens* emerged in northeast Africa. Behavioral patterns considered as indications of "modernity" have much older roots than previously realized.

TABLE OF CONTENTS

LIST OF FIGURES

LIST OF TABLES

ACKNOWLEDGMENTS

My deepest gratitude, first and foremost, goes to my beloved family whose presence in all aspects of my life has always encouraged me to take on tough journeys, such as this. Thank-you Dad, Yisehak, Betel and Daniel!

Cordial thanks go to my main supervisor Dr. David R. Braun for his invaluable assistance throughout my doctoral study. I have been so lucky to have a man of his energy and seriousness of purpose as my supervisor. Dave's dedication has enormously benefited my field and lab research in more ways than one; his ambitiousness has always made me think *outside the box*.

I thank my co-supervisor Prof. Judith C. Sealy whose close follow-ups of my research progress and critical comments on my work have always kept me on the right track. Judy's wisdom in addressing problems has taught me tons while her cordiality has made my "Capetonian" stay super pleasant and easy.

Thanks are due to Drs. Leah E. Morgan (Scottish Universities Environmental Research Centre) and Balemwal Atnafu (Addis Ababa University) for collaborations in the field and lab studies of the geochronology and stratigraphy of the Gademotta Fm. Thank-you also to Dr. W. Karl Hutchings (Thompson Rivers University) for collaboration in the initial identification of microfracture features on an assemblage of pointed artifacts from my study area.

I am greatly indebted to Dr. John J. Shea (Stony Brook University) for invaluable discussions and comments, as well as for the generous provision of raw metric data on the Omo Kibish and experimental lithic assemblages.

I thank Dr. Sarah Wurz (University of the Witwatersrand) for providing raw metric data on lithic assemblages from Klasies River main site; Dr. Katsuhiro Sano (Tohoku University) for discussions on macrofracture analysis and permission to reproduce a figure; and Dr. Philip Van Peer (Catholic University of Leuven) for discussions on the Nubian Techno-complex.

Special thanks go to all leaders of the Middle Awash Research Project (Drs. Tim D. White, Berhane Asfaw, Giday Wolde-Gabriel and Yonas Beyene) for kindly allowing me access to the lithic assemblages of Herto and Aduma,

and involving me in field research in the Middle Awash study area. I would particularly like to thank Dr. Yonas Beyene for his insightful suggestion of a renewed research at Gademotta, after a nearly four-decade hiatus, which gave birth to the present work.

I thank Dr. Gen Suwa (University of Tokyo) for assistance during microscopic analysis of pointed lithic artifacts in the National Museum of Ethiopia in Addis.

I am deeply indebted to *Ato* Tegenu Gossa (Arba Minch University) for his invaluable assistance in successive field seasons at Gademotta and lab analyses in the museum.

Thank-you to *Ato* Jara Hailemariam, former Director-General of the Ethiopian Authority for Research and Conservation of Cultural Heritage (ARCCH), for a considerate reply to my request for an exclusive research permit (Ref. No. 06/Kt-111/2 – Nov. 2009). The ARCCH is gratefully acknowledged for the provision of laboratory and curatorial facilities that have greatly benefited my research.

A number of other people contributed to the success of my study in one way or another, too many to mention them all. My cordial thanks are due and their kind support is very gratefully acknowledged.

Finally, but most importantly, I thank the Wenner-Gren Foundation for Anthropological Research for sponsoring my four-year doctoral study in Cape Town. Thanks are due to the Paleontological Scientific Trust (PAST) and its Scatterlings of Africa programs for financial support toward my dissertation field research for three years in a row, since 2010. Thank-you also to the Centre for African Origins (funded by the Vice-Chancellor's Strategic Initiative), UCT. Without the generous support of these organizations, the present research would never have been possible.

DEDICATION

To my beloved mother,
I can only wish you made it to this date

To my special father,
For being both a dad and mom for twelve long years

CHAPTER ONE

1. INTRODUCTION

Human evolution is a record of the rise of some hominin species and the vanishing of others. The earlier part of human evolution was an exclusively African phenomenon. To wit, the emergence, evolution, and disappearance of the earliest hominin species were geographically entirely limited to the African continent (*e.g.,* Brunet *et al.* 2002; Pickford & Senut 2001; Haile-Selassie *et al.* 2004b; White *et al.* 1994, 2006, 2009; M. Leakey *et al.* 1995, 1998; Dart 1925; Broom 1938; Johanson *et al.* 1978; Asfaw *et al.* 1999; Suwa *et al.* 1997; L. Leakey 1959; L. Leakey *et al.* 1964; Berger *et al.* 2010). Only after the emergence of the genus *Homo* did hominins disperse out of Africa, for the first time *ca.* 1.8 million years ago (Gabunia *et al*. 2000; Vekua *et al*. 2002; Rightmire 1991). The last major species-level hominin dispersal from Africa with far-reaching repercussions had to wait until *Homo sapiens* appeared much later on the continent.

Homo sapiens first appeared in east Africa between *ca.* 200 ka and 150 ka (McDougall *et al.* 2005; Clark *et al.* 2003; White *et al.* 2003). In the periods that followed, this species spread throughout the continent and beyond, absorbing and replacing residual populations of the same genus.

The rise of the earliest *H. sapiens* in Africa is supported by fossil as well as genetic evidence (*e.g.*, McDougall *et al.* 2005; White *et al.* 2003;

Ingman *et al.* 2000; Yotova *et al.* 2007). Controversies do exist, however, about the behavior of the earliest *H. sapiens*. In general, these contentions pertain to the timing, pace, and trajectory of the transition to behaviors accepted as *modern*. There is also a vibrant debate on whether these behaviors are exclusive to *H. sapiens* or were shared with other penecontemporaneous, non-modern populations/species (*e.g.*, Klein 2000, 2008; Mellars 2006; McBrearty & Brooks 2000; Nowell 2010; d'Errico 2003; Hovers & Belfer-Cohen 2006; Zilhão *et al.* 2010; Henshilwood & Marean 2003; Shea 2011).

There are several models of how these behaviors arose and which particular traits should be the focus of attention. However, testing these models has proved to be virtually inapplicable mainly due to the vague definition of what lines of behavior should be considered modern (Nowell 2010; d'Errico & Stringer 2011; Shea 2011). As a result, most mainstream researchers still have more differences than consensus on issues surrounding modern behavior. From a methodological perspective, an increasing number of works currently stress the need for the development of models that can link causes to outcomes (Stringer 2007; Richerson *et al.* 2009; Powell *et al.* 2009; Shea 2011; d'Errico & Stringer 2011), as opposed to far more abundant examples of scrutinizing what has been termed the "laundry list" of "traits of modernity". The empirical reality of testing some of the most appealing models (*e.g.*, Powell *et al*. 2009; Hovers & Belfer-Cohen 2006; Shea 2011) continues to be challenging, as archaeological contexts suitable

for such investigations are extremely rare on the African continent.

The prime focus of this dissertation is understanding the behavioral context across the evolutionary juncture when the first *H. sapiens* appeared in the broader rift valley in Ethiopia (i.e. the Omo Valley, the Main Ethiopian Rift and the Afar Rift). Through the analysis of lithic assemblages from sites in the Gademotta Fm., this dissertation elucidates the behavioral capacities of hominin populations that inhabited the same geographic region at different periods in the later Middle Pleistocene and earlier Upper Pleistocene.

This research capitalizes on the location of the major study area at the heart of the Main Ethiopian Rift: the Gademotta Ridge (Fig. 1.1). This region is almost equidistant between the sites of Herto and Omo Kibish that have yielded the earliest known fossils of *H. sapiens* dated to 160-154 ka and ~195 ka, respectively (Clark *et al.* 2003; White *et al.* 2003; McDougall *et al.* 2005, 2008; F. Brown *et al.* 2012; Fig. 1.1a). In addition, the region has several features that make it ideal to investigate behavioral variability throughout the Middle- and Upper Pleistocene. The Gademotta Ridge hosts a continuous cultural sequence that spans much of the MSA (Wendorf & Schild 1974; Wendorf *et al*. 1975; Laury & Albritton 1975), as well as high-confidence geochronological framework (Morgan & Renne 2008; Sahle *et al.* 2013). The locality has also benefited from extensive raw material sourcing and paleoenvironmental studies (Vogel *et al.* 2006; Negash *et al*. 2010; Basell 2008; *see also* Trauth *et al*. 2010; Blome *et al*. 2012; F. Brown

et al. 2009). The combination of these different features provides an ideal setting to investigate questions of the dynamics of behavioral capacities across the later Middle- and earlier Upper Pleistocene.

Some of the oft-cited models for modern human origins propose that a population ancestral to modern humans expanded in Africa and beyond between 350 ka and 250 ka (Lahr & Foley 1998; *see also* Weaver 2012). These models propose that cost-benefit ratios in adaptive strategies are affected by population changes that occur as a result of environmental and behavioral changes (Lahr & Foley 1998: 147-148). If this assumption holds, then variability in technology ought to follow the change in population density and ecological carrying capacity.

More favorable paleoenvironmental conditions in the broader Gademotta region (Basell 2008; Trauth *et al*. 2010; Vogel 2006; Negash *et al*. 2010) may have created an ecological equilibrium in which increased population sizes and greater behavioral variability could be supported across the later Middle Pleistocene. If variability in technological attributes such as metric properties of cores, flakes, and retouched tools in later Middle Pleistocene occupations at Gademotta is comparable with that from later periods, then the assumption that the area supported large populations as early as >279 ka is supported. These populations may later have expanded and created the demographic ground for the emergence of the first *H. sapiens* in the region.

Notwithstanding the lack of a widely employed lithic analysis

framework for the region, the mosaic of techno-typological variability in MSA sites in east Africa (*e.g.*, Clark 1988; Shea 2008; Yellen *et al*. 2005; Wendorf & Schild 1974, 1993) contrasts with comparable records elsewhere on the continent which represent "sharp breaks and horizon-wide transformations" (Lombard 2012: 142; Clark 1988). The implications of such a unique mosaic of variability among east African MSA sites for understanding the evolutionary context of early humans is clearly far-reaching. Finer-grained intra- and inter-regional comparisons of technological variability across the MSA allow the testing of the suggested evolution of the earliest humans in this part of Africa in an evolutionarily stable context. Through a direct comparison of technological behavior witnessed in sites within the wider rift valley in Ethiopia, this dissertation seeks to test more closely whether increased behavioral variability evolved in contexts of stable adaptation. In so doing, the dissertation will contribute additional data to an accumulating body of knowledge on the evolutionary dynamics that marked the wider period across the appearance of our species (Shea 2008; Basell 2008; Blome *et al*. 2012; Beyene 2010; Yellen *et al*. 2005; Brooks *et al*. 2006; Tryon 2008).

Specifically, this research employs renewed geochronological and stratigraphic investigations in order to attain a finer-grained contextualization of later Middle and earlier Upper Pleistocene occupations within the Gademotta type-site. Renewed excavations have enabled the recovery of assemblages from selected cultural horizons using modern

excavation techniques and procedures. Assemblages are studied with more emphasis on technological, rather than typological, variability while accurate spatial data are used to test hypotheses developed out of previous research in the area. Through the incorporation of nuanced approaches to lithic analysis this dissertation investigates how the technological behaviors of hominin populations that inhabited the Gademotta Ridge compare during different periods across the later Middle and earlier Upper Pleistocene. Specifically, the assessment of evidence for projectile technology and the analysis of "costs" and "benefits" in flake production in sites spanning a broad timescale are used as proxies for deciphering the behavioral capacities of hominin populations from as early as >279 ka *versus* those close to 105 ka.

Finally, in an attempt to obtain a more comprehensive, regional picture of behavioral variability across the critical period when the first *H. sapiens* emerged in the rift valley in Ethiopia, this dissertation employs data that I collected from sites within the wider region under discussion. Comparisons of patterns of technological behavior among sites from different regions and periods in the later Middle- and earlier Upper Pleistocene contribute to understanding better the behavioral context across the period when early *H. sapiens* appeared within the same rift system (McDougall *et al.* 2005; Shea 2008; Clark *et al.* 2003; White *et al*. 2003; Yellen *et al.* 2005; Haile-Selassie *et al*. 2004a). Results are used to evaluate closely the strength of previous suggestions that typological similarities

within and across MSA assemblages spanning wide temporal and spatial ranges in northeast Africa may represent relatively stable adaptations during the period of our species' evolutionary origin (Clark 1988; Shea 2008; Yellen *et al*. 2005, *see also* Basell 2008; Blome *et al*. 2012).

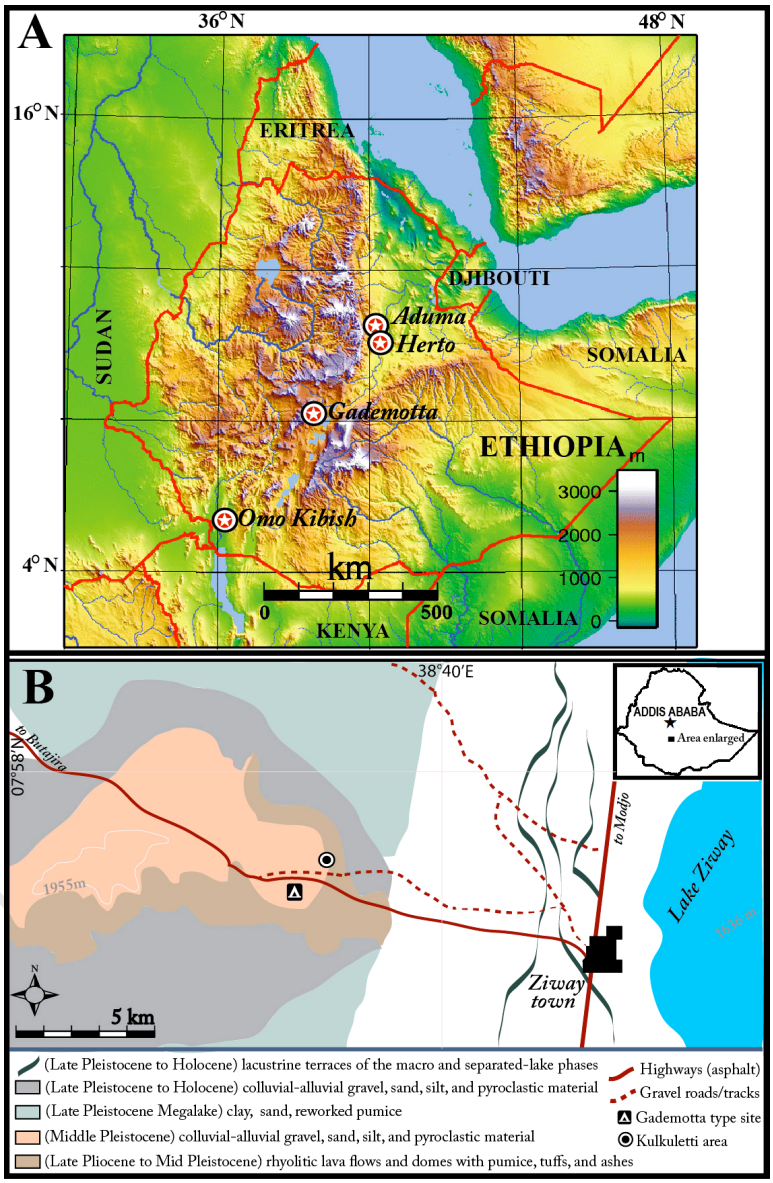

Figure 1.1 A map of Ethiopia showing (a) important MSA sites in the rift, (b) deposit classes in the Gademotta area and its environs (*After* Dainelli *et al*. 2001)

1.1 Behavioral context across the emergence of *Homo sapiens*: Approaches to the later Middle- and earlier Upper Pleistocene archaeology of sub-Saharan Africa

Is the emergence of anatomical modernity associated with behavioral changes that have marked the later Middle- and Upper Pleistocene? Did the earliest members of our species possess behavioral capacities that were dramatically distinct from their immediate predecessors, their contemporaries, and/or their Upper Pleistocene descendents? These are questions that have not been fully addressed as yet.

The dearth of securely dated sites that incorporate the anatomical and behavioral transitions across the latter part of the Middle Pleistocene (*e.g.*, Clark 1982, 1988; Tryon & McBrearty 2002), together with the presence of widely divergent opinions among researchers (*e.g.*, Klein 2000, 2008; Mellars 2006; McBrearty & Brooks 2000; Hovers & Belfer-Cohen 2006; Zilhão *et al.* 2010), continues to hinder investigations surrounding the above-stated questions. As a result, much of our current understanding of the evolutionary context across the emergence of our species relies on data from the more extensively researched southern African record. The best-described sites in the southern African record are largely limited to Upper Pleistocene contexts. Also, there has been a strong emphasis on the "behavioral modernity" approach to studying evidence from these contexts (*e.g.*, K. Brown *et al.* 2009, 2012; d'Errico 2007; Lombard 2007; Wadley *et al*. 2009, 2011; Henshilwood *et al*. 2011; Marean *et al.* 2007). In

comparison, the limited number of sites in east Africa document records from older contexts with superior geochronological resolution and skeletal evidence for the earliest *H. sapiens* (McDougall *et al.* 2005; Shea 2008; Clark *et al.* 2003; White *et al.* 2003; Yellen *et al*. 2005; Brooks *et al.* 2006; Haile-Selassie *et al.* 2004a; Deino & McBrearty 2002; McBrearty & Tryon 2006; Wendorf & Schild 1974; Morgan & Renne 2008; Sahle *et al*. 2013). The older age of these localities, coupled with research approaches commonly employed in the region (Shea 2012), often results in the construction of a framework whereby most of the localities are depicted as having little or nothing to contribute to the debates surrounding the emergence of complex behaviors.

Current inferences about the emergence of complex behaviors rely heavily on the search for traits which most researchers take to demonstrate behavioral modernity (McBrearty & Brooks 2000 *and references therein*; Henshilwood & Marean 2003; Nowell 2010; Klein 2000, 2008). These are traits that mostly marked the Middle-to-Upper Paleolithic transition in Europe, which also coincided with the arrival of *H. sapiens* in the continent and the subsequent disappearance of Neanderthals (Marean & Assefa 1999; Bar-Yosef 1998; Conard & Bolus 2003). Inherent limitations of such an approach are manifested in its failure to create the desired links between behavioral and biological modernity in Europe (*e.g.,* Zilhão 2006, 2011; Caron *et al*. 2011; d'Errico 2003; Mellars 2005; d'Errico & Stringer 2011). In Africa, these links are even more tenuous, often marked with the

"precocious" appearance of many of the hallmarks of sophisticated human behavior (*e.g.,* Barham 2002; Marean *et al.* 2007; K. Brown *et al.* 2009; Henshilwood *et al.* 2011).

Within the behavioral modernity approach, interpretations about the when and how of the emergence of the capacity for sophisticated behavior among our ancestors remain widely divergent. For some (Klein 1999, 2000, 2008; Klein & Edgar 2002; Mellars 1996, 2007) this was a relatively swift phenomenon that started only after *ca.* 50 ka. Other scholars (*e.g.*, Gamble 2007; McBrearty & Brooks 2000; Deacon & Wurz 2001) perceive this as a process with much older roots, involving an accumulation of traits over time. Even within the latter, long-chronology perspective, mainstream researchers do not agree on whether or how the emergence of skeletally fully modern humans is related to behavioral patterns in the African Middle Pleistocene. Detailed reviews of the different views on the timing, mode and tempo of the evolution of modern human behavior have been widely published elsewhere (*e.g.*, d'Errico & Stringer 2011; Nowell 2010; Shea 2011; Hovers & Belfer-Cohen 2006; McBrearty & Brooks 2000; Henshilwood & Marean 2003) and are beyond the scope of this dissertation. Instead, a brief summary is provided here in order to illustrate the inherent problems with the behavioral modernity approach and reinforce the necessity of more nuanced approaches.

Proponents of the short-chronology paradigm contend that Upper Pleistocene neural shifts brought about the capacity among *H. sapiens* to

exhibit "modern behavior" (Klein 1999, 2000, 2008; Klein & Edgar 2002). According to these researchers, the most important selective advantage of such mutations was the capacity for language, and this likely emerged among *H. sapiens ca.* 50 ka in Africa (Klein 2000: 27). However, the detection in Neanderthal DNA of the *FOXP2* gene (Krause *et al.* 2007) responsible for the purported later emergence of the capacity for language (Klein & Edgar 2002) has posed a critical challenge to this argument, suggesting that fully syntactical language may have evolved much earlier among the common ancestor of *H. sapiens* and Neanderthals.

The long-chronology view to behavioral modernity, mainly represented by McBrearty and Brooks's (2000) seminal paper, contends that such behavioral capacity was present among Middle Pleistocene hominins of Africa. According to this perspective, modern behavior is the result of better accretion of traits involving multi-directional trajectories that varied across space and time (McBrearty & Brooks 2000: 456). Critiques of this approach include: i) it fails to set out clearly, what d'Errico (2003: 189) calls "'the criteria to find the criteria'". As a result, the approach provides a list of behavioral traits that mostly arise out of those developed for the European Upper Paleolithic record; ii) it incorporates a tacit assumption, by considering the capacity for behavioral modernity as a cumulative process with given first appearance datums, of a dichotomy into *beginners* and *masters* of modern behavior among *H. sapiens*. However, such distinctions in the manifestation of these behaviors by *H. sapiens* may equally be the

result of taphonomic and methodological biases (Shea 2011: 4-5; Shea 2012). In other words, an apparent accumulation of traits may be the result better evidence from more recent periods (i.e. due to a lesser degree of geological attrition) and may not be a true representation of differences in the capacities for behavioral modernity once this had fully evolved among the African Middle Pleistocene *H. sapiens*.

A more critical approach within the longer-chronology view has put forward certain criteria to sift out behaviors that carried symbolic meaning as more compelling indicators of complex cognitive abilities among modern humans (Henshilwood & Marean 2003). This view stresses that the behavioral modernity approach is inherently problematic, but contends that not all traits in this approach are to be discarded. Rather, certain traits reflect symbolically organized behavior and can thus adequately define modern behavior. The capacity for symbolically mediated behavior is reflected in the use of symbolic thoughts to organize behavior and should be recognizable in the archaeological record. The most common evidence for external symbolic storage includes art, ritualized burial/mortuary practice, personal ornamentation, and use of social space (Henshilwood & Marean 2003: 635; Wadley 2001).

Yet, this too has been criticized (Chase 2003; Davidson 2003; Shea 2011) as merely a search for theoretically more convincing lines of evidence toward the same end – showing the presence of behavioral modernity.

In general, traits that are commonly considered indicative of modern

behavior include personal adornment, ritualized disposal of the dead, long-distance trade/exchange, exploitation of distant and/or difficult-to-procure resources, structured living space, composite tools, projectile technology, and regional technological styles (McBrearty & Brooks 2000 *and references therein*). Most of these traits are inferred from artifactual traces in the archaeological record, such as engraved ochre/eggshell (Henshilwood *et al*. 2009; d'Errico *et al*. 2012; Texier *et al*. 2010); processed ochre (Henshilwood *et al*. 2011; Lombard 2007); perforated beads (*e.g.*, Assefa *et al.* 2008; Bouzouggar *et al*. 2007); marine foods (Marean *et al*. 2007; Walter *et al*. 2000); grave goods/post-mortem manipulation of the dead (*see* McBrearty & Brooks 2000 *for a review of claims*); artifacts securely provenanced to distant sources (Merrick *et al*. 1994; Negash & Shackley 2006; Negash *et al.* 2010, 2011). A number of other traits are theoretically symbolically mediated and sophisticated but cannot be identified in the archaeological record as they do not leave material traces (Wurz 2012). Therefore, our perception of the capacity of hominin populations for what are taken as sophisticated behaviors relies on what traits we can infer from the archaeological record.

The conundrums of the behavioral modernity approach are larger and more complicated than has been summarized here. Yet, alternative approaches that attempt to provide nuanced theoretical and methodological grounds for the study of the behavioral capacities of our species have been slow to emerge. This has long deterred archaeologists from looking for

Afrocentric interpretations for African contexts (Shea 2011). As a result there is now an even longer list of the supposed hallmarks of behavioral modernity (*see* Nowell 2010 *for a recent review*) than there was only a little over a decade ago (*cf*. McBrearty & Brooks 2000). Furthermore, these criteria continue to be forced upon the African behavioral record although they derive from models developed decades ago for much younger and more geographically restricted European contexts.

A plethora of evidence is now showing that most of the traits in the behavioral modernity checklist first originated in Africa (*e.g.*, Marean *et al*. 2007; Henshilwood *et al.* 2011; K. Brown *et al.* 2009; Bouzouggar *et al*. 2007; Lombard & Phillipson 2010; Wadley *et al*. 2009). Some researchers, however, continue to term these behaviors as precocious or dismiss them as outliers. The entire trait-list-based approach proves problematic and has to be discarded altogether (Shea 2011). Unfortunately Paleolithic scholars have still not replaced the behavioral modernity paradigm with an understanding of what other *currencies* of behavior should measure human uniqueness. In his comment to the assessment of models for modern behavior by Henshilwood and Marean (2003), Davidson (2003: 638) warns us that searching for traces of behavior that are still dependent on our understanding of communications as evidenced in much later periods can be deeply methodologically flawed and inherently biased. The danger such an undertaking presents is that in the search for such behavioral traces we may be missing other lines of evidence for possible symbolic communications

(*see also* d'Errico & Stringer 2011: 1061; Shea 2011: 5, 10-11).

Perhaps the shortcomings of the behavioral modernity approach explain the apparent disconnect between the behavioral evidence in southern and eastern Africa. Despite the dramatic fossil evidence of *H. sapiens* at localities such as Omo Kibish, Herto, or Aduma in the Ethiopian rift, these sites bear barely any instance of the types of behavioral attributes widely highlighted in the southern African record. This incongruence is even more puzzling considering the notable absence of fossil evidence to assert the presence of *H. sapiens* even in the younger southern African record (Shea 2008; Clark *et al.* 2003; Yellen *et al*. 2005; Brooks *et al.* 2006; Marean *et al*. 2007; Herries 2011; *see* Feathers 2002; Groves & Throne 2000 *for discussion on the ages and taxonomic affinities of the Klasies River remains*). Differential preservation and the nature of sites in these regions are admittedly possible reasons. But this does not seem to answer the magnitude of the difference between behavioral evidence deriving from the two regions. Perhaps such evidence is not visible in the eastern African sites in forms we are expecting to see, rather than being absent altogether (Barham & Mitchell 2008: 257). Added to the spectacular preservation of non-lithic cultural evidence in the many coastal and near-coastal cave sites in South Africa is the advantage of greater research focus the period has received in this region. This introduces the issue of sampling as yet another important factor for the greater representation of the non-lithic evidence mostly interpreted as indicative of sophisticated behavior (Shea 2012). Such

disparity in the regional records of the evidence is what seems to have created the difference in the interpretation of behaviors across the period of our species' origin.

The question we should be asking ourselves, then, is why are we bound to this demonstrably problematic approach of behavioral modernity? Why, in the face of an accumulation of evidence from different regions on the continent, are we limited to reporting first appearance datums of certain behavioral patterns than investigate wider contexts that contribute to the development of sub-regional and regional pictures of the evolutionary dynamics marking the critical period in question (Lombard 2012)? As I have briefly summarized, the present paradigms cannot explain, in particular, the absence in east Africa of the widely accepted markers of modern behavior in the fashion documented in sites in southern and northern Africa. In other words, the apparent differences between later Middle Pleistocene hominin behaviors from eastern *versus* southern and north Africa can equally be the result of differences in the methods of interpretation of the archaeological records rather than a product of the records themselves (Shea 2012). In fact, as will be argued in the final chapters of this dissertation, there are several lines of evidence that make a strong case for the presence of behaviors among the later Middle Pleistocene denizens of the Gademotta and Herto regions that can be securely considered modern (Clark *et al.* 2003; Beyene 2010; Sahle & Beyene *forthcoming*; Shea 2011; Yellen *et al.* 2005). However, rather than

fitting the evidence into the trait list of modern behavior, a more meaningful analysis of the behavioral context in which these traits emerged will be provided here.

A further problem in the behavioral modernity approach relates to the definition of *modern*. If we support the view that modern behaviors are exclusive to *H. sapiens*, even within Africa, then many sites that have produced evidence of behavioral attributes referred to as modern could be questioned. This is largely because of the virtual absence of skeletal evidence to support the presence of *H. sapiens*, for instance, in many of the sites in southern Africa. Grand generalizations are often made *a priori* about the makers of material cultures that reflect behavioral modernity being *H. sapiens*. Such generalizations prove to be "untested, and . . . unnecessary" (Tryon 2011: 23), in particular as most views now favor the decoupling of behavioral and anatomical modernity (*e.g.*, Nowell 2010 *and references therein*; Zilhão 2011; Caron *et al*. 2011; Hovers & Belfer-Cohen 2006).

Despite the near unanimous acceptance of the many flaws of the behavioral modernity approach, the practicality of discarding it proves difficult. Are there other alternative approaches to studying the behaviors of the earliest *H. sapiens* and, for that matter, their immediate predecessors and contemporaries? A recent critique by Shea (2011) represents an attempt to call for the total abandonment of the behavioral modernity approach. In this thorough reappraisal of the behavioral modernity concept, Shea (2011) not only depicts the ineptness of this approach, but also proposes an alternative

approach as a better way to explain the behavioral context across the period immediately before and after the emergence of *H. sapiens*.

The *behavioral variability* approach, in particular to the study of the behavioral capacities of later Middle- and earlier Upper Pleistocene *H. sapiens* in Africa, is not necessarily a new one. Minichillo's (2005) dissertation, which reviews widely published interpretations on the behavior of MSA and LSA humans in the Western Cape Province of South Africa, indicates that the behavioral modernity approach has a number of deficiencies. In particular, Minichillo (2005) notes that the behavioral modernity approach fails to adequately explain the actual behavioral capacities of humans that occupied the same region during different periods. Refuting former conclusions of Klein (1999), which favored the presence of differential cognitive abilities between MSA and LSA populations in the Cape, Minichillo (2005: 239-240) views the behavioral modernity concept in light of what is called *phenotypic plasticity* – the ability to respond rapidly to certain ecological/cultural changes. Interestingly, he details that this can be expressed technologically through a noticeable increase in the variability of tool forms and can only be explained in the ecological/cultural context from which the particular finds derive. In his analysis of the Kibish assemblages, found in association with fossils of the earliest *H. sapiens*, Shea (2008) shows us that the measurement of flake cutting edge and metric variation in flake striking platform can be applied to infer costs and benefits reflected in the technological behavior of later Middle- and earlier Upper

Pleistocene hominin populations.

Unlike behavioral modernity, behavioral variability is a characteristic of all humans, as well as other species, and does not necessarily follow a diachronic trend. In addition, behavioral variability is shared by all hominins, can be expressed quantitatively, and has reversible trends (Shea 2011: table 1). While the identification of evidence of sophisticated behavior is important in itself, it does not lend itself to inferences that allow regional comparisons and broader pictures of human evolution (Shea 2011, 2012; Lombard 2012).

In this dissertation, the behavioral variability approach is employed to investigate the behavioral context across the period when *H. sapiens* appeared. Specifically, I will show that with the incorporation of additional techniques of studying technological capabilities of later Middle- and earlier Upper Pleistocene hominin populations, we can better explain behavioral patterns. Using data from multiple well-dated MSA occupations in the Gademotta Fm. (Wendorf & Schild 1974; Morgan & Renne 2008; Sahle *et al.* 2013) and other MSA sites in the wider rift valley in Ethiopia that have yielded fossils of the first *H. sapiens* (McDougall *et al.* 2005; Shea 2008; White *et al.* 2003; Clark *et al.* 2003; Beyene 2010; Haile-Selassie *et al.* 2004a; Yellen *et al.* 2005), I compare costs/benefits in flake production and the capacity for projectile technology. This allows me to explore behavioral variability among hominin populations from geographically and temporally discrete sites.

CHAPTER TWO

2. THE MIDDLE STONE AGE

The MSA represents a cultural phase between the Earlier and Later Stone Ages (ESA/LSA) and spans the period from >279 ka to *ca.* 40 ka (Sahle *et al*. 2013; Morgan & Renne 2008; Dieno & McBrearty 2002; McBrearty & Brooks 2000). Defined on the basis of techno-typological attributes, the MSA is commonly characterized by the presence of prepared core/flake technologies and blade tools, which stand in contrast to the large cutting tools of the preceding long-lived Acheulean tradition (Goodwin & Van Riet Lowe 1929; Deacon and Deacon 1999).

As opposed to long-held views, the transition from the ESA to the MSA has over the last few decades proved to be complex and gradual. At several sites in east and southern Africa, tool forms usually associated with the Acheulean tradition, and/or regarded as transitional (i.e. the Sangoan/Fauresmith), co-occur with those considered distinctly MSA, and vice versa (McBrearty & Tryon 2006; Tryon & McBrearty 2002, 2006; Johnson & McBrearty 2009; Porat *et al*. 2010; Van Peer *et al.* 2003; Shea 2008; Clark *et al*. 2003; Walter *et al*. 2000; Bruggemann *et al*. 2004). Some of these contexts have yielded skeletal evidence for the earliest *H. sapiens*, thereby introducing the need for a reconsideration of the attribution of certain technologies to a given taxon (Clark *et al*. 2003; Shea 2008). Similarly, the MSA-LSA transition occurred across a long period of time

and differs within and across regions. The earliest MSA-LSA transition in east Africa has been reported from the site of Enkapune Ya Muto in Kenya at >46 ka (Ambrose 1998) while surviving MSA elements in other sites have been documented from much later periods (*e.g.* Gossa *et al.* 2012; Willoughby 2007; McBrearty & Brooks 2000).

An exhaustive review of the MSA is beyond the scope of this dissertation. Instead, a summary of major MSA sites in sub-Saharan Africa that span the period of interest here (i.e. *ca.* 280 ka to ~80 ka) will be provided. More detailed descriptions are provided particularly on the MSA of the Gademotta Fm., the Kibish Fm. and the Middle Awash region as assemblages from these contexts make up the central part of this dissertation.

2.1 An overview of the MSA of sub-Saharan Africa prior to 80 ka

Evidence for the earliest MSA comes from sites in the Gademotta and Kapthurin Fms. (Sahle *et al*. 2013; Morgan & Renne 2008; Wendorf & Schild 1974; Dieno & McBrearty 2002; Tryon & McBrearty 2002, 2006; McBrearty & Tryon 2006). In the Kapthurin Fm. of the Kenyan rift, the earliest MSA occurs in interstratification with large bifaces of the Acheulean tradition in contexts dated to >284 ± 12 ka (Tryon & McBrearty 2002, McBrearty & Tryon 2006). At the Koimilot (GnJh-17; GnJi-74) and Rorop Lingop (GnJi-28) localities in the Kapthurin Fm. the early MSA is characterized by the Levallois technique and rare unretouched pointed

pieces (Tryon & McBrearty 2006: 503; McBrearty & Tryon 2006). The presence of the Levallois method as a common component of the Acheulean and early MSA in the Kapthurin Fm. indicates that the transition to the MSA was multi-directional, time-transgressive and gradual (McBrearty & Tryon 2006). In addition, the earliest MSA in the Kapthurin Fm. provides evidence of sophisticated behavior in the form of grindstones and pigments, which occur at site GnJh-15 in contexts >284 ka (McBrearty & Tryon 2006).

Like Kapthurin, the early MSA in the Sai Island of the Sudanese Nile Valley and at Abdur in the Eritrean Red Sea coast show an interstratification with industries considered Acheulean, at 223-152 ka and ~125 ka, respectively (Van Peer *et al*. 2003; Walter *et al*. 2000; Bruggemann *et al*. 2004). At site 8-B-11 in the Sai Island, the early MSA is depicted as containing the Sangoan transitional industry. Moreover, evidence for the processing of pigment (i.e. red and yellow ochre) and plant foods is documented from the same context (Van Peer *et al.* 2003). At Abdur, the MSA contains flakes and blades made on high-quality silicates such as obsidian (Walter *et al*. 2000; Bruggemann *et al*. 2004). The Red Sea coastal site shows some of the earliest evidence for marine resource exploitation (Walter *et al*. 2000; *cf*. Marean *et al*. 2007). The Kapedo Tuff archaeological sites of the Kenyan rift provide another instance where a typical MSA assemblage is found in association with a pick, in a context dated to between 135 ka and 123 ka (Tryon *et al*. 2008). Results of a comparison of

the Kapedo Tuff MSA with other sites in Kenya and southern Ethiopia suggest that the availability of lithic raw material is an important factor affecting variability defined on the basis of typology (Tryon *et al*. 2008).

At Lake Eyasi, in Tanzania, a broadly constrained (>132-82 ka) MSA sequence contains simple flakes associated with an archaic *H. sapiens* cranium (Domínguez-Rodrigo *et al*. 2008). The provenience of the cranial fragments is not conclusive. If these remains are as young as 132-82 ka, the contexts marks the latest instance where primitive morphological features among populations of our lineage continued (Domínguez-Rodrigo *et al*. 2008).

The early MSA record of the southern African region is rich, but often characterized by the lack of high-confidence dates and secure contextual data especially for fossil hominins (*see* Herries 2011; Lombard 2012 *for recent reviews*). An important early MSA site-complex in this region is found at Pinnacle Point, close to the southern tip of the continent. The early MSA at Cave 13B is marked by evidence of probable heat-treatment of stone materials, exploitation of marine resources, and the use of pigment from as early as *ca.* 164 ka (K. Brown *et al*. 2009; Marean *et al*. 2007; *see also* Watts 2010). At Blombos Cave, evidence of symbolic behavior includes incised and engraved ochre pieces dating to *ca*. 100-75 ka, and an ochre mixing kit ~100 ka old (Henshilwood *et al.* 2009, 2011). The MSA at Klasies River, in the Eastern Cape province of South Africa, documents a sequence spanning the period between *ca.* 115 ka and 60 ka (Wurz 2002).

The Klasies River MSA depicts the flexible subsistence strategies of inhabitants of the area, as inferred from widely studied faunal and lithic assemblages (Wurz 2002; Klein & Cruz-Uribe 1996; Milo 1998; Klein & Edgar 2002; *cf*. Minichillo 2005). Evidence of a deliberately engraved ochre pebble has been recovered from a context dated to 100-85 ka (d'Errico *et al*. 2012). In southeastern Africa, the Mozambican sites of Mikuyu and Ngalue provide evidence that MSA populations processed and consumed a wide range of starchy plant foods as early as ~105 ka (Mercader *et al*. 2008; Mercader 2009). Elsewhere in central Africa, evidence for ochre use comes from a broadly bracketed context at Twin Rivers, Zambia, dating to between 400 ka and 141 ka (Barham 2002). However, like most early MSA sites in the region (*e.g.* Grün *et al*. 1996; 2003*; see also* Herries 2011), the dates for this site are less secure. This stands in sharp contrast with some of the aforementioned east African sites where the MSA in its classical sense occurs in securely dated and older contexts.

2.1.1 The MSA of the Gademotta Fm.

The archaeological site-complex of the Gademotta Fm. was discovered and excavated four decades ago by a team of researchers led by Fred Wendorf of the Southern Methodist University (Wendorf & Schild 1974). Located in the central sector of the Main Ethiopian Rift (Fig. 1.1a), this open-air site complex represents a setting with few parallels in Africa. The interstratified tephra layers in this formation provide superior

stratigraphic controls for occupations spanning much of the MSA (Sahle *et al*. 2013; Morgan & Renne 2008; Fig. 2.1).

The Gademotta Fm. is located on a high ridge, which once made up a portion of an ancient, collapsed caldera west of the modern Lake Ziway (Laury & Albritton 1975; Fig. 1.1b). This formation rests unconformably over the volcanics of the Kulkuletti Fm. dated to *ca*. 1.3 million years ago (Vogel *et al.* 2006). Two major archaeological localities are known from previous investigations in the Gademotta Fm. These are the Gademotta type-site (*hereafter* Gademotta) and the Kulkuletti area. These two major foci of initial phase of research are located *ca*. 2.5 km apart along a southwest-northeast trending transect (Fig. 1.1b).

Previous research in the Gademotta Fm. determined the ages of two major tephra beds using the $^{40}K/^{40}Ar$ methods. These initial dating results suggested an age of 181 ± 6 ka (Wendorf *et al*. 1975) for the lowermost bedded-tuff of Unit 10; subsequent age estimations were reported on this tephra as 235 ± 5 ka (Wendorf *et al*. 1994; Fig. 2.1). Unit D represents a lapilli ash bed deposited during the filling of a large erosion feature that removed most of Unit 12 in the Kulkuletti area. This ash was dated at 149 ± 13 ka (Wendorf *et al*. 1975; Fig. 2.1). A recent $^{39}Ar/^{40}Ar$ geochronology revised the ages of Unit 10 to 276 ± 4 ka and Unit D to 183 ± 10 ka (Morgan & Renne 2008). Similar analysis on the uppermost Unit 15 ash could not yield a secure age (Morgan & Renne 2008). However, a recent geochemical correlation shows that the composition of this ash matches with

the Aliyo Tuff in the Kibish Fm., which is dated to 104 ± 1 ka (F. Brown *et al*. 2012).

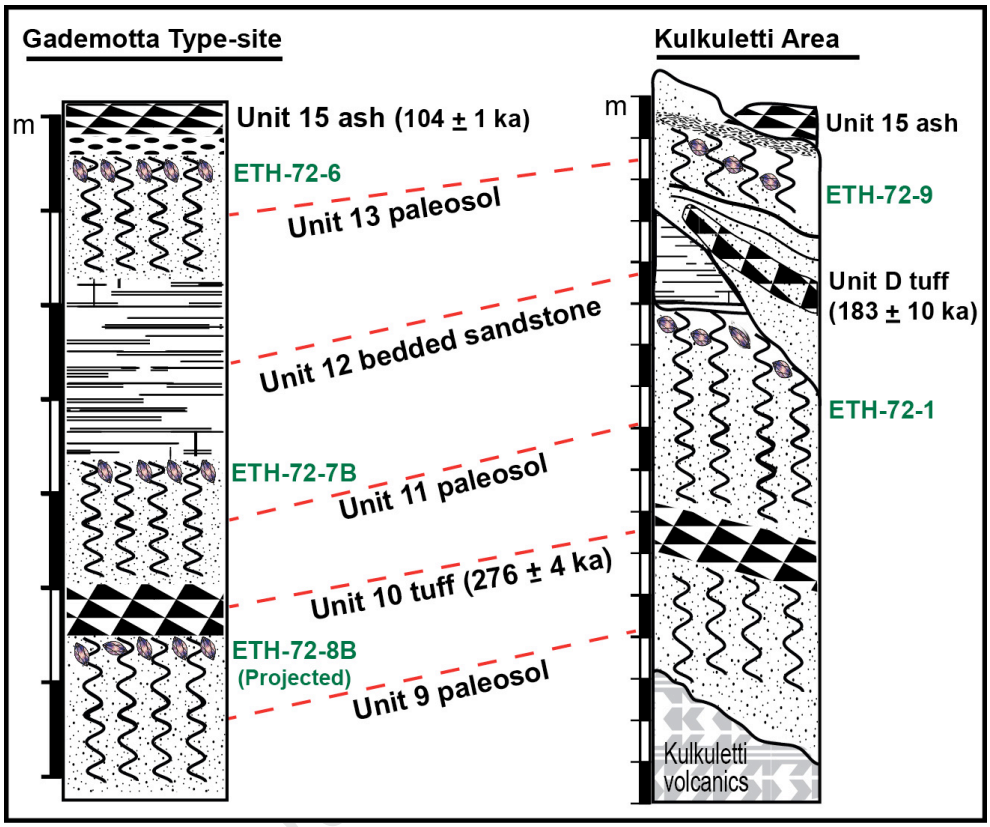

Figure 2.1 Stratigraphic sections of the cultural sequence and placement of previously excavated sites (in green) in the Gademotta Fm. (*After* Laury & Albritton 1975)

Major archaeological excavations conducted in 1972 both at Gademotta and Kulkuletti recovered a large collection of distinctly MSA assemblages from several sites. Most notable among these previously

excavated sites are ETH-72-1 and 72-9 in the Kulkuletti area, and ETH-72-8B, 72-7B and 72-6 in the Gademotta area (Wendorf & Schild 1974; Fig. 2.1). The high-quality obsidian quarried from a source near Kulkuletti, known as Worja, (Vogel *et al*. 2006) makes up the sole stone raw material used for the manufacturing of artifacts in all occupations (Wendorf & Schild 1974).

The availability of radiometric dates that extend into the Middle Pleistocene, together with the rich assemblages and spatial features, had long made the occupation at ETH-72-8B particularly dominant in discussions surrounding the beginning of the MSA (Wendorf & Schild 1974, 1993; McBrearty & Brooks 2000; Shea 2008; Yellen *et al*. 2005). This site represents an occupation in the Unit 9 paleosol, marking the lowermost MSA occurrence in the sequence. Based on physical correlations, this site was suggested to underlie Unit 10 (Laury & Albritton 1975; Fig. 2.1). As opposed to most other early MSA sites (*e.g.* McBrearty & Tryon 2006; Van Peer *et al*. 2003; Shea 2008; Clark *et al*. 2003; Bruggemann *et al*. 2004; Tryon *et al*. 2008), the earliest MSA at ETH-72-8B is characterized by the absence of any trace of an Acheulean occupation and abundant retouched tool forms attesting enormous techno-typological variability (Wendorf & Schild 1974; Wendorf *et al*. 1975).

ETH-72-8B yielded over 9,000 artifacts, nearly half of which is debris (Wendorf & Schild 1974: 84). Debitage, particularly primary flakes, and retouched tools dominate the non-debris assemblage while the Levallois

technique is well represented (Wendorf & Schild 1974: table 1, 2). In addition, the horizontal distribution pattern of artifacts at ETH-72-8B, specifically the rapid thinning out of artifact density from the center of the excavation, was interpreted as conforming to a roughly circular depression interpreted as marking the floor of a shelter (Wendorf & Schild 1974: 151). The suggested presence of a prehistoric "hut" needs further investigation and, if supported, would constitute some of the earliest known evidence for a housing feature, with implications for sophisticated behavior among Middle Pleistocene hominin populations (McBrearty & Brooks 2000).

Stratigraphically below ETH-72-8B, near the base of the Unit 9 paleosol (Fig. 1.2), small handaxes were recovered in surface contexts. This may be suggestive of a possible final Acheulean occurrence, although no cultural horizon attributed to this tradition was discovered *in situ* (Wendorf & Schild 1974: 48; Wendorf *et al*. 1975; Laury & Albritton 1975).

Sites ETH-72-7B and 72-1 both represent occupations in the Unit 11 paleosol and are bracketed between Units 10 and 12 (Laury & Albritton 1975: table 1; Fig. 2.1). An age of 183 ka on the Unit D tuff at Kulkuletti provided the most recent upper-capping date for these occupations (Morgan & Renne 2008; Fig. 2.1). Assemblages from these occupations, like those from ETH-72-8B, have been depicted as exhibiting tremendous technological variability that contrasts with substantially younger MSA sites in the region, such as Kibish and Herto (Wendorf & Schild 1974, 1993; Schild & Wendorf 2005; Shea 2008; Clark *et al.* 2003). In addition,

substantial similarity between attributes of assemblages from these younger sites in the Gademotta Fm. and the ETH-72-8B assemblage has been presented as indicative of a technological "stasis" spanning a period of almost 100 ka (Wendorf & Schild 1974; Morgan & Renne 2008).

Site ETH-72-6 and 72-9 were excavated into the Unit 13 paleosol at Gademotta and Kulkuletti, respectively (Wendorf & Schild 1974; Laury & Albritton 1975: table 1; Fig 2.1). The recent correlative age for the Unit 15 ash (F. Brown *et al*. 2012) provides a minimum age for these sites. Typological and technological patterns of assemblages from these sites are generally similar to the older sites described above, such that retouched tools and primary flakes make up the largest proportion of the assemblages and the Levallois method is an important component (Wendorf & Schild 1974).

A particular horizon that preserved fossilized bones was identified below the Unit 9 paleosol. This horizon has yielded numerous faunal remains, including a hippopotamus upper molar, an equid tibia (possibly *Dolichohippus grevyi)*, and dental and hemi-mandibular remains of wildebeest (possibly *Connochaetes taurinus*), hartebeest (possibly *Alcelaphus buselaphus*), and large- and medium-size antelopes (Gautier 1974). Although this fossiliferous channel fill has been tentatively considered contemporaneous with the occupation at ETH-72-8B, its stratigraphic relationship could not be confidently established (Wendorf & Schld 1974). As a result, the assumption that faunal remains recovered from

this secondary deposit possibly represent prey hunted by inhabitants of the ETH-72-8B occupation (Gautier 1974) must be treated with caution.

2.1.2 The MSA of the Kibish Fm.

The Kibish Fm. is situated in the Omo Valley of the rift valley in Ethiopia (Fig. 1.1a) and contains sites named KHS, AHS and BNS (Shea 2008; Fig. 2.2). The first two sites are dated to *ca*. 196 ± 2 ka, while the minimum age for BNS is 104 ± 1 ka (McDougall *et al*. 2005, 2008; F. Brown *et al*. 2012; Fig. 2.2). Fossils of *H. sapiens* recovered from this site complex include the Omo I and Omo II crania, and additional post-cranial elements at KHS and AHS (McDougall *et al*. 2005; Pearson *et al*. 2008). Despite missing facial parts, Omo I has been shown to fall well within the range of *H. sapiens* while the Omo II cranium represents an "archaic", near-modern individual (Day & Stringer 1991; *See also* Rightmire 2008; Tattersall & Schwartz 2008).

The non-debris assemblages from the Kibish sites are dominated by debitage. Retouched tools generally make up a small proportion of the whole assemblage. In addition, large cutting tools and bifaces were recovered from both *in situ* and surface contexts, although they are more common in the latter (Shea 2008). Fine-grained silicates, mainly chert, make up the most commonly utilized raw material type in the Kibish assemblages (Shea 2008: 467). Extensive refitting and analysis of spatial data provide rare insights into the natural and cultural site-formation processes witnessed

at BNS and KHS in the Kibish Fm. (Sisk & Shea 2008). Similarly, comparisons of patterns of cutting edge production and core exploitation at AHS, KHS and BNS suggest that denizens of these sites exhibited substantially similar technological behavior (Shea 2008). Certain patterns of behavior, such as the potentially non-utilitarian transport of opal, can be interpreted as indicative of the capacity of the Kibish early *H. sapiens* populations for symbolic behavior, if one is to employ commonly applied approaches (Shea 2011: 10-11).

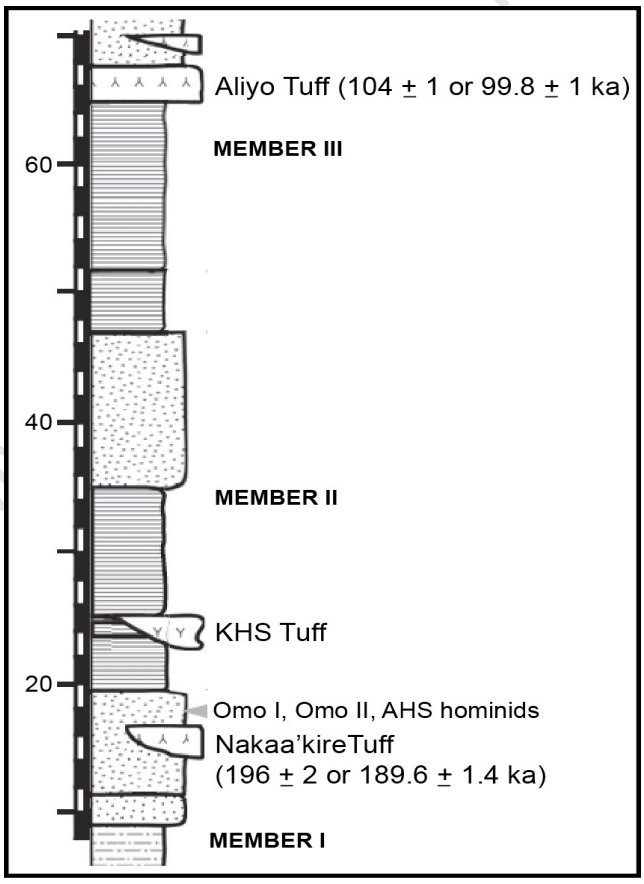

Figure 2.2 A composite stratigraphy of the Kibish Fm. (*After* F. Brown *et al.* 2012)

2.1.3 The MSA at Herto and Aduma, Middle Awash area

The sites of Herto and Aduma in the Middle Awash study area of the Afar Rift, northeastern Ethiopia (Figs. 1.1a, 2.3), represent MSA assemblages recovered from contexts that have yielded some of the earliest and best-known *H. s* fossils (Clark *et al*. 2003; White *et al*. 2003; Yellen *et al* 2005; Haile-Selassie *et al*. 2004a).

The Herto MSA assemblages represent both excavated and surface-collected materials that manifestly derive from the hominin-bearing sediments of the Upper Herto Member that are tightly constrained between 160 ± 2 ka and 154 ± 7 ka (Clark *et al*. 2003; Fig. 2.3). Major discoveries at Herto include three well-preserved hominin crania (including one juvenile) of *H. sapiens* that represent a new paleosubspecies named *idaltu* (White *et al*. 2003).

In general, the Herto assemblages are primarily composed of flake debitage and retouched tools, including those produced with the Levallois technique. Most of the retouched tools occur in the forms of scrapers and points, in addition to retouched blades. Large bifaces also make up a significant portion of the assemblages (Clark *et al*. 2003: 750-751). Fine-grained basalt was used as the predominant raw material type for both flakes and tools. Points and blades were, in contrast, more often made on obsidian (Clark *et al*. 2003: 750-751, supp. info.; Beyene 2010: 46).

Little has been published on the inferred patterns of behavior among the Herto humans (Clark *et al*. 2003; Beyene 2010), although independent

arrays of evidence from Herto can be used to make a strong case for the capacity of the earliest human populations for sophisticated behavior (Sahle & Beyene *forthcoming*). All three of the Herto crania witness bone surface modifications interpreted as evidence for "post-mortem manipulation and curation of human remains as part of mortuary practices" (Clark *et al*. 2003: 751). Not far away, within the Middle Awash region, defleshing cutmarks on the Bodo skull have provided even earlier evidence of a special post-mortem treatment, rather than cannibalization, by a non-*sapiens* species of the genus *Homo* at ~600 ka (White 2000; Clark *et al.* 1994). Herto provides much stronger evidence in that the cutmarks appear on all of the crania discovered at the site (Clark *et al*. 2003: 751). In addition, only cranial elements were found at Herto in a context that also preserved such delicate fauna as the cranium of a juvenile individual. This absence of postcrania is, hence, provocative as it may indicate curation of specific parts of the dead, most plausibly for similar ritual purposes to those documented ethnographically (Beyene 2010: 51; Sahle & Beyene *forthcoming*; Clark *et al*. 2003; White 2000).

Another line of independent evidence suggestive of the capacities of the Herto people for complex behavior comes from a recent geochemical provenancing work in the wider Afar Rift (Negash *et al*. 2011). This study confirms the procurement of obsidian raw material by the Herto humans from a remote source 289 km distant (Negash *et al*. 2011). This is particularly interesting because these people had a number of other available

obsidian sources within much closer range (Negash *et al*. 2011). This work could not confirm whether this source was directly quarried and transported by the Herto humans or whether a long-distance obsidian exchange was involved (Negash *et al*. 2011: 671). Yet one can conclude that these people possessed knowledge and control of resources over a wider geographic range and/or embraced the practice of some form of social interaction. It is possible that trade/exchange of resources with other groups from these distant sources is responsible for the evident pattern (Sahle & Beyene *forthcoming*).

The Aduma assemblage from ADU-VP-1/3 represents surface collections from the Ardu B sediments, with an estimated age of 100-80 ka (Yellen *et al*. 2005: 35; Fig. 2.3). The discovery of the most complete of the Aduma partial crania from freshly eroding sediments (Haile-Selassie *et al*. 2004a) necessitated the collection of securely associated archaeological material from this locality (Yellen *et al*. 2005: 41, 49). Craniometric and morphological analyses put all of the Aduma Upper Pleistocene crania within the range of anatomically-modern *H. sapiens* (Haile-Selassie *et al*. 2004a).

As at Herto, the Aduma artifacts are made mainly on basalt whereas cryptocrystalline raw materials (primarily obsidian and chert) are similarly well represented. Analysis of the Aduma assemblage shows that inhabitants of the area responded to dynamic ecological conditions through flexible behavior, such as subsistence scheduling and technological variability, in a

fashion common among contemporary hunter-gatherers (Yellen *et al.* 2005; Brooks *et al*. 2006).

Sites at Herto and Aduma show a mix of technological affinities that reflect the complexities of the ESA-to-MSA and MSA-to-LSA transitions. The Herto sites mentioned above provide one of the last appearance datums for the Acheulean tradition in Africa, at 154 ka (Clark *et al*. 2003; *cf*. Bruggemann *et al*. 2004; Tryon *et al*. 2008). Certain sites in the younger sections of the Ardu sequence at Aduma (Fig. 2.3) show that the transition to the LSA was neither straightforward nor swift (Brooks *et al*. 2002).

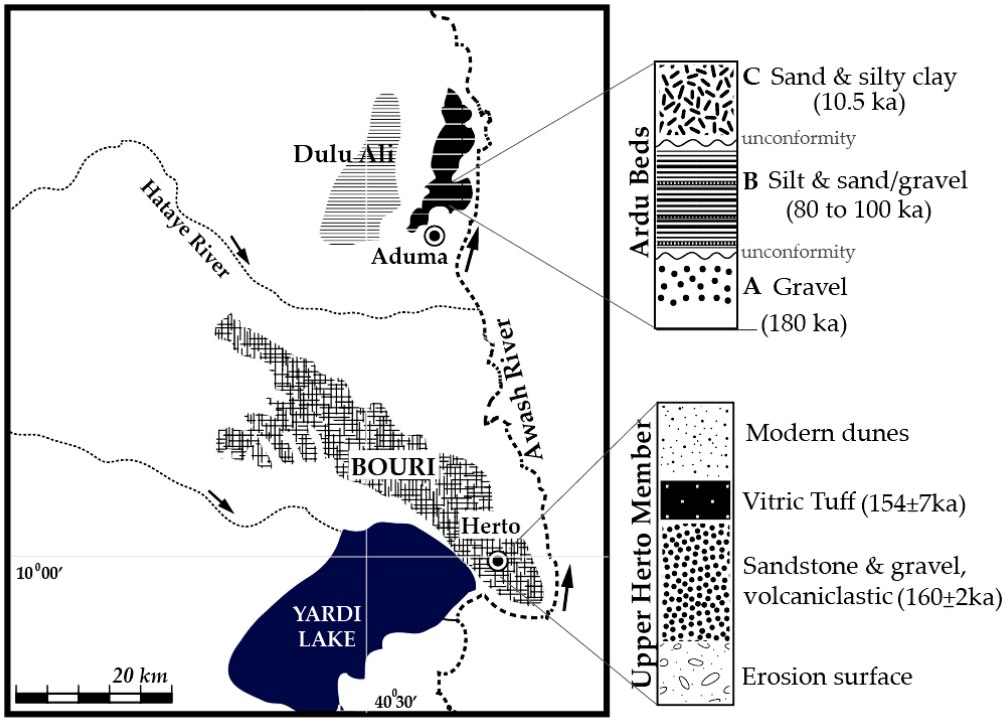

Figure 2.3 A map showing the relative locations and composite stratigraphies of Herto and Aduma, Middle Awash (*after* Yellen *et al.* 2005; Clark *et al*. 2003)

2.2 Summary and Discussion

The general picture depicted here shows that the MSA prior to *ca*. 80 ka encompasses evidence not only for the earliest *H. sapiens*, but also patterns of behavior commonly associated with the latter part of this time period. In addition, the record shows that the Acheulean-MSA transition was a complex, diachronous and gradual process (Fig. 2.4). On the one hand, evidence for behaviors commonly considered quintessential to humans occur sporadically and "precociously" across a wide range of time and space. On the other, certain techno-typological attributes that define the preceding Acheulean tradition persist past the early-late MSA divide. An exception to this general picture comes from the Gademotta Fm. where even the world's earliest MSA occupation does not retain elements attributable to the transition from the Acheulean period (Wendorf & Schild 1974; Wendorf *et al*. 1975; Fig. 2.4). As such the pattern attested by the Gademotta early MSA sites supports current perceptions that the Acheulean-to-MSA transition was complex. More importantly, it invites questions as to why and/or how such a pattern emerged at Gademotta as early as >279 ka while other later Middle Pleistocene sites in the region exhibit patterns quite different from it (Fig. 2.4). Answering these questions requires a closer examination of inferred patterns of technological behavior and the testing of models of modern human origins.

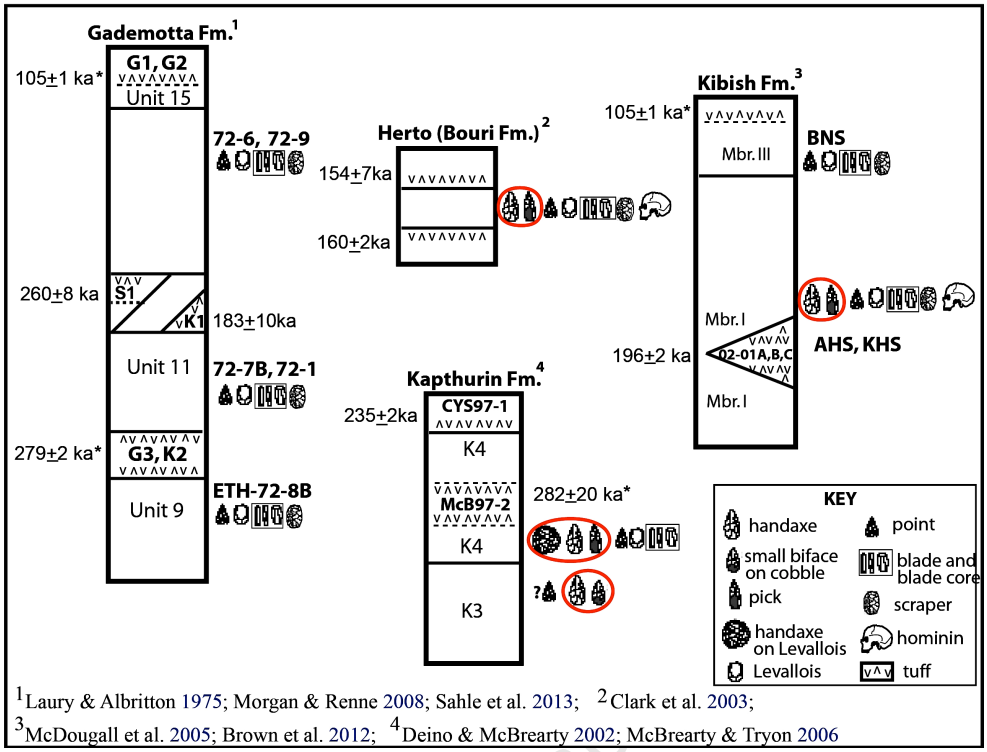

Figure 2.4 A schematic representation of the cultural stratigraphic succession of some of the best-known early MSA sites from east Africa

CHAPTER THREE

3. MATERIALS AND METHODS

3.1 Excavation and lithic analysis

3.1.1 Excavation

Renewed archaeological research in the Gademotta area undertaken for this dissertation started with an extensive field reconnaissance of the wider region in 2010, almost four decades after the discovery and initial investigation of the site complex (Wendorf & Schild 1974). Detailed topographic maps, figures, sketches and geographic coordinates from the existing literature were used to relocate previous excavations, geological trenches and tephra sampling localities (Wendorf & Schild 1974; Laury & Albritton 1975; Wendorf *et al*. 1975; Morgan & Renne 2008: data rep.). In particular, site ETH-72-6 of Wendorf and Schild (1974: fig. 36, 37) retains standing sections that are still visible and easily identifiable due to the unique shape of a relatively large (33m^2) excavation that indicates little sign of backfill. This excavation was used as a reference to georeference a more comprehensive map of the Gademotta type locality. Once the maps produced by Wendorf and Schild (1974) were rectified, it was possible to relocate the other less visible sites, such as ETH-72-8B. Total stations (Leica TC307 and Leica Builder 505) borrowed from the Department of Archaeology, University of Cape Town (UCT), were used to collect spatial

data. A series of datums were also established to enable detailed mapping.

Excavations were made in selected localities of the Gademotta type area. Major excavations included GDM7, which was excavated adjacent to site ETH-72-8B, and GDM 10, which lies adjacent to ETH-72-7B (Fig. 4.1; Wendorf & Schild 1974). Grids were set in meters, using the total station, with the smallest grid unit a 1 x 1m square. Excavations followed artificially established spits of 10cm, as there are no fine natural stratigraphic distinctions to follow. Excavations were conducted primarily using trowels. Broad-tipped chisels were occasionally used to dig carefully into consolidated sediments. All excavated sediments were screened through a 5mm wire mesh. Artifacts recovered from the screening activities were bagged into their respective squares and levels.

Each artifact recovered *in situ* that was >2cm in any dimension was mapped using total station and individually numbered and bagged. Each mapped artifact was identified with specimen type and individual field ID. Artifacts too small to plot were picked and bagged into the respective levels from which they derive. Point data collected using the total station were plotted in ArcMap 10.1 (ESRI) and NewPlot (McPherron & Dibble 2002) to provide high-precision relational data, such as artifact distribution and orientation patterns.

3.1.2 Lithic Analysis

There is no single, consistently employed framework of lithic analysis for the MSA of east Africa (*cf.* Clark *et al*. 2003; Yellen *et al*. 2005; Shea 2008; Wendorf & Schild 1974; Tryon *et al*. 2005; Van Peer *et al*. 2003). For the present study, the framework described by Shea (2008: appendix) in his analysis of the Kibish MSA assemblages has been largely adopted due to its comprehensiveness and Kibish's temporal and geographical proximity to Gademotta. A detailed description of this framework is provided in Appendix-1 of this dissertation.

Detailed morphometric and technological analyses of flakes and cores can help us understand how ancient hominins incorporated costs and benefits as part of their technological adaptive strategies (*e.g.,* Braun *et al.* 2005, 2008; Potts 1998; Shea 2008). Previous studies of variation in assemblages from sites in the Gademotta Fm. relied mainly upon European-style typological analysis (Wendorf & Schild 1974; Bordes 1961). These studies suggested that technological strategies remained largely constant from the oldest through younger MSA occupations (Wendorf & Schild 1974). In contrast, the technological analysis component of this research measured two major aspects of behavior pertaining to stone tool production, use and discard. These are: i) the analysis of cost and benefit of stone tool production; ii) the assessment of projectile technologies.

3.1.2.1 Cost/Benefit Analysis

The analysis of costs/benefits in technological adaptations mainly encompasses the measurement of curation levels (*sensu* Shott 1989, 1996) as inferred from the dimensions of flake cutting edge, and core-exploitation strategies.

A comparison of costs and benefits in assemblages allows the measurement of how different populations responded to diverse ecological contingencies (*e.g.*, Blumenschine *et al*. 2008; Bousman 2005). This in turn can be used to compare the capacities for behavioral variability among hominin populations using the most abundant, and most durable of archaeological evidence – stone tools (Shea 2011).

For this dissertation research, I collected whole-flake measurements on assemblages from sites in the Gademotta type area, as well as those from the Herto and Aduma MSA sites (Fig.1.1). All whole-flake measurements on the previously excavated Gademotta assemblage from ETH-72-6, as well as on assemblages from the Middle Awash MSA sites of Herto and Aduma, were conducted under a laboratory permit from the Ethiopian Authority for Research and Conservation of Cultural Heritage (ARCCH) and the consent of active research permit holders. Whole-flake raw metric data on the Kibish assemblages were generously provided by Dr. John J. Shea. All metric measurements were collected using a digital caliper accurate to 0.01mm and following protocols detailed in Appendix-1. A discussion of the conceptual basis of measurements is provided in Chapter Six of this dissertation.

3.1.2.2 Macro- and microscopic analysis of pointed pieces

The presence of projectile weaponry in the archaeological record is often considered as a major innovation with important evolutionary advantages, especially with regards to subsistence strategies and dietary/niche breadth (*e.g.*, Churchill 1993; O'Connell 2006). A confident identification of the earliest projectile technologies in the Paleolithic record has long proved difficult (Thieme 1997; Shea 1988, 2006; Brooks *et al*. 2006; Holdaway 1989). On the basis of morphological-metrical attributes and use traces, "complex" projectiles are suggested to have originated among *H. sapiens* in Africa, sometime between 100 and 50 ka (*e.g.*, Shea 2006, 2009; Shea & Sisk 2010; Brooks *et al.* 2006; Lombard & Phillipson 2010).

Pointed artifacts made on obsidian in the Gademotta Fm. bear morphological features, such as small size and diagnostic impact fractures, often associated with the use of projectile weapons. However, these features can only inform on the likelihood of pointed pieces having been used as projectile weapons (Sisk & Shea 2011). None of these morphological criteria alone can speak to the actual use of a tool as a projectile. A more confident assessment must rely on the application of various independent approaches to the identification of projectile weaponry (Lombard 2011).

This research employed three independent approaches in order to assess whether any of the Gademotta pointed artifacts were actually used as projectile weapons. These methods included: i) the identification and

measurement of impact-induced microfracture features on the surface of pointed pieces to determine the velocity of the weapon and impact delivery mechanism (Hutchings 1997, 2011); ii) the documentation of edge-damage patterns on the pointed pieces (Fischer *et al*. 1984; Bergman & Newcomer 1983; Sano 2009; Lombard 2005); iii) an assessment of the suitability of the morphology of a pointed piece for hafting and use as the tip of projectile weapons (Shea 2006; Shea & Sisk 2010; Sisk & Shea 2011).

The study of microfracture features involved multiple stages of analysis: i) the determination of the material properties of the obsidian used by the Gademotta hominins; ii) the microscopic investigation of fracture fronts on pointed pieces; iii) the capturing of fracture features in photomicrographs; iv) the measurement of dimensions of fracture feature; v) the calculation of the instantaneous fracture velocity.

Fracture features, such as Wallner lines, appear on the fracture surface of fine-grained materials as characteristic undulations resulting from the interaction of the propagating crack with shear waves emanating from the crack force (Wallner 1939; Ravi-Chandar 2004). Wallner lines are created when the normally curved crack-front propagation is perturbed by intrinsic imperfections or terminal fracture, thereby creating shear waves radiating at a given velocity on the local fracture surface. It is possible to determine the crack velocity from the geometric configuration of these lines (Ravi-Chandar 2004: 98). Fracture wings (*hereafter* FW) represent special types of microscopic fracture features and form from similar mechanisms. FWs are

"V" shaped, with their wings opening up toward the direction of fracture propagation and attenuating relatively rapidly than do Wallner lines (Fig. 5.2). A detailed review of related literature on the type, nature and use of these microfracture features to determine the speed and direction of impacts producing them is provided by Hutchings (1997, 1999, 2011).

Dr. Braun and I collected obsidian samples (n=32) from the Worja source near Kulkuletti to facilitate the study of material properties of the obsidian used by the Gademotta hominins (Vogel *et al.* 2006; Negash *et al.* 2010). I trimmed raw material samples into slabs of 5cm thickness each using a lapidary saw. Two of these samples were first brought to UCT for initial tests. A comprehensive material analysis of the Worja obsidian was conducted in the National Museum of Ethiopia (NME), Addis Ababa, using portable ultrasonic transducers (NDT James Instruments MK IV) (Appendix-3).

Young's Modulus (E) and Poisson's Ratio (v) for the Worja obsidian were determined by the pulse method using the ultrasonic transducer. These properties were used to calculate the Modulus of Rigidity (G). The distortional wave velocity (C_2) of the Worja obsidian was then computed from G and the material density. Material density (ρ) of the Worja obsidian was measured in the Concrete Materials and Structural Integrity Research Unit (CoMSIRU) of the Department of Civil Engineering, UCT.

The following formulae detailed by Hutchings (2011) were used in the calculation of the physical properties of the Worja obsidian:

$$C_2 = (G/\rho)^{1/2} \quad \textit{and} \quad G = E/2(1+v)$$

Individual readings of E and v for the Worja obsidian are provided in Appendix-3. Averages of the E and v values were used to calculate C_2 and G. Since readings for E were collected on the ultrasonic transducers as pound/inch^2 (*psi*), values were converted into Newton/m^2 (*pa* [pascal]) (*cf.* Hutchings 2011: table 1).

Velocity dependent fracture surface features were documented on bifacial and unifacial points from several sites in the Gademotta Fm. using a Keyence VHX-600 (3CCD) digital microscope, with a magnification power of 20 to 200x, housed in the NME, Addis Ababa. Initial attempts to identify microfracture features were inconclusive as a leading expert, Dr. W. Karl Hutchings of Thompson Rivers University, could not confidently confirm the presence of these features from photomicrographs of certain features on pointed artifacts from the Gademotta. As a result, the next phase of this research involved Dr. Hutchings visiting Addis Ababa to examine the pointed artifacts in order to identify microfracture features. As explained in Chapter Five, I subsequently conducted more thorough microfracture analyses, using the same digital microscope in the same laboratory in Addis Ababa. The measurement of relevant dimensions of microfracture features was carried out by Dr. Hutchings, and independently by myself.

Instantaneous fracture velocity (C) is calculated from the angles of FWs once they have been positively identified. FWs are microfracture

ripples and can appear in two forms: curved and plain. Computations for FWs with plane crack fronts are conducted using the formula that the ratio of C to C_2 is equal to the cosine of the semi-angle of divergence of an FW. Mathematically, $C/C_2 = \cos(\psi/2)$; where ψ is the angle of divergence of an FW. FWs with curved crack fronts will, in addition, include a measurement of the angle of curvature (Hutchings 2011: 1740, fig 6b).

Photomicrographs of FWs were collected using a microscope housed in the NME, Addis Ababa, first by Dr. Hutchings, and later independently by myself. Measurements of angle of divergence were conducted on the digital versions of photomicrographs using the software on the Keyence microscope, and independently using the MB Ruler 4.0 (http://markus-bader.de/MB-Ruler) ImageJ 1.440 (http://imagej.nih.gov/ij) and external software.

Detailed documentation of edge-damage patterns was conducted on pointed pieces that have yielded measurable microfracture features. Macroscopic damage patterns were carefully analyzed on these pointed pieces to link damage patterns with the most probable tool function. Identification of edge damage was made largely using the naked eye, and seldom with the help of a hand lens and the microscope, providing magnifications of up to 20x. Damage patterns were classified using Sano's (2009) comprehensive methodological summary.

Tip Cross Section Area (TCSA) and -Perimeter (TCSP) were calculated following methods detailed by Shea (2006), and Sisk and Shea

(2011). For TCSP, values from the more restrictive measure of triangular (rather than rhomboidal) cross-section were used, as recommended by Sisk and Shea (2011: 3). Results were compared with values for assemblages from experimental spear points replicated from Levantine Middle Paleolithic assemblages (Shea *et al*. 2001). Dr. Shea provided raw metric data for these experimental spear points. Also, comparison was conducted with an archaeological assemblage of MSA pointed pieces from the Klasies River main site (KRM), South Africa. Raw metric data for the Klasies River main site point assemblage were generously provided by Dr. Sarah Wurz.

3.2 Dating and stratigraphy

3.2.1 $^{40}Ar/^{39}Ar$ geochronology

Renewed archaeological field research I conducted in 2010, alongside Dr. Braun, enabled me to find out that the actual stratigraphic relationship between the lowermost dated tepha bed of Unit 10 and the ETH-72-8B occupation horizon projected to underlie this tuff (Wendorf & Schild 1974; Laury & Albritton 1975; Morgan & Renne 2008) was not clear. Tephra sample for the most recent $^{40}Ar/^{39}Ar$ geochronology was collected from hundreds of meters away from the site, where the Unit 10 tepra crops out prominently (Morgan & Renne 2008: data rep.). As a result, despite reporting a much older age for Unit 10, this work depended on previous stratigraphic correlations that put site ETH-72-8B under the dated tuff (Morgan & Renne 2008; Laury & Albritton 1975).

In 2011, with the help of Dr. Balemwal Atnafu of the Department of Earth Sciences, Addis Ababa University (AAU), I collected several tephra samples and excavated geological trenches across a large area in the type-site. This undertaking included the sampling of datable material from immediately above site ETH-72-8B (Wendorf & Schild 1974). In addition, a localized ash layer that had never before been dated was sampled from Unit 12 of Laury and Albritton (1975) in order to obtain a better minimum age for occupations between this unit and Unit 10 (Wendorf & Schild 1974; Laury & Albritton 1975; *cf*. Morgan & Renne 2008).

Early in 2012, I conducted an additional brief geological fieldwork alongside Dr. Leah E. Morgan of the Scottish Universities Environmental Research Centre and sampled the uppermost Unit 15 ash (Wendorf & Schild 1974). Analysis of this ash is currently in progress.

$^{40}Ar/^{39}Ar$ analyses of the Unit 10 and the Unit 12 tephra samples were conducted by Dr. Morgan. In addition to sampling, I conducted initial sample preparation in the Sedimentology Lab at AAU, where I washed, dried and sieved bulk samples. I then took all samples to Vrije Universiteit, Amsterdam, where they were prepared further. Both preparation and measurement followed the procedures and protocols for previous analyses from the same area (Morgan & Renne 2008). Samples were irradiated in aluminum disks with the Alder Creek sanidine standard (Nomade *et al.* 2005) using the Oregon State (USA) TRIGA reactor housed in the Cd-shielded CLICIT facility. Samples were degassed using a Synrad CO_2 laser;

resulting gas was purified using SAES getters and a Polycold cryocooler. Argon isotopic relative abundances were measured by peak hopping on a Mass Analyzer Products 215-50 mass spectrometer. Backgrounds were measured between every one to two analyses; corrections were made via long-term integration of background measurements. Mass discrimination was measured with an air pipette analysis between every *ca* four to 14 analyses; corrections were made by a long-term average and standard deviation of air pipette analysis. Production ratios used follow Renne *et al*. (2005). Decay constants and standard ages follow Renne *et al.* (2011); both these and values computed using Steiger and Jäger (1977) and Renne *et al*. (1998) are provided in Appendix-2, also to facilitate comparison with previously reported data (Morgan & Renne 2008: data rep.). Calculations were made using the spreadsheet provided by Renne *et al.* (2011). Uncertainties reported in text and figures are provided at the 1σ level and include full analytical and systematic uncertainties; reported values are standard error of the mean (*SEM*), except where the Mean Square of Weighted Deviates (*MSWD*) >1, where uncertainties are equal to (*SEM*)* $\sqrt{MSWD}$.

In addition to results of new analyses reported here, ages published for some sites have been revised using the new standards published by Renne *et al*. (2011). These revisions are made in order to maintain methodological consistency in the discussion of ages of sites that are important for discussions in this dissertation. Accordingly, the revised age for the Aliyo Tuff in the Kibish Fm. was made using the published Ar data (McDougall *et*

al. 2005, 2008) and a spreadsheet provided by Renne *et al*. (2011). The revised age for the Kapthurin Fm. was made in two steps – first, by separate raw data provided by Dr. Deino (Morgan & Renne 2008) that allowed calculation of an inverse isochron; second, by converting that age into the revised value by using the spreadsheet from Renne *et al*. (2011).

3.2.2 Stratigraphy

Stratigraphic investigations were conducted across the entire Gademotta type-site. The field aspects of these studies focused on the identification of marker beds and sediment features in the multiple units of the type-site and involved expert assistance from Dr. Atnafu. The monotonous succession of sediments of Units 9 though 12 necessitated the digging of trenches across the area. Step-trenches of 1m width were opened in two major loci across the type-site in order to enable a comparison of the stratigraphic sequence closer to site ETH-72-8B and farther north where the Unit 10 ash forms a prominent bed. Additionally, a series of sediment samples were collected from these trenches and analyzed in the sedimentological lab at AAU. Section drawings were finally developed in order to enable a holistic comparison of the sequence across space.

Using results from the new $^{40}Ar/^{39}Ar$ geochronology, and additional field investigations, I developed a new understanding of the chrono-stratigraphy of later Middle Pleistocene sections. This data allowed me to develop a chronological framework for the archaeological sites of the

Gademotta Fm. that were excavated by previous as well as renewed research (*cf*. Wendorf & Schild 1974; Wendorf *et al.* 1975, 1994; Laury & Albritton 1975).

CHAPTER FOUR

4. RENEWED RESEARCH IN THE GADEMOTTA FORMATION

4.1 Renewed $^{40}Ar/^{39}Ar$ geochronology and the context of *early* MSA occupations at Gademotta

The Unit 10 bedded-tuff is the most widespread tephra in the Gademotta Fm. and outcrops prominently in both the Gademotta and Kulkuletti areas (Laury & Albritton 1975). The most recent geochronological analysis of the Unit 10 ash yielded ages of 283 ± 4 ka* (sampled at Kulkuletti) and 279 ± 2 ka* (sampled at Gademotta) (Morgan & Renne 2008). (Unless otherwise noted, uncertainties are provided at 1σ here and throughout, excepting ages reported by Laury and Albritton [1975] for which confidence levels are not provided). Surveys I conducted with Dr. Braun in 2010 relocated the ETH-72-8B excavation in the Gademotta type area (Wendorf & Schild 1974; Laury & Albritton 1975; Fig. 4.1) and identified that Unit 10 is not easily recognized near the ETH-72-8B archaeological site. At ETH-72-8B there is a resistant ledge that extends across some 200m north of the site (Fig. 4.1). All along this resistant ledge the Unit 10 ash does not form a prominent outcrop. This is a sharp contrast to the ~60cm thick bed that Unit 10 forms some 400m farther north, from where samples for the most recent $^{40}Ar/^{39}Ar$ analysis were collected (Morgan & Renne 2008: data rep.; Fig. 4.1).

*All ages marked by asterisks throughout this dissertation represent those recalculated from original publications using decay constants and standard ages of Renne *et al.* (2011).

The stratigraphic placement of site ETH-72-8B was previously based on a physical correlation of sediment successions from the southern part of the Gademotta region where the tuff is not easily visible with an area farther north where the Gademotta type section was developed (Laury & Albritton 1975: 1005, fig. 9). However, the presence of abruptly changing geomorphological features and differential sedimentary representations across the type-site rendered this projection uncertain. A confident stratigraphic placement of ETH-72-8B consequently required independent $^{40}Ar/^{39}Ar$ geochronology on datable separates sampled from directly above the occupation horizon represented by ETH-72-8B (Fig. 4.1). Tephra sample I collected from this unit was given a field ID of *Unit 10_TB'*.

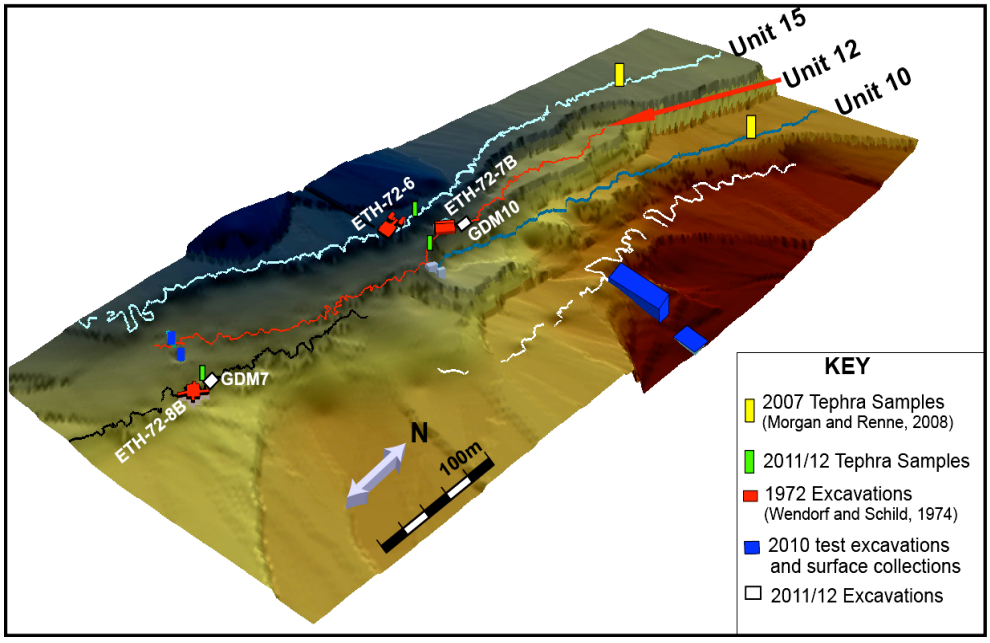

Figure 4.1 A digital terrain model of the Gademotta type area showing major excavations and tephra sampling localities

Analysis of the Unit 10_TB' sample yielded an inverse isochron age of 275 ± 6 ka (Fig. 4.2a, b; Appendix-2). This result is analytically indistinguishable from previous results (i.e. 276 ± 4 ka; now recalculated using Renne *et al*.'s [2011] decay constants and age standards to 279 ± 2 ka) for sample from Unit 10 (Morgan & Renne 2008). This reaffirms the age of the underlying sites of ETH-72-8B and GDM7 as 279 ± 2 ka. As reported in Sahle *et al*. (2013), ages for this oldest MSA occupation in the Gademotta Fm. do account for excess ^{40}Ar that was trapped in sanidine crystals upon eruption, which has been assessed through the isochron method (Fig. 4.2a, b; Appendix-2). This makes the occupation horizon at ETH-72-8B the world's oldest currently-known MSA occupation. Until now, an age of 287 ± 12 ka* for cultural horizons in the Kapthurin Fm. in Kenya has been widely cited as the oldest date for an MSA occurrence (Deino & McBrearty 2002). The application of similar isochron methods to the analysis of the Kapthurin samples shifts the age of 287 ± 12 ka* (Deino & McBrearty 2002) to 282 ± 20 ka*, making it substantially less precise than the age for the oldest MSA at Gademotta.

The presence of a cemented ash layer in the uppermost parts of the Unit 12 bedded sandstone (Fig. 2.1) was reported in previous work (Wendorf & Schild 1974: fig 7). These tephra deposits occur in the form of localized bedded pumice pebbles directly overlain by a thin layer of fine ash sediments. ^{40}Ar/^{39}Ar analysis was conducted on samples I collected from the fine ash (Sample Unit12_T1s1) as well as pumice pebble deposits

(Sample Unit12_T1s2). These yielded analytically indistinguishable isochron ages of 270 ± 10 ka (for T1s1) and 252 ± 11 ka (for T1s2) (Fig. 4.2c, d; Appendix-2). As these dates are analytically indistinguishable, and since the samples come from the same sub-unit, a combined analysis was conducted. This yielded an isochron age of 260 ± 7 ka as the age of the top layer of Unit 12 (Fig. 4.2c, d; Appendix-2).

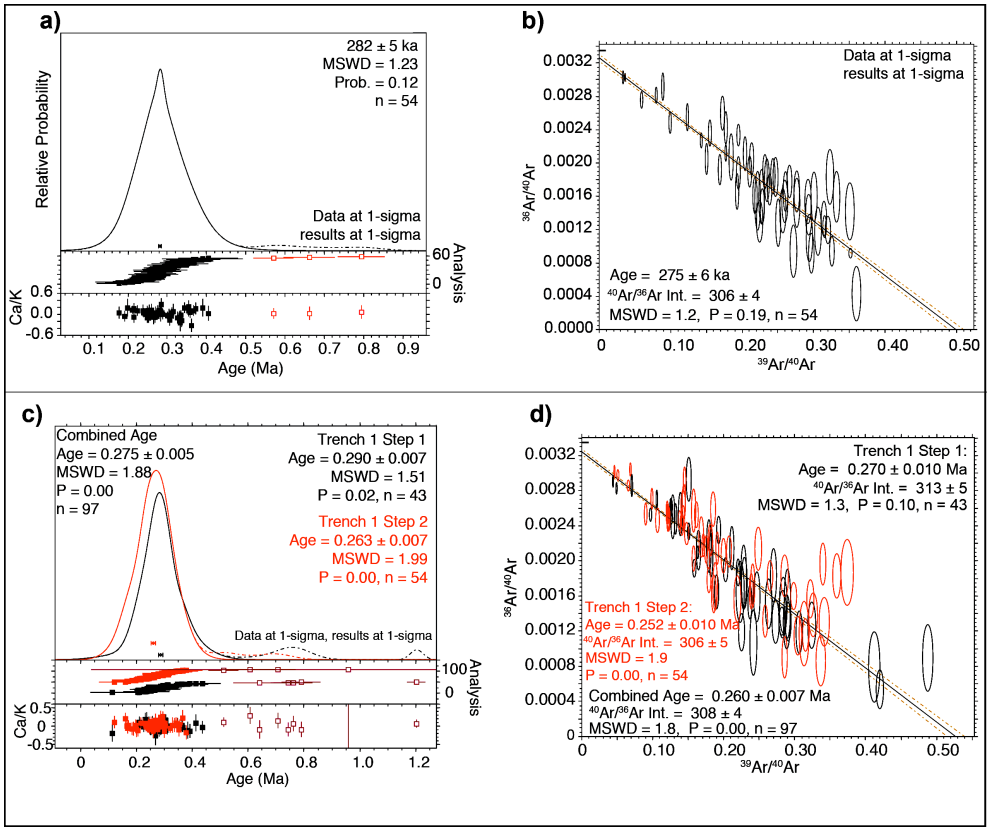

Figure 4.2 Graphs of relative probability and inverse isochron of single crystal total fusion analyses for sanidines for (a, b) sample Unit 10_TB', (c,d) combined results from samples T1s1, and T1s2 (in red). Xenocrysts are shown in pink on the relative probability graphs (and are excluded from age calculations); they are not included on the inverse isochron graphs

Recent geochemical analysis has identified that the uppermost tephra bed in the Gademotta Fm. (Unit 15) correlates with the 105 ± 1 ka* Aliyo Tuff in the Kibish Fm. (F. Brown *et al*. 2012; Fig. 2.1, 4.1). Work is currently in progress to obtain direct and precise age constraints on Unit 15. A confident age attribution for this unit would provide a more secure minimum age estimate for occupation horizons represented by sites ETH-72-6 and 72-9 within the Gademotta Fm. (Wendorf & Schild 1974; Laury & Albritton 1975).

The stratigraphic aspects of this research focused on comparing the sequence near site ETH-72-8B with that farther north near where a previous study developed the type section for the Gademotta area (Laury & Albritton 1975; Wendorf & Schild 1974). As mentioned earlier, the absence of a conspicuously outcropping Unit 10 ash layer south of a geomorphological feature described as Cut XII by Laury and Albritton (1975; Fig. 4.3) and the presence of differential sediment thickness/representation have complicated the interpretation of Gademotta sequence. Two major step-trenches, 1m wide and several meters high, were excavated into Units 9 through 12. Trench 1 was excavated into the portion of the type-site north of Cut XII where the Unit 10 and 12 ash beds are easily identifiable; Trench 2 was excavated south of Cut XII, closer to site ETH-72-8B (Fig. 4.3).

As illustrated in the sections in Figure 4.3, there are noticeable differences in the thickness and magnitude of representation of sediments between the two parts of the Gademotta area. Sediments are the thickest just

north of Cut XII and abruptly thin out to the south (Fig. 4.3). Although positively identified, the Unit 12 bedded sandstone is notably thinner where Trench 2 is as compared to Trench 1. Moreover, the bedded tuffaceous pumice pebbles and the thin, fine ash layer that mark the top of this unit in Trench 1 are totally absent in Trench 2. Paleosol units 9, 11 and 13 are all represented in both sections, albeit with different thicknesses. The ~60 cm-thick bedded ash of Unit 10 cannot be easily identified with the naked eye in Trench 2. At the top of Unit 9, where a Unit 10 equivalent sediment would be expected, a weathered sediment is deposited. The clay skins in this package of sediment make it hard to distinguish it from the underlying Unit 9 paleosol. However, abundant volcanic glasses can be easily identified in this sediment with the help of a hand lens. Further lab analyses of sediment samples collected from the different layers in the trenches prove that the sediment directly above the Unit 9 paleosol contains rich volcanic material and is different from the Unit 9 clayey soil and ashy colluvium sediments.

Using the data from the new geochronological analyses and from the stratigraphic studies detailed above, a revised chrono-stratigraphic framework is provided in Figure 4.4. The earlier units of the Gademotta Fm (i.e. Units 1 through 8) are laterally discontinuous as they filled an irregular surface (Laury & Albritton 1975: 1003-1004). This has been noted in the Gademotta area where the Unit 9 paleosol near site ETH-72-8B rests directly on the Kulkuletti volcanics (*see also the section for Trench 2 in*

Fig. 4.3). Starting from the Unit 9 paleosol, all sediments are represented in both the Gademotta and Kulkuletti areas (Fig. 2.1), albeit in various degrees of prominence. The upper part of Unit 9 in the Gademotta area contains a rich cultural horizon represented by ETH-72-8B. In contrast, no cultural horizon has been identified in Unit 9 at Kulkuletti (Laury & Albritton 1975). Unit 10 was deposited across the region and can be physically traced between Gademotta and Kulkuletti. However, for the few hundred meters south of Cut XII (Fig. 4.3) this unit does not represent a prominent ash bed as it does elsewhere in the Gademotta and Kulkuletti areas. Field observations and lab analyses confirm that despite its inconspicuous occurrence, the Unit 10 ash does overlie Unit 9 in the locality near site ETH-72-8B (Fig. 4.3, 4.4). This has been confirmed by independent geochronological analysis on a sample from directly above the archaeological horizon at ETH-72-8B.

The bedded sandstone of Unit 12 is laterally continuous both in the Gademotta and Kulkuletti areas (Fig. 4.3, 4.4). In the area between site ETH-72-7B and Cut XII, in the Gademotta area, this unit contains pumice and ash sediments. In the Kulkuletti area, this unit is partly cut and filled by sediments that contain a lapilli ash named Unit D (Fig. 2.1). The cut and fill process at Kulkuletti took place once Unit 11 and Unit 12 were deposited (Laury & Albritton 1975). As a result, the recent age of 185 ± 5 ka* for Unit D (Morgan & Renne 2008) provided the minimum age for sites ETH-72-7B and 72-1, which are excavated into the upper part of the Unit 11

paleosol at Gademotta and Kulkuletti, respectively. The new combined isochron age of 260 ± 7 ka reported here for the upper part of Unit 12 now provides a better minimum age for these cultural horizons in Unit 11 (Fig. 4.4).

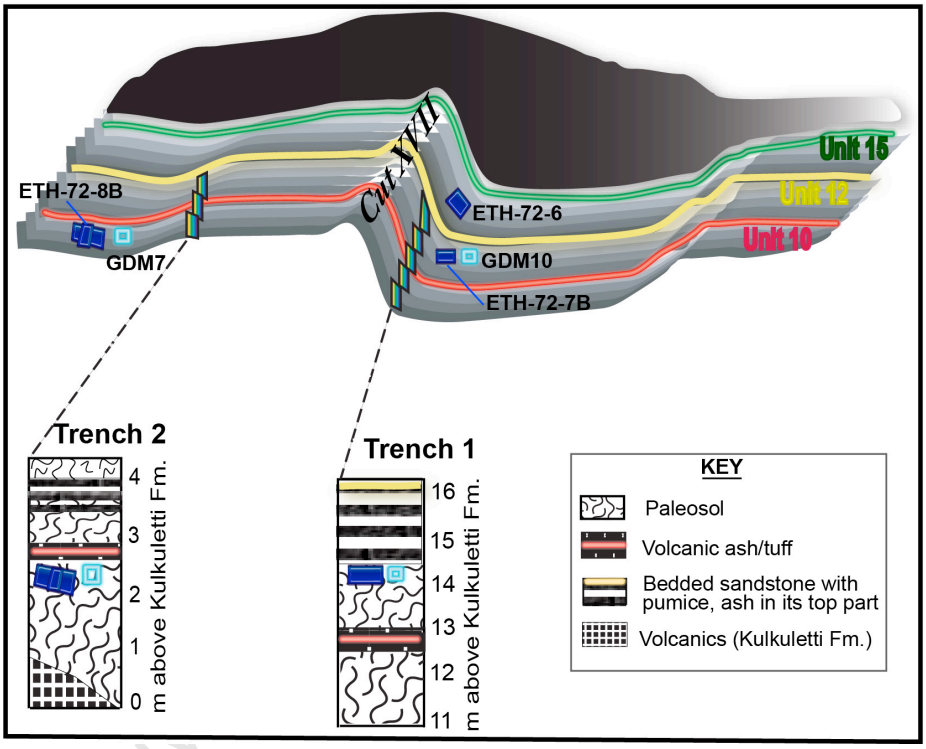

Figure 4.3 A schematic representation of the Gademotta type-site showing major geological trenches and sequences

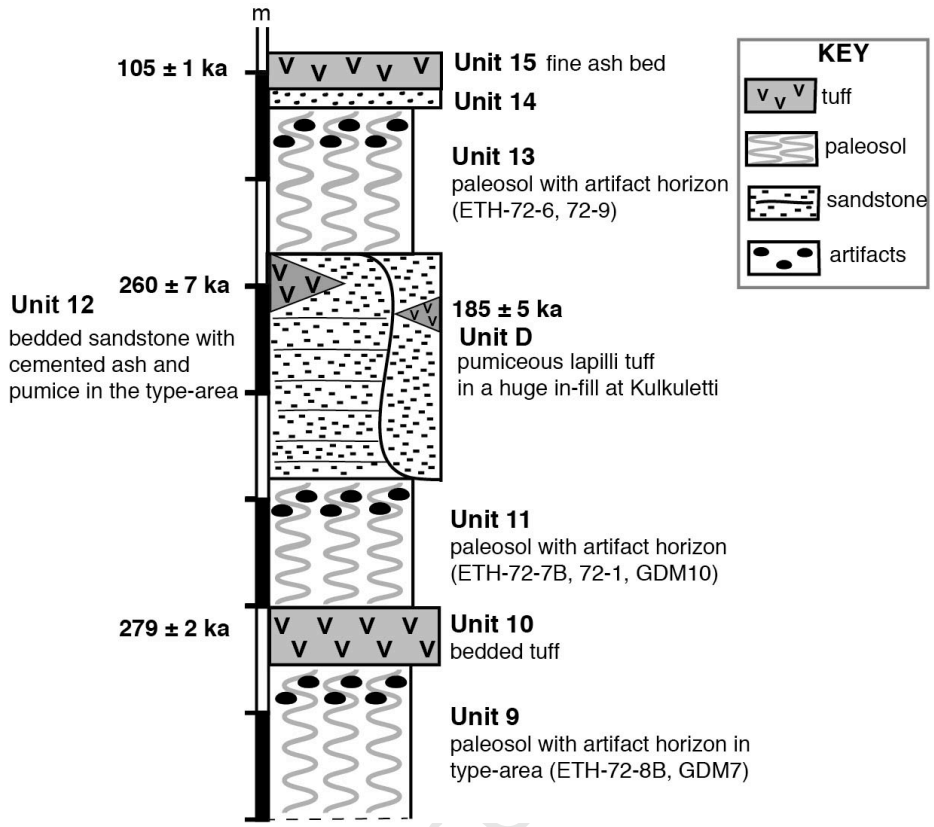

Figure 4.4 A composite, revised stratigraphy of the Gademotta Fm. Thickness of deposits is based on observations of the type section; the cut-and-fill in Unit 12 is projected from the section of the Kulkuletti area (*cf.* Fig. 2.1)

4.2 Renewed excavations and analyses in the Gademotta type area

Following the confident identification of the actual locations of previously excavated major sites in the Gademotta area, excavations were made in selected localities. Major excavations included GDM7 and GDM 10, excavated adjacent to sites ETH-72-8B and 72-7B, respectively (Wendorf & Schild 1974; Fig. 4.1, 4.3).

4.2.1 GDM7

GDM7 represents a 3 x 3m excavation adjoining, within less than a meter, the northwestern limits of ETH-72-8B (Fig. 4.1). This excavation was designed to recover an additional artifact assemblage using modern excavation techniques where stratigraphic details and artifact distribution patterns would be better documented (*cf.* Wendorf & Schild 1974). GDM7 recovered a total of 4,909 artifacts (Table 4.1). The artifact-rich level is confined to a 20-30cm fine colluvium horizon at the base of this 70cm-deep excavation (Fig. 4.5).

The non-debris (*see* Appendix-1 *for a definition of debris*) assemblage from GDM7 is dominated by debitage but also includes retouched tools – such as formal scrapers as well as unifacial and bifacial points (Table 4.1). Moreover, the Levallois technique is well represented (Fig 4.6). Blade production is exhibited in both the debitage as well as tool categories. Core types are generally similar to those documented for ETH-72-8B (Table 4.1). On average, GDM7 cores exhibit 4.90 flake scars and 2.35 removal surfaces. The average extent of retouch for the retouched tools is about 60% (i.e., 5/8th on an eight-point polar coordinate [Appendix-1]). 58.5% of tools in the GDM7 assemblage have more than half of their circumferences retouched. Of these, nearly 17% are wholly retouched. Table 4.3 provides a summary of artifact dimensions within each major category.

A comparison of flake surface area-to-thickness ratio (FSA/T) in whole flakes *versus* that in retouched tools within a given assemblages has

been suggested as an additional tool for measuring the amount of reduction a given tool has experienced as a result of attrition from use as well as resharpening retouch (Shea 2008: 447). Flake surface area is calculated as the product of the technological length and midpoint width of a flake. The quotient of this value and the midpoint thickness of a flake provides an estimate of the amount of cutting edge a flake contains (Dibble 1997; Davis & Shea 1998). (A detailed discussion of this concept is presented in Chapter Six).

Whole flakes in the GDM7 assemblage (*n=54*) yield a mean FSA/T value of 150.52 while for retouched tools (*n=159*) this is 135.75 (Table 4.3). The difference between these values is 14.77. Taking the FSA/T value as the amount of potential utility presented by the GDM7 whole flakes, one can obtain a quick estimate, from the difference in FSA-to-T ratios, of the amount of utility actually extracted from these assemblages. Retouched tools were, of course, produced from whole flakes. Assuming that these retouched tools entered the archaeological record when deemed exhausted, it appears that the utility extracted from the GDM7 tools is relatively small (*cf.*, Shea 2008: 447). The result, therefore, can be used to infer the presence of low degrees of curation. More robust approaches to inferring the realized utility of a retouched tool require knowledge of the original dimension of the actual tools. In ethnographic contexts, this can be directly measured (Sahle *et al*. 2012; Shott & Weedman 2007). In the archaeological record, original tool dimensions must be inferred from the platform (*e.g.*, Dibble

1995; Shott *et al*. 2000), and/or other morphometric attributes of the exhausted piece (*e.g.*, Kuhn 1992; Clarkson 2002; Eren *et al*. 2005). Unfortunately, the morphometric approaches (i.e. geometric/volumetric indices) are usually applicable to certain tool forms, mostly unifacial end scrapers. These tool forms are very rare in the GDM7 assemblages. In addition, less than half of the GDM7 retouched tool assemblage retain their platforms (Table 4.3).

Raw material exploitation at GDM7 proves to be by and large dominated by obsidian, which accounts for 95.6 % of the non-debris assemblage (Table 4.1). This clearly pertains to the availability of this high-quality silicate rock at the Worja source, near Kulkuletti (Vogel *et al.* 2006; Negash *et al*. 2010). Rhyolite, which is more ubiquitously available at the base of gulleys near the site, represents the other raw material type exploited at GDM7, accounting for *ca.* 2.4% of the total non-debris assemblages. Other volcanics account for only about 2% of the total non-debris assemblages (Table 4.1).

Cortical pieces in the GDM7 assemblage account for around 10% of the total assemblage. Out of the non-debris assemblages, around 32% retain cortex in various percentages. The most frequent cortex percentage both in the debris and non-debris assemblages is 31 to 50% (Appendix-1). Initial cortical flakes (>50% cortex) account only for about 4.6% of the debitage classes. However, judging from the abundance of debris and a relatively higher percentage of cortical pieces within the non-debris assemblage, it can

be concluded that there was initial core preparation activity at GDM7. This pattern is not surprising as the raw material source is only about 2.5 km away from the site.

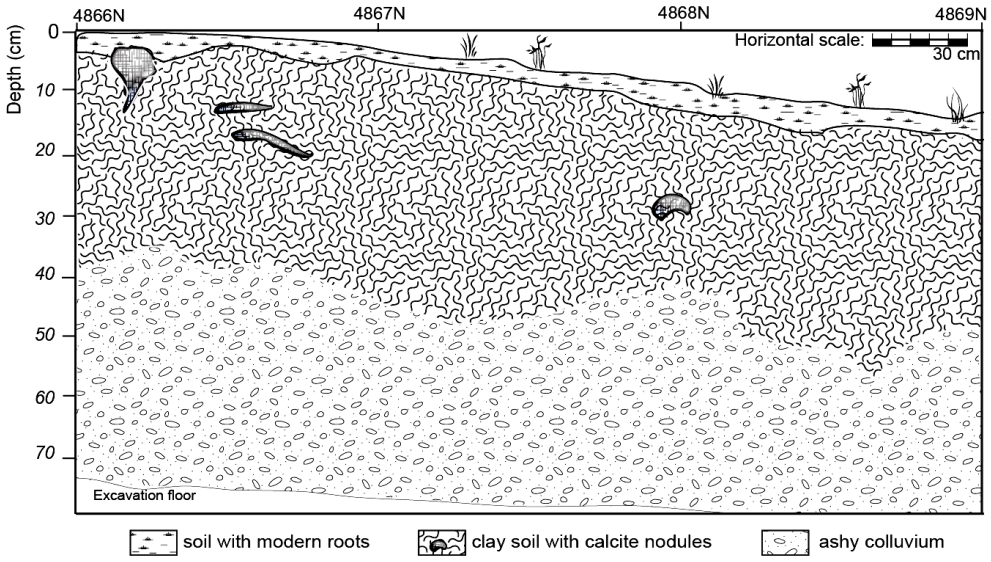

Figure 4.5 Stratigraphic profile of the western wall of the GDM7 excavation

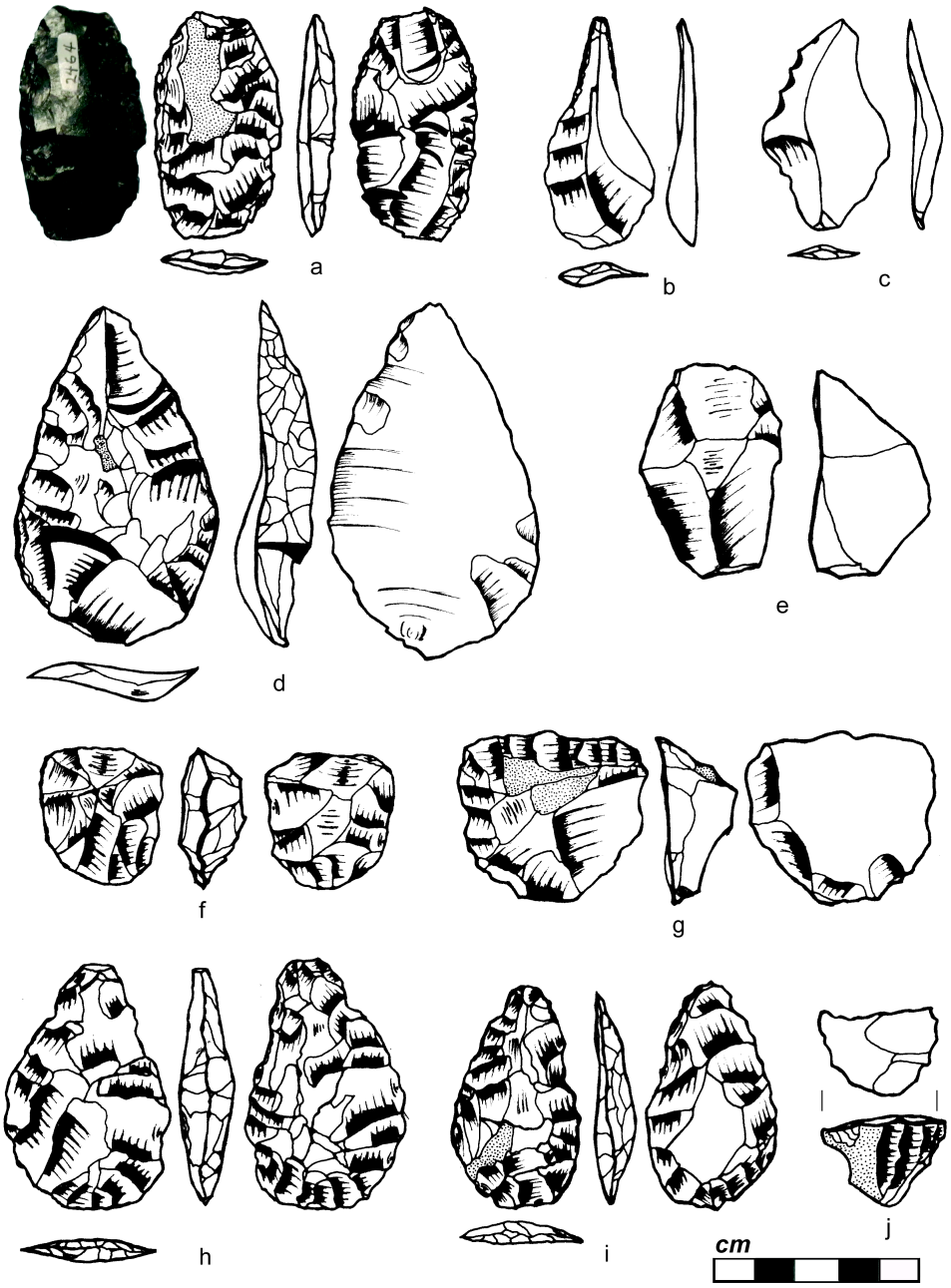

Figure 4.6 Illustrations of selected artifacts from GDM7 [(a) bifacial point with fluted impact fractures on both proximal and distal tips, (b) awl, (c) denticulate, (d) unifacial foliate point with burin-like fracture on the disto-lateral tip, (e) single platform core, (f) discoidal core, (g) Levallois core], and GDM10 [(h) bifacial foliate point, (i) bifacial Levallois point, (j) prismatic bladelet core]. Artifact 'e' is made on rhyolite; all the rest are on obsidian

Table 4.1 GDM7 assemblage typology and raw material use

Typology	Count	% without debris	Raw material		
			Obsidian	Rhyolite	Other
CORE					
Bifacial chopper	1	0.09	-	-	1
Discoid/Partial discoid	6	0.56	6	-	-
Core scraper	3	0.28	1	1	1
Levallois core	3	0.28	3	-	-
Core on flake	19	1.77	17	2	-
Core fragment	12	1.12	11	1	-
Other core	16	1.49	12	2	2
Subtotal	***60***	***5.59***	***50***	***6***	***4***
RETOUCHED TOOL					
Point/triangular flake					
unifacial	15	1.4	15	-	-
bifacial	18	1.68	18	-	-
Scraper				-	-
side	41	3.82	41	-	-
convergent	21	1.96	21	-	-
transverse	26	2.42	26	-	-
double	26	2.42	26	-	-
Awl/borer	2	0.19	2	-	-
Denticulate	2	0.19	2	-	-
Other retouched tool	8	0.75	8	-	-
Subtotal	***159***	***15.58***	***159***	***0***	***0***
DEBITAGE					
Cobble fragment	4	0.37	3	-	1
Initial cortical flake	39	3.64	37	1	1
Residual cortical flake	114	10.63	110	4	-
Levallois flake	72	6.72	71	-	1
Levallois blade	15	1.4	15	-	-
Pseudo-Levallois point	4	0.37	4	-	-
Prismatic blade	23	2.14	19	4	-
Core-trimming element	95	8.86	95	-	-
Biface-thinning flake	42	3.92	41	-	1
Kombewa	12	1.12	11	1	-
Angular fragment	93	8.67	89	2	2
Non-cortical flake	275	25.65	274	-	1
Split flake	13	1.21	13	-	-
Snapped flake	51	4.76	51	-	-
Subtotal	***852***	***79.47***	***833***	***12***	***7***
DEBRIS	***3837***		***3581***	***256***	***-***
HAMMERSTONE	***1***	***0.09***	***-***	***1***	***-***
Grand Total	**4909**	**100**	***4623****[94.1%]*	***275****[5.6 %]*	***11****[0.22 %]*

4.2.2 GDM10

Excavation at GDM10 covered a 2 x 3m area and extended ETH-72-7B northwards (Fig. 4.1). As in GDM7, this excavation was designed to recover assemblages from a previously documented archaeological horizon (*cf*. Wendorf & Schild 1974: 103). GDM10 was excavated into the resistant ledge formed by the bedded-sandstone layers of Unit 12 and the Unit 11 paleosol, which overlie the Unit 10 bedded tuff (Fig. 4.3, 4.4). The GDM10 excavation results in a total of 1,790 artifacts (Table 4.2). The artifact horizon is found in the upper parts of the Unit 11 paleosol. A few artifacts are also recovered from the lower layers of Unit 12; these are, however, indicated to have been probably reworked into this unit from the underlying Unit 11 (Laury & Albritton 1975). The highest concentration of artifacts is in levels "*h*" and "*i*" (i.e., 50cm to 70cm below the Unit 12-Unit 11 contact) (Fig. 4.7).

The GDM10, non-debris assemblage is dominated by debitage, followed by a large number of retouched tools (*cf*. Table 4.1; Shea 2008). About half of the cores are partial discoids while the Levallois technique is represented by a single core. There is one single-platform pyramidal core that appears very similar to the bladelet cores noted from much younger sites elsewhere (Fig. 4.5j; *cf*. Gossa *et al.* 2012: fig. 4).

GDM10 cores exhibit an average of 7.5 flake scars and 4.3 removal surfaces. The average extent of retouch for the retouched tools is 61% (i.e., 5/8th on the eight-point coordinate [Appendix-1]). About 76.3% of tools in

the GDM7 assemblage have more than half of their circumferences retouched. Of these, about 15.3 % are wholly retouched. Table 4.3 provides a summary of artifact dimensions per category.

FSA/T ratio for whole flakes and retouched tools in the GDM10 assemblage are 197.95 and 114.08, respectively (Table 4.3). The difference between these two values, at 83.87, further substantiates the high retouch intensity inferred above from the coordinate-based invasiveness measure.

Raw material use is almost entirely (>99.5%) limited to obsidian, the exception being 8 pieces of rhyolite debris (Table 4.2). About 22% of the total GDM10 assemblage retain cortical surface in various percentages. Within the non-debris assemblage, 23.5% of the artifacts have cortex. This probably has to do with the relatively more exhaustive flake utilization pattern observed from the relatively high retouch intensity and FSA/T ratio in the GDM10 assemblage.

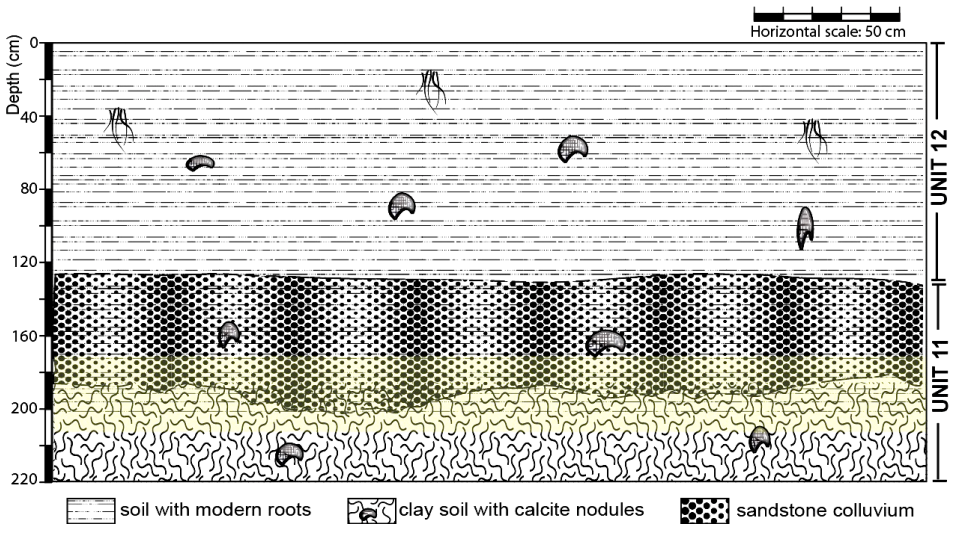

Figure 4.7 Stratigraphic profile of the western wall of the GDM10 excavation. Yellow shade represents the richest artifact horizon

Table 4.2 GDM10 assemblage typology and raw material type

Typology	Count	% with debris	Raw material		
			Obsidian	Rhyolite	Other
CORE					
Bifacial chopper	-	-	-	-	-
Discoid/Partial discoid	4	1.29	4	-	-
Core scraper	-	-	-	-	-
Levallois core	1	0.32	1	-	-
Core on flake	1	0.32	1	-	-
Core fragment	-	-	-	-	-
Other core	3	0.97	2	-	-
Subtotal	***9***	***2.9***	***8***	***0***	***0***
RETOUCHED TOOL					
Point/triangular flake					
unifacial	4	1.29	4	-	-
bifacial	6	1.94	6	-	-
Scraper					
side	20	6.45	20	-	-
convergent	5	1.61	5	-	-
transverse	5	1.61	5	-	-
double	12	3.87	12	-	-
Awl/borer	1	0.32	1	-	-
Denticulate	3	0.96	3	-	-
Notched	1	0.32	1	-	-
Other retouched tool	2	0.64	2	-	-
Subtotal	***59***	***19.03***	***59***	***0***	***0***
DEBITAGE					
Cobble fragment	-	-	-	-	-
Initial cortical flake	3	0.97	3	-	-
Residual cortical flake	6	1.94	6	-	-
Levallois flake	35	11.29	35	-	-
Levallois blade	6	1.94	6	-	-
Pseudo-Levallois point	-	-	-	-	-
Prismatic blade	27	8.71	27	-	-
Core-trimming element	53	17.1	53	-	-
Biface-thinning flake	21	6.77	21	-	-
Kombewa	2	0.64	2	-	-
Angular fragment	23	7.42	23	-	-
Non-cortical flake	36	11.6	36	-	-
Split flake	2	0.64	2	-	-
Snapped flake	28	9.03	28	-	-
Subtotal	***242***	***78.05***	***242***	***0***	***0***
DEBRIS	***1481***		***1473***	***8***	***0***
HAMMERSTONE	***-***	***-***	***-***	***-***	***-***
Grand Total	**1791**	**100**	***1782****[99.5 %]*	***8****[0.5%]*	***0***

Table 4.3 Summary statistics of dimensions (mm) of cores, whole flakes and retouched tools from GDM7 and GDM10

Artifact category + Statistics	Length	Width	Thickness	SP* Width	SP Thickness
GDM7					
CORE (*n*=60)					
Mean	46.05	33.7	18.46		
StDev†	11.12	9.97	8.07		
Range	49.37	42.49	42.99		
WHOLE FLAKE (*n*=54)					
Mean	44.86	29.15	8.83	19.12	7.81
StDev	10.15	8.42	2.59	7.7	4.81
Range	39.78	40.56	11.85	32.37	33.86
RETOUCHED TOOL‡ (*n*=159)					
Mean	40.01	28.23	8.86	18.79	7.36
StDev	12.96	9.46	3.32	7.59	3.12
Range	81.62	58.64	19.22	32.65	14.88
GDM10					
CORE (*n*=8)					
Mean	34.63	29.53	10.62		
StDev	7.12	11.02	3.48		
Range	23.47	37.55	10.75		
WHOLE FLAKE (*n*=27)					
Mean	41.3	28.23	6.92	19.12	7.81
StDev	10.63	8.52	3.79	7.7	4.81
Range	48.88	32.19	18.35	39.44	9.17
RETOUCHED TOOL (*n*=59)					
Mean	33.09	21.96	6.71	14.38	5.44
StDev	13.29	7.55	2.78	7.55	2.39
Range	58.28	32.25	10.23	29.5	10.81

*Striking platform; †Standard deviation; ‡Platform dimensions collected on only 73 (~46%) of the GDM7 and 22 (~37%) of the GDM10 retouched tools.

4.3 Inter-assemblage comparisons

Detailed typological and functional analyses from previous studies on assemblages from ETH-72-8B, 72-7B and other sites within the Gademotta Fm. have contributed enormously to our knowledge of early MSA technological behavior (Wendorf & Schild 1974, 1993). These analyses document that assemblages from the earliest MSA occupations display remarkable typological variability. Also, little change was noted in terms of the technological repertoire of inhabitants of ETH-72-8B and those of younger sites within the Fm., namely ETH-72-7B and 72-1 (Wendorf & Schild 1974: 154). Analysis of the GDM7 and GDM10 assemblages confirm that the archaeological horizons represented by ETH-72-8B and 72-7B do not show marked differences in terms of typological representation of artifacts as well as technological strategies.

The most important aspect of this current research is that new dates reported here for Unit 12 now provide tighter constraints for these younger occupations, showing that the minimum difference in age between the occupations at ETH-72-8B/GDM7 and ETH-72-7B/GDM10 is much smaller than previously established – a mere 19 ± ka rather than ~100 ka (*cf.* Wendorf *et al*. 1975; Morgan & Renne 2008). As a result the lack of major technological difference between these two assemblages is less notable; it might be expected that they would share substantial aspects of the technological repertoire.

Raw material exploitation patterns noted at the previously excavated

sites of ETH-72-8B and 72-7B as well as at GDM10 stand in some contrast to those evident at GDM7 where even certain non-debris pieces were made on rhyolite. The selection of obsidian over rhyolite by inhabitants of the occupation at GDM7/ETH-72-8B is clearly the result of several superior qualities of the former (ease/control in knapping, sharpness of edge, etc). However, the exploitation of rhyolite witnessed in the GDM7 assemblage remains intriguing. What factors led to the occasional choice of this relatively poor-quality material over obsidian? At this stage, no pattern can be discerned from the rhyolite formal tools. As a result it is difficult to determine if rhyolite use is associated with specific functional and/or technological choices. The difference in raw material exploitation patterns between GDM7 and the younger sites of ETH-72-7B and GDM10 does not appear to be substantial enough to talk of a temporal trend toward an exclusive use of obsidian by hominins in the later periods.

Certain techno-typological assumptions made previously about specific tool production techniques in the Gademotta MSA prove to be weakly supported. For instance, the presence of burin-like scars on a large proportion of pointed pieces has raised some interest and required further investigation. Two features have been used to argue that these burin-like fractures are the result of an intentional technique of cutting edge rejuvination – the *tranchet blow*. Firstly, previous research noted these pseudo-burin scars mostly on the right distolateral tips (dorsal face for unifacial points) of the pointed forms. Secondly, microwear patterns

indicative the use of these pieces as projectile tips could not be clearly documented. These led previous researchers to suggest that the burin-like fractures are the result of intentional burination and the points were probably used for cutting and/or scraping, rather than as projectile tips (Wendorf & Schild 1993; *see also* Douze 2010). The present study identified a number of pointed pieces with burin-like fractures on the left distolateral tips on the dorsal sides of unifacial points, both in the newly-recovered and previously collected Gademotta assemblages. In addition, even where burin-like fractures are present on the right-hand dorsal sides of pointed pieces, some of these points bear clear fracture patterns that suggest they were used in a longitudinal fashion (*e.g*, Fig. 4.8; *see also* Sahle *et al*. 2013). Also, intentional burination is distinguishable from impact burination in that the latter does not retain the bulb of force as it is produced from a bending fracture (Cotterell & Kamminga 1987).

A detailed discussion of the function of pointed pieces, with examples of pseudo-burin scars on the left distolateral tip of the dorsal side and associated microfracture data, from the Gademotta Fm. is provided in the next chapter. As it stands now, the small dimension of the burinated edges relative to the overall tool dimensions, and the otherwise mostly fully retouched circumference of most of the pointed pieces depicted to bear *tranchet blow* (*e.g.* Fig. 4.8, 4.5d) argue against the interpretation of these macrofracture as the result of attempts to produce a long cutting edge, such as those seen in long blade tools.

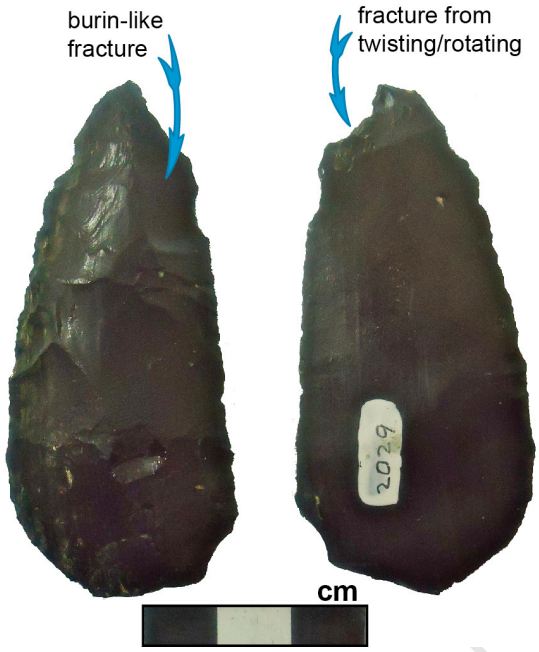

Figure 4.8 Pictures of a unifacial foliate point from GDM7 with a pseudo-burin scar on the dorsal face and a macrofracture typical of twisting/rotating of a thrust spear tip upon impact (*cf.* Rots *et al.* 2011)

As part of the objective of comparing occupations in the Middle- and Upper Pleistocene, a general reassessment of the ETH-72-6 assemblage was conducted. Data collected on whole flakes from this assemblage are discussed in Chapter Six. Here, a unique technological pattern noted during a reassessment of the ETH-72-6 assemblage will be highlighted. I have noted that some of the ETH-72-6 cores exhibit the typical Nubian Techno-complex whereby they are preferentially reduced to produce pointed flakes from laterally trimmed surfaces (Fig. 4.9). Personal communications with

Dr. Phillip Van Peer (June 8, 2012 Addis Ababa) collect opinion that these cores resemble ones from the Late Nubian Tradition. The fine lateral retouch on these cores are typical of the Late Nubian Tradition where the lateral remnant ridges are further used to produce elongated flakes/blades with inherent backing. The presence of these cores has a lot of implications to the inferred behavior of hominin populations in the Gademotta area as well as in the wider northeast African region.

The Nubian Techno-complex represents a regionally distinct variant of the preferential Levallois technique of manufacturing points and is unique to the broader northeastern African region (Van Peer 1992). In Ethiopia, this tradition has been reported from the K'one MSA site, only *ca*. 100 km northeast of Gademotta within the Main Ethiopian Rift (Kurashina 1978). The Nubian cores from ETH-72-6, and K'one, show additional features to the general attributes documented as typical of this northeast African techno-complex (Van Peer, *pers. comm*). There are no secure dates for the MSA at K'one (Williams *et al*. 1977). Based on regional chronology, an age estimate of 70-60 ka has been assigned to the K'one MSA (Kurashina 1978; Brandt 1986). The ages of ETH-72-6 and K'one broadly conform to the generally established temporal range for the Late Nubian Techno-complex – Marine Isotope Stage 5 (between ~128 ka and 74 ka) (Van Peer & Vermeersch 2007). Outside of the Nile Valley and the wider northeastern African and Horn of Africa regions, the Nubian tradition has been documented at Dhofar in Oman, suggesting the presence of intra-regional

cultural contacts and inter-regional population expansions (Rose *et al*. 2011). In addition, the presence of technological industries specific to a region is considered as one indicator of modern human behavior (McBrearty & Brooks 2000 *and references therein*).

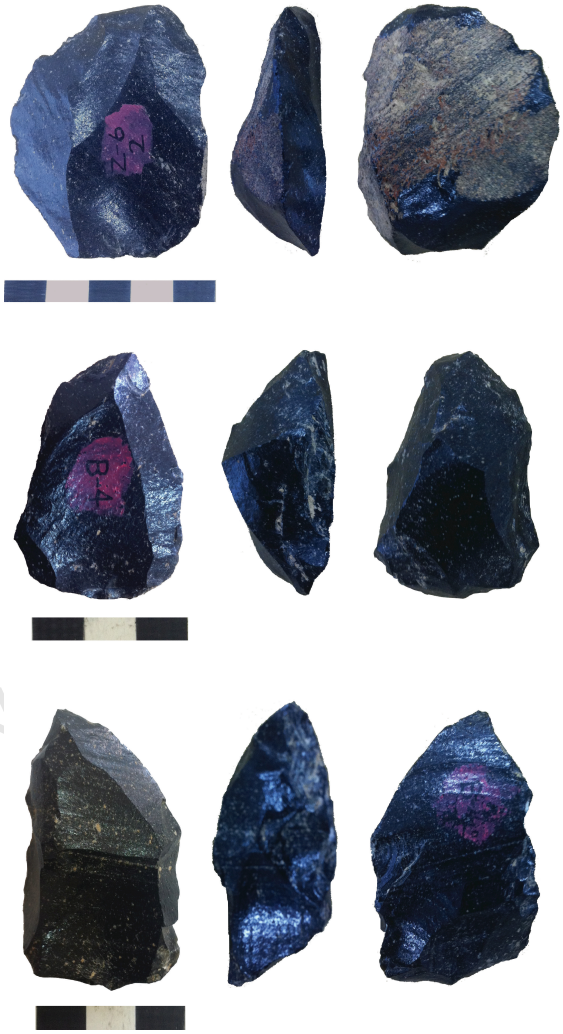

Figure 4.9 A sample of preferential Levallois cores from Site ETH-72-6 that exhibit the Nubian Type-1 preparation

4.4 Comparison of the spatial distribution and density of artifacts

Wendorf and Schild (1974: 81-84) suggested that a "roughly circular shallow concavity" at ETH-72-8B represented traces of a housing feature. They argue that the horizontal distribution of artifacts follows a concentric pattern with the highest clustering at the center of what they assumed was a "hut" (Wendorf & Schild 1974: 150-151).

Distinct use of space, such as for residential areas, has often been depicted as one marker of modern behavior (McBrearty & Brooks 2000). Since the behavioral implications of a housing structure at >279 ka will be intriguing, the present research tested this hypothesis forwarded by Wendorf and Schild (1974: 150-151). If the observed artifact distribution pattern at ETH-72-8B and its conformity with a shallow depression at the center of this excavation indeed represents a housing structure, then it is expected that an excavation adjoining ETH-72-8B will yield artifact densities comparable with the margins of ETH-72-8B. If, on the contrary, artifact density from an excavation adjoining ETH-72-8B is comparable with, or greater than, that reported for the center of ETH-72-8B, then the hypothesis that the presence of the concavity and artifact distribution patterns are indicative of a housing structure can be rejected.

A detailed comparison of artifact distribution patterns at ETH-72-8B with the GDM7 excavation is not possible as there are no published data on the vertical distribution of artifacts recovered from the former site. Artifact density at ETH-72-8B is rather represented by a 2D scatter diagram

(Wendorf & Schild 1974: fig. 25). The plotting of a similar scatter diagram for the GDM7 excavation meant superimposing distributions from multiple excavation levels. Even this yielded a spatial distribution pattern that exhibits the highest concentrations at the northern edge of the concentric circles originally identified by Wendorf and Schild (1974; Fig. 4.10a). As a result the data from GDM7 run counter to what would be predicted if there were a housing feature in the center of the ETH-72-8B excavation. Although situated outside of the artifact distribution circles, the concentration of artifacts at GDM7 is comparable with the innermost concentric circle of the hypothesized artifact concentration zone at ETH-72-8B (Fig. 4.10; Wendorf & Schild 1974: fig. 25).

More simplistic figures of non-debris artifact classes per square meter prove to be higher for GDM7 (122 artifacts/sq m) than for ETH-72-8B (57.78 artifacts/sq m) (Wendorf & Schild 1974: table 1). Also, several other factors, (*see* Sahle & Negash 2010; Sahle *et al*. 2012 *for insights from ethnographic cases*), seem to have been underestimated in the explanation provided for residential and activity area choice (Wendorf & Schild 1974: 150-151). The artifact distribution data, both horizontal and vertical (Fig. 4.10), collected during the present research suggest that the occupation horizon at ETH-72-8B and GDM7 was more laterally extensive than previously depicted. The hypothesis that the excavation at ETH-72-8B represents a hut feature with a high concentration of artifacts at its center is, therefore, not supported by the GDM7 excavation (Sahle *et al*. 2011).

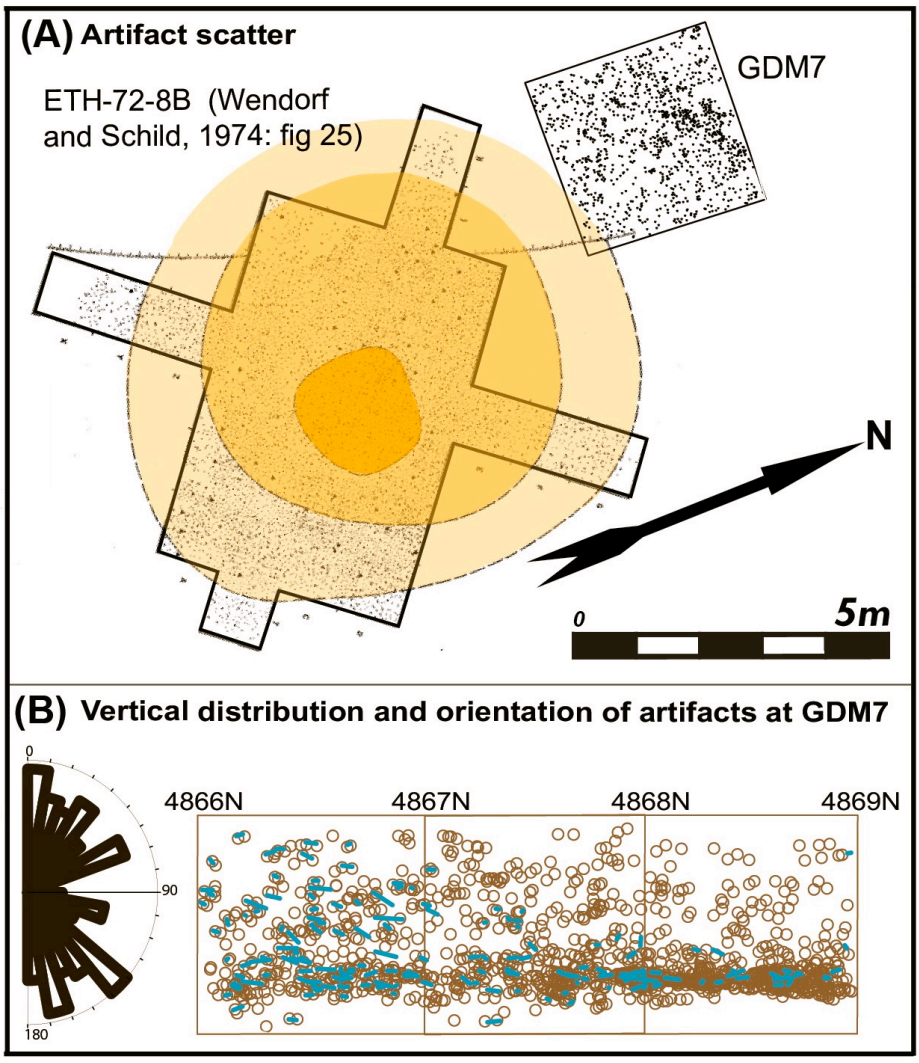

Figure 4.10 Comparisons of artifact distribution patterns of ETH-72-8B and GDM7. Contour intervals in 'A' show concavity while each black dot represents an artifact; turquoise lines in 'B' represent specimens with orientation (Note the correction on the north arrow [*cf.* Wendorf & Schild 1974: fig. 25])

4.5 Summary and Discussion

Previous research in the Gademotta Fm. has provided invaluable behavioral and contextual data on MSA occupations (Wendorf & Schild 1974, 1993; Wendorf *et al*. 1975, 1994; Laury & Albritton 1975). Other important questions this earlier study did not address had to wait for the next four decades until the present renewed research was initiated. This recent round of research was partly encouraged by results of new geochronological analyses (Morgan & Renne 2008). Research carried out for this dissertation has established the precise stratigraphic placement of later Middle Pleistocene occupations. Further excavations using modern data recovery techniques have enabled a finer-grained analysis of hominin technological behavior across this important period.

In spite of the presence of multiple tephra beds yielding radiometric dates, the stratigraphy in both the Gademotta and Kulkuletti areas has long presented a considerable degree of complexity (Brandt 1986). In addition to the marked difference in the thickness and representation of certain units across the site-complex, significant cut-and-fill processes at Kulkuletti have complicated the stratigraphic placement of excavated sites (Laury & Albritton 1975). The geochronological results reported here provide a more detailed and improved picture of the stratigraphy at both Gademotta and Kulkuletti. Through independent geochronological analyses, conducted in collaboration with a geochronology expert, it is now possible to confirm that ETH-72-8B is stratigraphically below the Unit 10 ash and is, therefore,

the world's oldest-dated MSA site (Sahle *et al*. 2013; *cf*. Deino & McBrearty 2002).

A new date obtained for Unit 12 provides a better minimum age for the occupation horizon sampled by ETH-72-7B/GDM10. Former stratigraphic correlations have estimated the age of this occupation to be similar to ETH-72-1 (Laury & Albritton 1975: table 1; Morgan & Renne 2008). The previous minimum age for these sites came from Unit D at Kulkuletti, dated recently at 185 ± 5 ka* (Morgan & Renne 2008). The cut-and-fill processes at Kulkuletti postdated the development of the Unit 11 paleosol as well as the deposition of the Unit 12 bedded sandstone layers (Laury & Albritton 1975: 1007). As a result, it can be securely concluded that all sites within the Unit 11 paleosol are not only older than Unit D but also older than Unit 12, hence >260 ± 7 ka (Fig. 4.3). This result also explains why there seems to be little discernable temporal trend in terms of technological variability between assemblages recovered from occupations within the Unit 11 paleosol (ETH-72-7B; 72-1) *versus* that marking the oldest MSA horizon (ETH-72-8B) (Wendorf & Schild 1974). Marked differences in terms of technological and/or typological attributes of assemblages from these occupations may not be expected considering the possibility of a short time window (19 ± 8 ka) that separates these later Middle Pleistocene sites.

Renewed archaeological research at Gademotta specifically focused on the type-site as it preserved, in contrast to the Kulkuletti area, an

exclusively MSA occupation horizon under the lowermost tephra bed of Unit 10. New excavations, conducted adjoining previously excavated important early MSA sites, recovered thousands of artifacts through state-of-the-art excavation techniques. Both GDM7 and GDM10, which were excavated into the cultural horizons previously sampled by ETH-72-8B and 72-7B, respectively, yielded assemblages that are in most respects similar to those recovered from the latter sites.

As a distinct feature of most sites in the Gademotta Fm., debitage and retouched tools make up a substantial portion of the non-debris assemblages at GDM7 and GDM10. Scrapers, blades, pointed tools, and the Levallois technique characterize the retouched tool components. Both in terms of their abundance and exclusiveness, the distinctly MSA assemblages of GDM7 and ETH-72-8B stand in sharp contrast to the pattern exhibited by sites in the Kapthurin Fm. (McBrearty & Tryon 2006; Tryon & McBrearty 2006). At such localities as Rorop Lingop and Koimilot in the Kapthurin Fm. elements of the MSA occur as part of the Acheulean tradition and are represented by cores and flakes that attest to the Levallois method and by unretouched pointed pieces (McBrearty & Tryon 2006). The geochronological analysis reported here now confirms the age of the Gademotta early MSA occupation represented by ETH-72-8B and GDM7 as >279 ka. While the pattern witnessed in the Kapthurin Fm. shows that the earliest MSA and the transition from the Acheulean was complex and time-transgressive, the Gademotta MSA at a similar, but more precise, minimum

age shows an exclusive occurrence of this tradition. What is represented at Gademotta is a comprehensive transition into the MSA. While inter-site difference in the timing and trajectories of this technological transition are clear (*cf.* Van Peer *et al*. 2003; Clark *et al*. 2003; Walter *et al*. 2000; Bruggemann *et al*. 2004; Tryon *et al*. 2008; Fig. 2.4) the pattern witnessed in the earliest MSA at Gademotta suggests that the MSA has even older roots and the transition into this tradition is even more complex and multi-directional than depicted thus far.

Better analyses of the technological behaviors of hominin population that inhabited the Gademotta area across the later Middle- and earlier Upper Pleistocene are conducted by assessing the capacity for projectile technology and comparing the cost/benefit in flake production between occupations >260 ka *versus* one that is <185 ka. GDM7 and GDM10 both represent occupations prior to 260 ka; an occupation from a much younger context (185-105 ka) in the Gademotta area is represented by ETH-72-6 (Wendorf & Schild 1974; Fig. 4.1, 4.3, 4.4). The ETH-72-6 assemblage is similar in several ways to those from the older contexts. The Levallois technique is represented well and retouched tools make up a good portion of the assemblage. Peculiar patterns of the assemblage from ETH-72-6 are the prominence of Levallois core preparation flakes and single platform bladelet components (Wendorf & Schild 1974: 107-117, table 1).

CHAPTER FIVE

5. AN ASSESSMENT OF POINTED ARTIFACTS FROM THE GADEMOTTA FM. FOR USE AS WEAPON TIPS

5.1 Introduction

The innovation of projectile weaponry represents a crucial turning point with far-reaching evolutionary advantages. Projectile weapons provided enhanced hunting efficiency though wider impact range, broader ecological niche, and reduced confrontation with dangerous prey species (Churchill 1993). Thus, they were a significant technological advance over thrusting spears (Wilkins *et al*. 2012). "Complex"/mechanically-assisted projectile weaponry, such as the bow and stone-tipped arrow, (*e.g.*, Shea & Sisk 2010; O'Connell 2006; Lombard & Phillipson 2010; Churchill 1993) are believed to have enabled *H. sapiens* to successfully spread within and out of Africa (Shea & Sisk 2010; *see also* Churchill 1993).

The earliest evidence for projectile weapon use has been suggested from Schöningen, Germany, where pointed wooden spears were recovered in association with "hunted" fauna from a context dating to *ca*. 400 ka (Thieme 1997). Whether these spears were actually thrown remains inconclusive and far from being readily accepted (Shea 2006; Schmitt *et al*. 2003). Long-range projectile weapons, namely the bow-and-arrow and the spearthrower-and-dart, are suggested to have originated among *H. sapiens* in Africa during the earlier Upper Pleistocene, sometime between 100 ka

and 50 ka (Shea 2006; Shea & Sisk 2010; Brooks *et al.* 2006; *but see* Villa & Lenoir 2006 *for opinion on whether the spearthrower-and-dart existed in the African Stone Age record*). These suggestions are based on approaches that use morphometric attributes and artifact weight thresholds as proxies for identifying pointed stones deemed ideal for use as the tips of certain types of projectile weapons. Microscopic approaches provide direct evidence of whether a pointed stone artifact was actually hafted. The identification of microscopic use-traces – such as edge damage/rounding, polish, striation, and organic residue – are shown to provide unique insights into a tool's hafting history and direction of use (Lombard 2011; Lombard & Phillipson 2010). However, these analyses, too, suffer similar inferential difficulties. Hafting traces do not show whether a certain pattern evident on a hafted point is necessarily indicative of projectile weapon use (*e.g.*, Lombard 2011; Rots *et al.* 2011; Rots 2012). Consequently, unequivocal identification of projectile technologies in the archaeological record remains difficult.

The identification and measurement of velocity-dependent microfracture features that are created on the artifact surface as a result of impact damage provide a non-subjective approach to assessing the presence, and even specific delivery mechanisms, of projectile weapons (Hutchings 1997, 2011). This approach studies microscopic fracture features most often identified on the surface of artifacts (Hutchings 2011). Unlike the other approaches to the identification of prehistoric hunting weapons, the

applicability of the impact-induced fracture velocity approach is, however, limited to fine-grained silicates, such as obsidian and chert/flint, which exhibit clear microfracture features. Moreover, the approach requires the establishment of physical properties of the raw material on which the artifacts under investigation are made (Hutchings 1999, 2011). Consequently, the application of this approach to the assessment of potential hunting weapons from Paleolithic records has been limited.

It has been demonstrated experimentally that the velocity-based microfracture approach can inform one on the specific delivery mechanisms of projectile weapons, i.e. thrust spears; javelins (i.e. hand-cast spears); arrows; and darts (Hutchings 2011). This attribution of weapon delivery mechanisms relies on the precursory loading rates of an artifact, which is in turn inferred from impact-induced microfracture features. Precursory loading rates have been determined experimentally and set as *quasi-static*, *rapid*, and *dynamic* on the basis of ranges recorded for various impact types and weapon delivery mechanisms (Hutchings 1997, 1999, 2011). However, the practical attribution of specific impact types to an artifact recovered from an archaeological context based solely on its instantaneous fracture velocity (C) values is virtually impossible. This is because of the equifinality that several possible impact types can produce values within the quasi-static and rapid loading rate regimes. As a result, this approach proves to work best for identifying darts and arrows, which are the only weapon delivery mechanisms that register fracture velocity values in the dynamic

loading range (Hutchings 2011: fig. 8; Fig. 5.1).

In the present study, different independent approaches to the identification of archaeological hunting weapons have been incorporated in order to avoid exclusive reliance on data from only one type of analysis and the limits of inference each of these approaches poses. Data have been, accordingly, collected from i) velocity-dependent microfracture features; ii) macrofracture patterns; iii) morphometric attributes of pointed pieces.

5.2 Analysis

For the present study, typological pointed pieces from 6 sites (ETH-72-8B, 72-7B, 72-1, 72-6, GDM7, and GDM10) were analyzed for the three independent lines of data mentioned above. A total of 141 pointed pieces were separated as possible hunting tools, from a larger assemblage of convergent pieces, mainly on the basis of morphological features. Microscopic analysis was conducted on all of these since even the smallest fragment of an artifact can document microfracture features (Hutchings 1997). Certain pointed artifacts from this selection had to be excluded from the other methods of analysis either because they were not suitable for specific morphological measurements or did not provide velocity-dependent microfracture data to encourage further analysis specifically using the macrofracture approach to edge damage patterns.

5.2.1 Analysis of velocity-dependent microfracture features

Velocity-dependent microfracture features are produced on fracture fronts of cryptocrystalline artifacts as a result of the perturbation of impact-induced crack force (Ravi-Chandar 2004). Fracture wings (FWs) are, for instance, created due to the interaction of the propagating crack force with intrinsic imperfections of the fracturing material. Using an electro-microscope and external light source, FWs were positively identified on 18 pointed artifacts from GDM7, ETH-72-8B, 72-7B, 72-6 and 72-1. Two of these points yielded FWs on additional crack fronts, hence enabling the documentation of a total of 20 relevant fracture feature loci (Table 5.1).

Fracture velocity measurements obtained from two of the 18 pieces (specimens ETH-72-7B_C2 and 72-8B_D1_12) were excluded from further analysis and interpretation. Fracture velocity data on the first piece was documented on a fresh fracture front, possibly resulting from sullegic and/or trephic factors, and produced the lowest *C* at 521 m/s. This could be attributed to damage from pressure contact, or very light percussion contact with a soft substance, such as a wooden drawer or table during handling and storage. This piece has, hence, been excluded from further investigations of projectile weaponry after concluding the fracture most plausibly resulted from post-collection damage. Fracture velocity on piece ETH-72-8B_D1_12 was documented on a fine fracture surface identical to several other contiguous fracture surfaces along the edges of the piece. The fracture surfaces associated with this piece are morphologically different from those

considered to be the result of impact from weapon use. For this reason, the FWs on this particular piece were regarded, without the need for further analysis, as produced by manufacturing/retouch rather than damage from weapon impact. The remaining 18 fracture velocity measures were obtained from fracture surfaces on 16 pieces and appear to be the result of damage from weapon impact.

Before discussing fracture velocity results from the Gademotta pointed pieces, it is necessary to provide more details on certain methodological issues due to the specialized application of this analysis. All of the angle of divergence measurements on the FWs collected by Dr. Hutchings were greater by ≥2º from those I collected independently. Dr. Braun carried out additional independent measurements on photomicrographs of Dr. Hutchings' and mine. Dr. Braun's measurements also yielded results that are lower than those of Dr. Hutchings' and very close to those of mine. Small discrepancies in measurement error are important to note because of the sensitivity of this measure to the resultant inference of behavior. A difference of 1º for measurements between 130º and 150º, for instance, increases the *C* value by an average 32.5 m/s. For a given hypothetical FW on a plane crack front with an angle of divergence of 140º, *C* will be:

= [Cos (140º/2)] * C_2 (i.e. 3995 m/s for the Worja obsidian)
= [Cos (70º)] * 3995 m/s
= 0.342 * 3995 m/s
= 1366.37 m/s.

If we change the angle measure to 138º, the result will become 1431.68 m/s.

Measurement variations are unavoidable in every science and have to do with a number of factors. In the particular case under discussion, such variations may be attributable to the resolution of photomicrographs, which is in turn governed by the light adjustment, perspective of the microscope lens, etc. However, the largest difference here seems to emanate from the observer's opinion of where exactly the arms of an FW are to be marked. Even intra-individual variation in the measurement of angle of divergence for an FW on a fracture surface of one of the Gademotta pieces, conducted by Dr. Hutchings, has been noted to account for a difference of up to 1.1º (i.e. a *C* value of 36 m/s).

While my personal opinion is that even the most conservative of angle of divergence measurements for the majority of the Gademotta pieces are substantially smaller than those collected on the same pieces by Dr. Hutchings, I have deliberately adopted his angle measurements for the present study due to the following reasons. First, the interpretation of *C* values collected on the Gademotta pointed pieces relies on loading rate thresholds and the correlation of these with particular impact delivery mechanisms set using experimental analysis where all angle measurements were collected by Hutchings (1997, 2011). As a result, the only way in which consistency in measurement can be assured is by adopting measures on the Gademotta pieces by the same individual. Second, where there are no methodological guidelines to constrain variations in the measurement of

angles of divergence from FWs, there are no grounds to argue which observation is a more accurate approximation of the actual divergence. Third, the highest angle of divergence measurements are associated with the lowest *C* values for a given pointed piece. Estimates that err on generous side therefore provide minimum values for impact velocity. Thus measures of impact velocity reported here represent the most conservative interpretation. Clearly, one is making substantial inferential leaps (*e.g.*, from FWs to *C*, and from *C* values to impact types and/or weapon delivery mechanisms) when extrapolating hunting behavior from fracture features. In this instance conservative measures are most prudent.

A summary of angular measurements and corresponding *C* values for every piece is presented in Table 5.1. Impact types and *C* values have been categorized into precursory loading-rate ranges set based on experimental work using the Glass Butte (Oregon, USA) obsidian. The Glass Butte material has nearly identical physical properties (*see* Hutchings, 2011: table 1) to that of the Worja obsidian used at Gademotta (Appendix-3). Figure 5.1 depicts *C* values for the Gademotta pieces plotted against impact types and associated precursory loading rate thresholds set using experimental work on the Glass Butte obsidian (*see also* Hutchings 2011: fig. 8, table 2).

Thirteen of the 18 *C* values collected on the Gademotta pointed pieces are in excess of those expected for thrusting spears, but are within the range of direct- and indirect-percussion, as well as javelin, arrow, and dart use. Four of the highest C values (i.e., those >1080 m/s) are attributable to a

more restricted range of fracture events; specifically, hard hammer percussion, javelin, arrow, and/or dart impact (Table 5.1; Fig. 5.1).

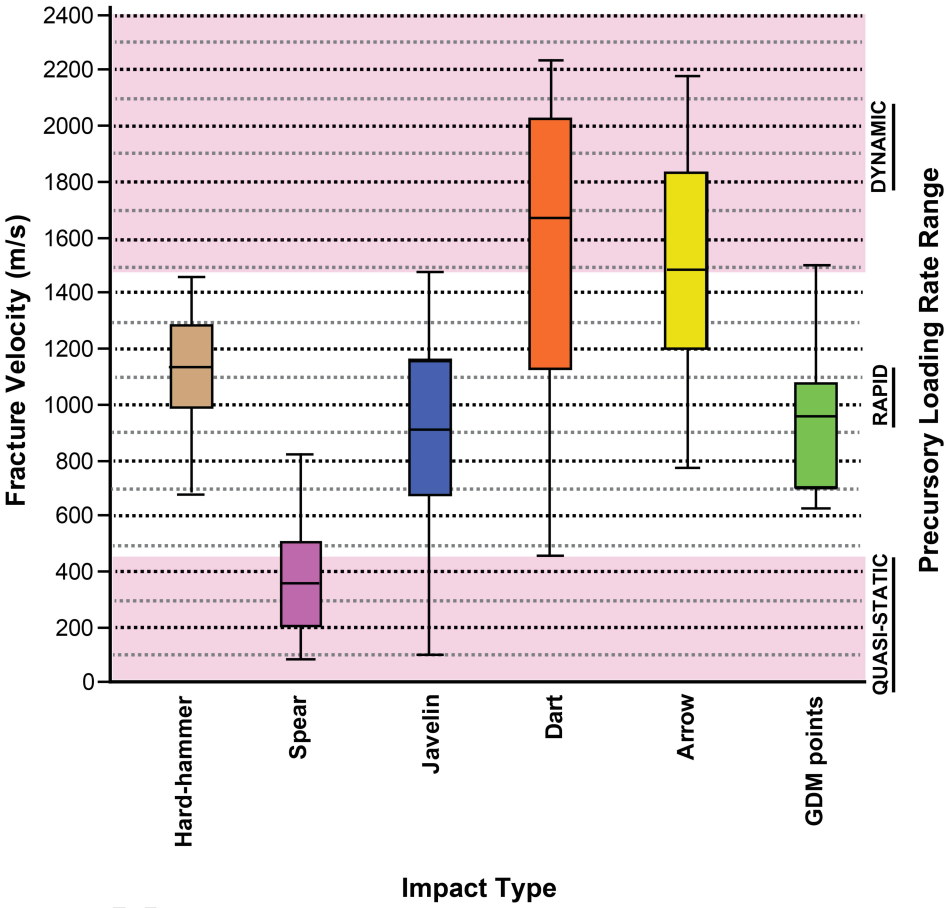

Figure 5.1 Reduction/impact types, corresponding *C* values, and loading rate ranges based on experimental work on obsidian raw material with a C_2 value of 3865 m/s. Raw *C* data for all experimental impact types obtained from Hutchings (1997; *pers. comm.*)

The velocity-based microfracture approach works through an exclusion of impact types that cannot explain the loading rate documented on a particular piece (Hutchings 2011: 1745). However, such exclusion based solely on *C* values (and their experimentally established impact/weapon delivery correlates) can only be used to identify pieces with dynamic loading rates (Fig. 5.1). The fracture velocity approach alone cannot provide conclusive evidence for the majority of loading rates (those in the quasi-static and rapid regimes). In the seminal work that introduced this approach to the identification of prehistoric weaponry, 35.8% of experimental darts and 46.7% of experimental arrows yielded *C* values within the rapid loading range (Hutchings 1997: table 13,14,18). These are indistinguishable from other impact types within the same loading rate range on the basis of their *C* values alone. Specimens recovered from an archaeological context can only be confidently identified as darts and arrows using this methodology if they register *C* values in the dynamic loading range.

For the present study, only one of the pieces, artifact ETH-72-8B_C6_3, yielded a *C* value in the dynamic range (at 1497 m/s). The other 17 readings record *C* values within the rapid range and are, on the basis of *C* data only, attributable to any of the overlapping correlative impact types (Table 5.1; Fig. 5.1). Therefore, for the majority of the Gademotta pointed pieces, a confident interpretation of the *C* data can only be attained through additional micro- and macroscopic analyses that aim to identify a specific

impact type by systematically ruling out other possible impact types with *C* values in the same loading rate regime.

In all but two of the 16 pieces the FWs are associated with fracture fronts on the tips of the artifacts (Fig. 5.2). The locations of these fracture features suggest that they were produced by impact from use of the tips of these pieces in a longitudinal fashion. It is very unlikely that impact from reduction processes would result in an almost universal placement of breakage at the tips of these pointed forms. Even on pieces documenting FWs on a fracture surface near their base, the possibility that the tips of these pieces were used in a longitudinal manner cannot be dismissed. It is possible for a piece to yield to an impact by way of medial/basal snapping from the resultant bending fracture (*e.g.*, Haynes 1980; Bergman & Newcomer 1983).

As reported elsewhere (Sahle *et al.* 2013), the interpretation of the fracture velocity data collected in collaboration with Dr. Hutchings proved largely inconclusive. Documentation of the precise location of the measured FWs on every piece was not considered very important when Dr. Hutchings examined the artifacts. This hindered a detailed analysis of the computed *C* values in relation to the location of impact-induced microfracture features. Results were consequently limited to certain inferences about the possible impacts that may have produced the measured *C* values (Sahle *et al*. 2013). As a result, in order to collect the additional details and more exhaustively examine if FWs are present elsewhere on the pieces other than where they

had already been documented, I conducted a subsequent, independent round of microscopic studies of these specimens.

All of the 16 pieces from which the 18 relevant fracture velocity data were collected were reanalyzed using the same instruments housed in the NME and following the same procedures. If microfracture features yielding the documented *C* values on the pieces were produced by percussive impact from a reduction process, then it is expected that there would be FWs in a range of locations on the pointed pieces. If these fractures indicate use as projectile weapon, we would expect damage concentrated on the tips and, less frequently, on transverse bending fractures along the medial-basal sections of a piece. If occurrence of the pertinent microfracture features is limited mostly to the tips of the tools, as noted during the earlier stage of the study, I will infer that the damage patterns are best attributed to impact from use of these tools in a longitudinal way, as weapon tips.

A thorough examination of the 16 pointed pieces documented the exact locations of every fracture feature from which data had been collected. In addition this re-analysis enabled me to collect a number of photomicrographs of these surfaces at different levels of magnification. The earlier stage of analysis focused exclusively on the tips and snapped surfaces of the pointed pieces. In contrast, the subsequent analysis investigated all edges of every piece at magnifications of 20 to 150x.

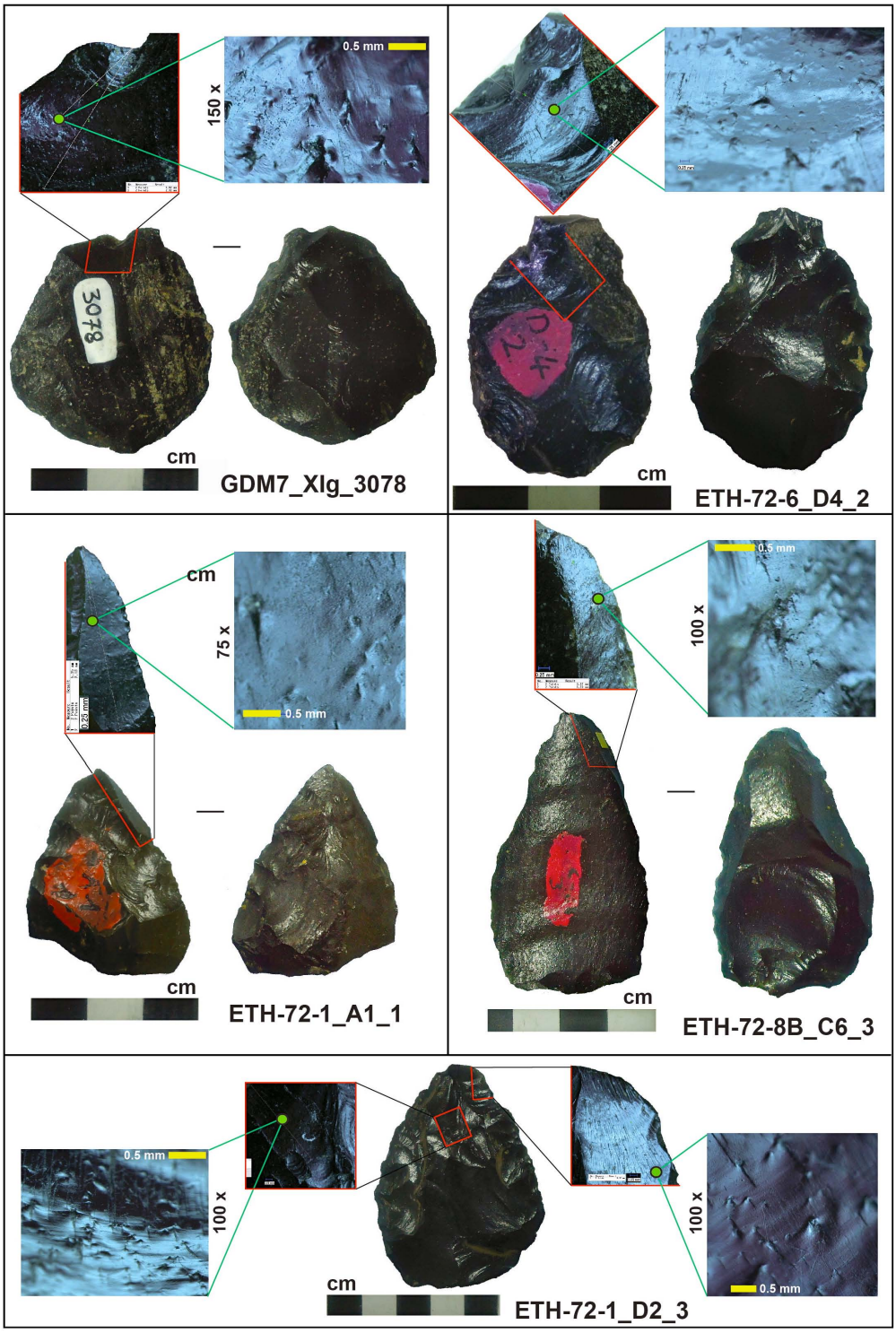

Figure 5.2 Photomicrographs of some of the pointed pieces with the location of fracture surfaces and features yielding *C* values

Table 5.1 *C* values and macroscopic damage categories of points. % fracture length (FL) represents where FWs are measured on the fracture front (FF)

No.	Specimen ID	ψ (°)	*C* (m/s)	%FL	Damage details
1	ETH-72-8B_C1_23	162	625	46	Tip; bending fracture with step termination; FL=6mm; proximal end thinned.
2	ETH-72-6_C2_3	162	625	54	Tip; unifacial spin off on dorsal; FL=5.2 mm; FF is obliquely aligned with typological axis.
3	ETH-72-6_Z9_2	160	694	49	Tip; bending fracture with step termination; FL=8 mm on the left disto-lateral tip (ventral face); FF is oblique with the typological axis; impact typical of rotating/twisting of piece upon contact, common in thrusting spears.
4	ETH-72-1_D2_3	160,155	694,865	56,56	Tip; (*i*) bending fracture with step termination FL=13.5 mm; *ii*) burin-like fracture with step termination; FL=16 mm; the two FFs are contiguous; proximal and lateral edges of the piece bear fractures with step termination.
5	ETH-72-6_C2_1x	160	694	63	Tip; step terminating fracture; FL=5.6 mm; base snapped; faint FWs visible on the basal bending fracture too.
6	ETH-72-6_D3_1	156	831	57	Tip; bending fracture with step termination; FL=4.6 mm; FWs documented on an overlying unifacial spin-off fracture.

Table 5.1 (cont'd)

No.	Specimen ID	ψ (°)	C (m/s)	%FL*	Damage details
7	ETH-72-8B_A3_5	153	933	21	Tip; burin-like fracture with step termination. FL=17mm; FWs are on a medial bending fracture surface; pseudo-burin scar, extends from tip of the piece to the end of the right mediolateral section on the ventral face.
8	ETH-72-6_D4_2	153	933	46	Tip; a transverse bending fracture; FL=9mm; bending snaps off entire tip of piece; FWs are on bending fracture surface with step termination; FFs on with similar patterns on either sides of this bifacial piece
9	ETH-72-8B_A3	152	966	28	Tip; bending fracture with step termination; FL= 6 mm in length for two step terminating fractures; very tip is snapped; a small (~2mm) spin-off fractures exist within one of the bending FF
10	ETH-72-8B_D4_4	150	1034	80	Tip; two burin-like fractures; FL=10.2 mm for the more prominent; FWs collected on the narrower burin-like FF running from the tip of the piece to the side of the bigger pseudo-burin scar; undulations and the orientation of FWs on the latter scar indicate fracture was initiated obliquely from the side, rather than the very tip.
11	ETH-72-8B_ C15_17	150	1034	69	Base; bending fracture snapping piece; FL is 33 mm; piece does not bear any other discernable damage fracture

Table 5.1 (cont'd)

No.	Specimen ID	ψ (°)	C (m/s)	%FL*	Damage details
12	ETH-72-7B_C4_1	150	1034	46	Tip; unifacial spin-off fracture with feather termination (on dorsal side); FL is 4.2 mm; a burin-like fracture with feather termination contiguous to it to the right
13	ETH-72-8B_A3_4	149,142	1068,1301	29,50	Base; transverse fracture; FWs documented on the basal snapped surface; a step-terminating burin-like fracture 9.5mm from the tip to the right distolateral on the dorsal side; contiguous transverse fractures with feather and step termination on a plain ventral side (possibly related to the impact on the dorsal side).
14	GDM7_IXg_3078	143	1268	57	Tip; transverse fracture with feather termination; FL is 7 mm; fracture removes entire tip of piece on one face; a narrow, feather terminating fracture initiated from same spot on the very tip
15	ETH-72-1_A1_1	139	1399	38	Tip; burin-like fracture; FL=14.5 mm and extends from the very tip of the piece to the lateral; proximal end is snapped.
16	ETH-72-8B_C6_3	136	1497	24	Tip; burin-like fracture; FL= 30mm; located on the right side of the ventral face, extending from the very tip to the mediolateral edge of the piece; a step-terminating fracture (8.5 mm long) at proximal tip on the dorsal side; proximal retouch scars visible on the ventral side.

Most of the microfracture features documented on these pieces prove to be restricted to the artifact tips. Where FWs were identified in more than one fracture front, they remain limited to contiguous fracture fronts on the tips of the pieces or opposite sides of a transverse fracture along a snapped tip or basal surface. FWs present on contiguous fracture surfaces appear to be clearly the result of whatever impact produced the measured FWs on the pieces. This inference is substantiated by the orientation of the FWs, which indicates the direction of impact propagation. A case in point illustrating this scenario is specimen ETH-72-1_D2_3, which retains two contiguous fracture surfaces with FWs on its distal tip (Fig. 5.2).

The combined results of the microfracture analysis strongly suggest that the impacts on the Gademotta pointed pieces were caused by use of the tool tips in a longitudinal manner. As a result, the damage on these pieces can be securely attributed to their use as weapon tips rather than the result of knapping blows. Furthermore, even relying only on the experimentally set threshold of precursory loading rates for different impact types, one of the pieces (ETH-72-8B_C6_3) with a *C* value in the dynamic loading rate is the result of impact that has never been documented from any known manufacturing process (Hutchings 1997, 2011; Fig. 5.1).

The fracture velocity approach enables one to distinguish between impacts from thrusting spears *versus* those from javelin use for *C* values that fall outside the range experimentally documented for thrusting spears (Hutchings 2011). About three-fourths (72.8%) of the Gademotta pieces

exhibit C values that are beyond the range experimentally established for thrusting spears (Table 5.1; Fig. 5.1). Due to reasons pointed out above, one can distinguish impact from arrows and darts from those produced by other weapon delivery mechanisms and manufacturing processes if and only if the pieces document *C* values within the dynamic range. It is impossible to be certain, based on *C* values alone, whether any of the Gademotta pointed pieces were used as arrows and/or darts. Ruling out the hypothesis that damage on the Gademotta pointed pieces were produced by a reduction process makes the documented *C* values for at least 72.8% of the pieces attributable to javelin impact. The remaining ~27% of specimens can be considered a result of use of these pieces as thrusting spears and/or javelins. The *C* value of specimen ETH-72-8B_C6_3 makes it attributable to arrow/dart impact. However, since this piece appears to be dimensionally outside the range documented for ethnographic and experimental arrows/darts (Shea 2006; Sisk & Shea 2011; Brooks *et al*. 2006), it cannot securely be ascribed to an arrow/dart tip. Instead, the proximity of its *C* value to the maximum value documented for experimental javelins (Hutchings 2011: table 3), and the morphometric range for archaeological and experimental spear tips (Shea *et al*. 2001; Shea 2006; Sisk & Shea 2011) mean that a more secure interpretation of the function of this piece is likely as a javelin tip.

The assemblage-level pattern observed for the C values from the Gademotta points is, in addition, consistent with those of the experimental

javelins. The pooled fracture velocity data from the 16 Gademotta pointed pieces are statistically indistinguishable from those documented on experimental javelins (Brunner-Munzel generalized Wilcoxon [BMgenW] test [Neuhäuser & Ruxton 2009] =0.57, p=0.57) (Hutching 1997: table 16).

5.2.2 Macrofracture analysis

A confident identification of the presence of projectile armatures is less likely to come from a single proxy for ancient behavior. Rather, a complete assessment of the technology and its behavioral implications requires a comprehensive knowledge of other artifact attributes and contextual data. A solid case for projectile weapon use in the Stone Age record can, hence, be made through the incorporation of multiple lines of evidence (*e.g.*, Sisk & Shea 2011; Brooks *et al*. 2006; Lombard 2005; Rots 2012). In the interest of obtaining the benefits of such additional approaches, a macrofracture analysis was conducted on the 16 Gademotta pointed forms on which fracture velocity data were collected. This involved the documentation of macroscopic damage patterns and locations on the tools. Hand lenses and low-power microscope (offering magnifications between 3 and 20x) were used, where necessary, to view fracture initiation and termination types in better detail.

Macroscopic fracture types most commonly depicted as diagnostic of impact result from use of a pointed piece in a longitudinal manner (for stabbing, thrusting, and 'distance penetrating') include: i) burin-like

fractures removing pseudo-burin spalls from the lateral margin(s) of the distal/distolateral tip of a pointed piece; ii) transverse fractures with terminations other than snaps that were inflicted after the tool was retouched; iii) unifacial spin-off fractures with a fracture length of >6mm ; iv) bifacial spin-off fractures; v) flute-like fractures (Bergman & Newcomer 1983; Fischer *et al.* 1984; Odell & Cowan 1986; Ho Ho Committee 1979; Sano 2009). Bending fractures with step terminations have often been presented as an additional, distinct type of fracture diagnostic of projectile impact (Fischer *et al*. 1984; Lombard 2005). However, according to Cotterell and Kamminga (1987), all impact fractures are bending, rather than conchoidal, fractures. In order to avoid confusion, bending fractures are treated here as part of Sano's (2009; Fig. 5.3) *transverse* or *flute-like fracture* category. Fractures that retain negative bulbs and those with feather terminations are often indicative of a manufacturing process, rather than impact damage, as these are often percussion induced (Bergman & Newcomer 1983). As a result, they require a more careful examination (Fig. 5.3). Furthermore, it has to be noted that impact fractures are not exclusively limited to the distal tips of pointed pieces and can be produced along the medial or proximal portion of a pointed piece used as a weapon tip. Impact-induced fractures on the proximal end of a pointed artifact can be distinguished from other fractures, such as knapping related percussions associated with proximal thinning. These types of removal often have step- or hinged-termination (Rots 2012; Villa *et al*. 2009). Comprehensive

summaries of the types of fractures most commonly associated with damage from projectile impact are widely available (*e.g.*, Lombard 2005; Sano 2009). For the present study, a combination of the criteria detailed in the above references has been adopted to describe damage patterns. Specifically, Sano's (2009) summary of criteria has been mostly applied here due to its comprehensiveness (Fig. 5.3).

A description of macrofracture patterns on the Gademotta pieces is presented in Table 5.1. Edge damage is mostly limited to the distal tips of the artifacts. Damage types on these pieces range from burin-like fractures to transverse (i.e. including what are also separately called bending fractures) and spin-off fractures. Some artifacts document more than one type of damage. Bending fractures account for about half of the damage patterns evident on the pieces while burin-like fractures are documented on about 40% of the pieces. Unifacial spin-off fractures occur on a few pieces (Table 5.1). Some of the pieces with bending fractures are snapped transversely across their medial-to-basal sections, suggesting that they yielded to stress from the impact damage by way of snapping while in the haft. Most of the macrofractures on the 16 pieces which yielded fracture velocity data are different in overall nature from fractures observed along the margins of the artifacts. In two pieces (namely, ETH-72-6_D3_1 and 72-8B_A3_5; Table 5.1; Fig. 5.4) the measured FWs were found in fracture surfaces other than those diagnostic of projectile impact.

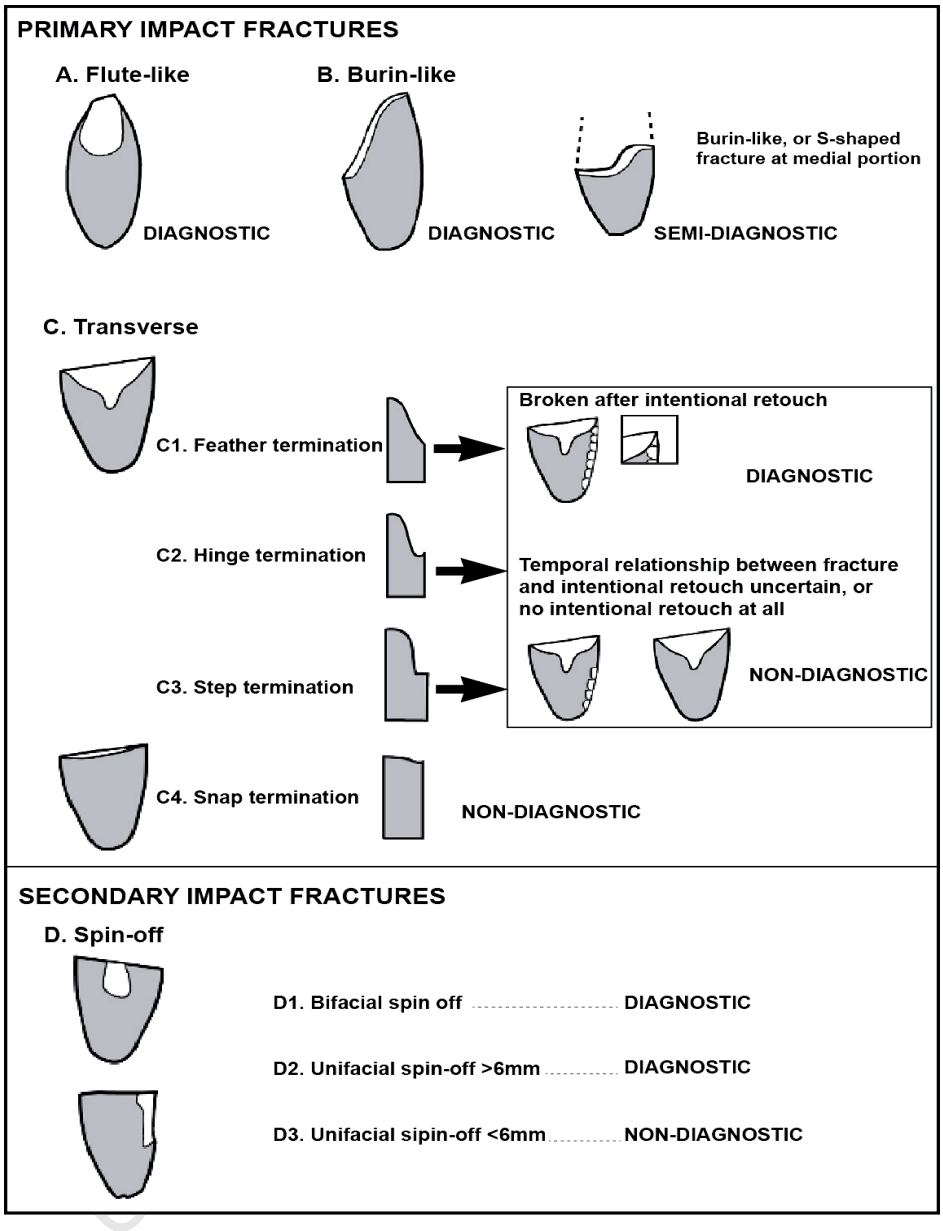

Figure 5.3 A schematic summary of impact fracture types and their interpretation (*After* Sano 2009: fig 15)

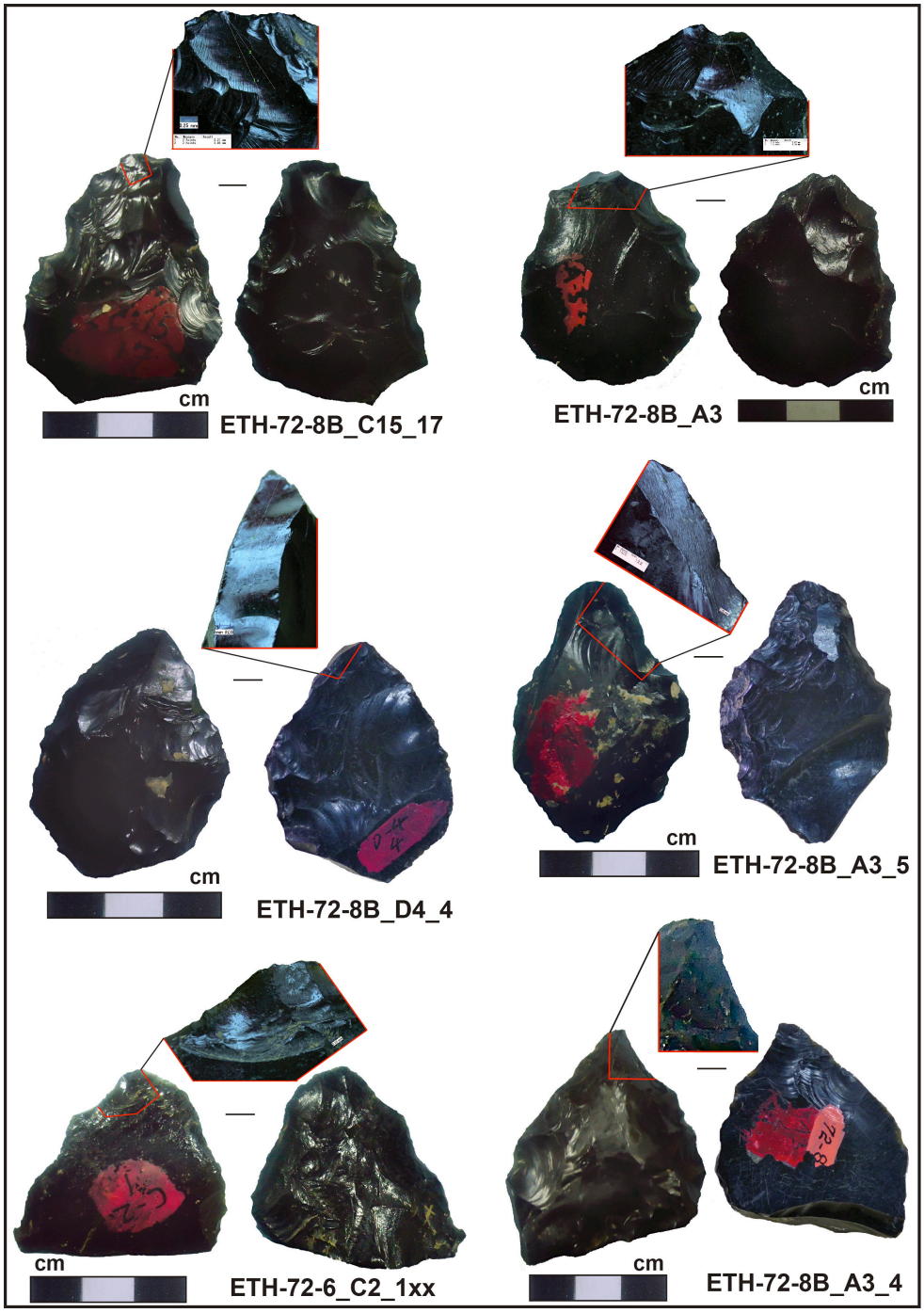

Figure 5.4 Images of selected artifacts with macrofractures diagnostic of projectile impact. See Table 5.1 for a description of macrofracture damage patterns

The interpretation of fracture types as diagnostic of projectile impact remains a difficult task as is clear from the previous discussion. Following the more restrictive and comprehensive criteria forwarded by Sano (2009; Fig. 5.3), 13 out of 16 of the Gademotta pieces under discussion bear impact fractures that will be considered diagnostic of damage from projectile use (Table 5.1; Fig. 5.4). The other 3 specimens retain damage that is not diagnostic of impact from weapon use. ETH-72-6_C2_3 and 72-7B_C4_1 retain spin-off fractures that are too small to be considered diagnostic of projectile impact. A single piece (72-8B_A3_4) does not bear any discernable damage on its distal tip. FWs on this latter piece were documented on the snapped surface near its base (Table 5.1).

5.2.3 Morphometric analysis

Much of the discourse surrounding the presence of projectile weapons in the Paleolithic record involves morphometric analyses that are thought to diagnose the ability of pointed artifacts to be used as a projectile weapon (*e.g.*, Brooks *et al.* 2006; Shea 2006). Although these measurements on their own are not adequate for understanding the use of tools as projectile weapons, they can provide an additional dimension to assessing the applicability of certain points as projectile weapons. The most widely used morphometric analyses, Tip Cross-Section Area (TCSA) and Tip Cross-Section Perimeter (TCSP), provide a tool for measuring the likelihood that points were hafted for use as effective weapon tips (Shea 2006; Sisk & Shea

2011). TCSA and/or TCSP values allow inference as to the suitability of a given point assemblage for use as a specific type of hunting weapon. These estimates are based on comparisons with thresholds established from ethnographic and experimental hunting points (Shea *et al*. 2001; Shea 2006; Sisk & Shea 2011).

For the present study, dimensional measurements were collected on 113 out of the 141 pointed pieces from ETH-72-8B, 72-7B, 72-1, 72-6, GDM7 and GDM10. The remaining 28 points were deemed unsuitable for this analysis because they retain only a small portion of their original tool dimensions. In addition to measurements I collected on the Gademotta pointed pieces, raw metric data for an experimental spear point assemblage were obtained from Dr. Shea. These were used for statistical comparisons and a calculation of their TCSP, which was not provided elsewhere (Shea *et al*. 2001; Shea 2006). Similarly, raw metric data for an assemblage of points from the Klasies River main site (KRM), South Africa, were obtained from Dr. Sarah Wurz. For all assemblages, TCSP was calculated using the formula for triangular, rather than rhomboid, cross-section as it provides a more restrictive measure (Sisk & Shea 2011: 3). TCSA is calculated as the product of maximum width and maximum thickness of a pointed piece divided by two (Shea 2006; Sisk & Shea 2011). TCSP, for triangular cross-section, was calculated using the following formula:

$$\text{TCSP} = \text{width} + \left(2 * \sqrt{[width/2]^2 + [Thickness]^2}\right)$$

Statistical summaries of the TCSA and TCSP of the Gademotta pointed pieces and comparative experimental and archaeological assemblages are provided in Table 5.2. Both TCSA and TCSP for the Gademotta point assemblage fall within the range for experimental spear points (Shea *et al.* 2001; Shea 2006; Fig. 5.5). In addition, these values are very similar to those documented for point assemblages from much younger MSA sites from elsewhere in Africa (*e.g.*, Aterian tanged points from Izouzaden and triangular MSA I points from KRM [Shea 2006: table 3; Sisk & Shea 2011: table 2]) which are commonly interpreted as hunting weapons on the basis of artifact morphology and/or associated fossil fauna.

Comparisons show that differences between Shea *et al.*'s (2001) experimental assemblage of spear points produced to replicate Middle Paleolithic Levantine point assemblages and the Gademotta point assemblage are not statistically significant both for TCSA and TCSP (Table 5.2). Similarly, differences between triangular points from MSA I at KRM and those from Gademotta are not statistically significant (Table 5.2). These results are interesting considering that the assemblage of experimental points has been suggested to represent morphometric attributes ideal for successful spear points. Similarly, the KRM MSA I points derive from a context as young as 90 ka, and in association with a rich fossil faunal assemblage (Milo 1998; Wurz 2002). Pointed pieces from even younger contexts at KRM (MSAII Lower and Upper) have even larger TCSA and TCSP values in comparison with those for the Gademotta assemblage.

Table 5.2 TCSA and TCSP values for the Gademotta *versus* experimental and archaeological points

	Gademotta (GDM) *(n=113)*	Experimental *(n=28)*	KRM MSA I *(n=71)*
TCSA (mm²)			
Mean	171.6	167.98	167.71
StDev*	84.6	89.3	59.39
TCSP (mm²)			
Mean	72.18	76.94	71.51
StDev	16.75	21.22	12.59
BMgenW Test *(vs GDM)*			
TCSA		-0.3242; *p*=0.7475	0.4409; *p*=0.6598
TCSP		1.0672; *p*=0.293	-0.1211; *p*=0.9037

*StDev = Standard deviation

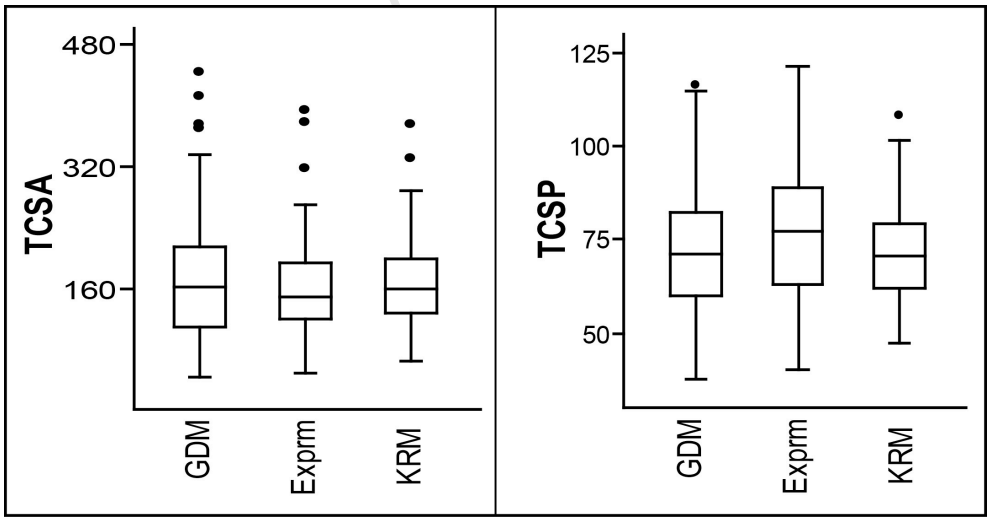

Figure 5.5 A box-plot comparison of TCSA and TCSP values for pointed pieces from Gademotta (GDM), Klasies River main site MSA I (KRM), and Shea *et al.*'s (2001) experimental study (Exprm)

5.3 Summary and Discussion

Launched armatures are recognized to be an important component of hunter-gatherer lifestyle (*e.g.*, Churchill 1993). Consequently, their presence in the Paleolithic record has often been considered an important innovation, as these technologies enhance hunting efficiency by increasing hunting range and avoiding direct confrontation with dangerous prey species (e.g., McBrearty & Brooks 2000 *and references therein*; Shea & Sisk 2010; Wadley *et al.* 2009). The production and use of such weapons requires assembling certain components – the shaft, the haft, and the action piece – and the launching of the weapon from a "safe" distance. This indicates complex cognitive capacities among users (*e.g.*, Wynn 2009; *cf*. Lombard 2011). Based on delivery mechanism, and the associated velocity of the specific mechanism, researchers sometimes dichotomize projectile weapons into "complex", and "simpler" forms (Shea & Sisk 2010; Sisk & Shea 2010). "Complex" forms incorporate the spearthrower-and-dart and the bow-and-arrow, which are mechanically projected and provide high velocity impacts. "Simpler" projectiles include javelins, i.e. hand-thrown spears, with lower velocity and reduced lethal range (Sisk & Shea 2010; Lombard & Phillipson 2010; Hutchings 2011).

Extant studies of Paleolithic projectile technologies focus predominantly on artifact tip morphology and overall dimensions, macro-fracture patterns, and proximal hafting traces of pointed artifacts thought to represent weapon armatures (*e.g.*, Shea 2006; Brooks *et al.* 2006; Sisk &

Shea 2011; Wadley *et al.* 2009; Rots *et al.* 2011; Lombard & Phillipson 2010; Sano 2009; Villa *et al.* 2009). These studies show whether an artifact was suitable for hafting or was in fact hafted. However, they fail to provide conclusive evidence for the actual use of a hafted tool. Hafted points can be used in a variety of ways and for a variety of functions. As a result, empirical evidence for the hafting of pointed artifacts is not the same as obtaining empirical evidence for *hunting at a distance*.

In more recent contexts where projectile technologies are known to have existed, hafting traces, macrofractures and morphometric attributes may be acceptable evidence for assigning functional interpretations to pointed artifacts. In the investigation of archaeological pointed assemblages from remote periods, however, data from these methods need to be taken as permissive and treated with caution. Arguments for particular delivery mechanisms in remote time periods must be supported by additional lines of evidence that substantiates a specific pattern, rather than depend largely on a single pattern alone (Iovita 2011; *cf. the claim for the presence of projectile weapons by* K. Brown *et al*. 2012). Even the non-subjective, fracture-velocity-based approach to assessing whether pointed pieces can be considered as tips of hunting armatures (Hutchings 1997, 1999, 2011) frequently fails to provide incontrovertible evidence for archaeological pieces with precursory loading rates attributable to a number of possible impact types (Fig. 5.1). As a result, the best application of this approach alone remains restricted to the identification of arrows and darts with

loading rates within the dynamic range. *C* values below the dynamic range may have been produced by impact from any of the overlapping mechanisms experimentally modeled and so pose the problem of equifinality.

Employing a combination of different approaches to the identification of projectile weapons in the archaeological record results in a sound and confident interpretation. In the present study, data collected from the different approaches outlined above provide a unique position from which sound interpretations can be made. In the following few paragraphs, I will try to show how the incorporation of the various lines of evidence from the approaches employed here has contributed to providing a concrete insight into the function of the pointed pieces from Gademotta.

The measurement of fracture velocity collected on 16 pointed pieces from several sites within the Gademotta Fm. yielded conservative estimates for *C* values that span the entire upper ranges of javelin impact established using experimental assemblages (Hutchings 1997, 2011; Table 5.1; Fig. 5.2). As such, the fracture velocity approach works through a justifiable exclusion of one or more potential impact types that may have produced given microfracture features (Hutchings 2011: 1045). For the Gademotta fracture velocity data, the possibility of all impact types other than javelin can be ruled out. The absence of microfracture features anywhere on the pieces except on the tips and, in two cases, snapped surfaces removing the entire base, suggests that the documented FWs were produced by fractures

indicating use of these tools in longitudinal fashion. This excludes the possibility that the documented microfacture features resulted from percussion. This conclusion is further supported by the damage patterns documented on the pointed pieces. Impact from use of these pointed forms as tips of thrusting spears is a possibility. However, only ~27% of pieces record *C* values within the range of experimental thrusting spears. The absence of *C* values within the dynamic loading range excludes use as arrow tips. However, the lines of evidence from multiple avenues of investigation are consistent with javelin use during the later Middle Pleistocene at Gademotta.

Macrofracture patterns evident on the measured pieces are also diagnostic of projectile impact damage (Sano 2009). This provides strong substantiating evidence for the interpretations based on fracture velocity. Almost all of these pieces exhibit macrofractures on their distal tips and follow a pattern commonly considered diagnostic of impact from projectile weapon use. There is one exception to this pattern. Artifact ETH-72-8B_C15_17 (Fig. 5.4) records a relatively high *C* (1034 m/s) on a basal bending fracture, but bears no discernable macrofracture that can be considered a result of impact damage. However, even for this piece, the basal bending fracture coupled with the high *C* suggests the possibility of impact fracture from use of this piece as a weapon (*cf*. Hayens 1980). ETH-72-8B_A3_4 documents diagnostic macrofractures on its distal tip, although FWs were documented on its snapped base (Fig. 5.4; Table 5.1).

Morphometric data (i.e. TCSA and TCSP) from a larger assemblage of pointed pieces from Gademotta show that they are statistically not different from experimental and more recent archaeological assemblages interpreted as effective hunting spear points (Shea *et al.* 2001; Shea 2006; Sisk & Shea 2011; Wurz 2002).

Currently, there is no criterion to distinguish spear points that were used for thrusting *versus* those that were thrown based on morphometric or macroscopic approaches (Shea 2006; Lombard *et al*. 2005; Villa & Lenoir 2006). More work is needed to understand the biomechanical capabilities of African Middle Pleistocene hominins (Churchill & Rhodes 2009). A throwing-capable hominin could use spears for both thrusting and throwing (Villa & Lenoir 2006), making it difficult to distinguish which spear tip was used for what type of weapon delivery. This makes deciphering the timing of the technological innovations associated with the earliest forms of hafted projectile armatures challenging.

The multi-stranded data on the Gademotta points provide a unique insight into the function of the tools and the innovation of projectile armatures. Data from the fracture-velocity-based approach provide a way to distinguish between spear tips used for thrusting versus those used as javelin tips (Hutchings 2011). Macrofracture analysis documents damage patterns. Morphometric data support the assertion that the Gademotta points are suitable for use as spear tips. The majority of the Gademotta pointed pieces for which evidence from these different approaches provide overlapping

insights were used as javelin tips; a smaller number may have been used as thrusting spears as well.

Direct evidence for stone-tipped projectile armatures is not well known until late in the Upper Pleistocene (Lombard & Phillipson 2010; Lombard 2011; *cf*. Villa *et al*. 2009). Because of the unique evolutionary advantages pointed out above, the presence of stone-tipped projectile armatures at Gademotta as early as >279 ka has implications for discussion of hominin lifeways.

CHAPTER SIX

6. AN INTER-ASSEMBLAGE COMPARISON OF COSTS AND BENEFITS IN FLAKE PRODUCTION FROM SITES IN THE MAIN ETHIOPIAN AND AFAR RIFTS

6.1 Introduction

At the center of behavioral ecological approaches to human evolution is the identification of evolutionarily significant dimensions that can be used to understand aspects of hominin behavioral variability (*e.g.*, Shea 2011; Minichillo 2005). The measurement of efficiency in flake production provides a method to quantitatively infer the behavioral capacities of hominin populations across time (Shea 2008, 2011). Efficiency in flake production can be quantified by using hypothetical costs and benefits of particular technologies within the context of sites across a given period of time. In turn, this provides insights into the technological responses of hominin populations to ecological necessities (Bird & O'Connell 2006; Potts 1998; Shea 2008, 2011).

The basic idea of the cost-benefit approach is that hominin responses to ecological requirements reflect adaptative behaviors. Put otherwise, the underlying assumption is that the responses of prehistoric knappers to costs and benefits involved in flake production can be discerned from the artifacts they produced (Dibble 1997; Shea 2011). Costs and benefits in the production and use of artifacts can be measured in several ways. For

example, reduction intensity in retouched tools has been widely used as a proxy for measuring the amount/degree of curation (i.e. realized relative to potential utility [Shott 1996]) with implications for responses of a group(s) to costs, benefits and/or risks (*e.g.*, Sahle *et al*. 2012; Bousman 2005; Kuhn 1991; Eren *et al*. 2005). In debitage classes, Shea (2008) has employed a methodology for measuring costs and benefits from the various dimensions of whole flakes.

The effectiveness of flake production can be assessed from the acquisition of desired flakes from a core using the smallest possible striking platform per flake. Accordingly, "efficiently" produced flakes can be identified by the small striking platform width (SPW) relative to striking platform thickness (SPT) that they retain (Davis & Shea 1998; Dibble 1997). In other words, the more striking platform a flake takes away from a core, the smaller the potential for making subsequent flakes because the striking platform on the core has been reduced. More "costly" approaches to flake production have greater platform widths (Shea 2008: 476; *see also* Tryon & Potts 2011: 382). Cost in flake production can, therefore, be calculated as SPW divided by SPT. Platform variables – such as its width, thickness and exterior angle – were most likely actively controlled by MSA knappers to obtain flakes of the desired dimension and morphology (Dibble 1997: 151; Dibble & Rezek 2009). It follows that flakes detached from cores using a narrower striking platform relative to SPT involved lower production cost, and vice versa.

In the model employed by Shea (2008, 2011) benefit in flake production can be estimated as the production of flakes with more cutting edge per flake. This model emphasizes that the prime concern of Stone Age knappers was attaining the largest possible cutting edge per flake. Benefit (i.e. cutting edge) in whole flakes can be calculated as the ratio of flake surface area (FSA) to mid-point thickness (T), where FSA is the product of technological length (L) and mid-point width (W) (Davis & Shea 1998). Accordingly, the higher the FSA-to-T ratio, the more benefit a knapper extracted from flake production activities, and vice versa.

This study collected dimensional measurements on whole flakes that are >30mm in their technological length from different sites at Gademotta (i.e. GDM7, GDM10, and ETH-72-6) and in the Middle Awash study area following protocols detailed in Appendix-1. The Middle Awash assemblages studied here come from sites BOU-A19A, A19B, A19HT, A26A, A26B, A26C and A29 at Herto, and ADU-VP-1/3 at Aduma (Fig. 2.3). At Herto, assemblages from BOU-A19B and A19HT were recovered through excavation whereas those from the rest of the localities were recovered from controlled surface collections whose context was verified through the recovery of *in situ* artifacts exposed by erosion, preservational characters, clinging matrix and/or geomorphological makeup (Clark *et al*. 2003: 750). In addition, raw whole-flake metric data on MSA assemblages from the Kibish Fm. (i.e. sites AHS, KHS and BNS) supplied by Dr. Shea are used in the present comparisons. While the comparison of cost and

benefit values from the different sites and regions in itself has been shown to provide insights into hominin core utilization and cutting edge production behavior (*e.g.*, Shea 2008, 2011), a comparison of cost-to-benefit ratios is imperative for more comprehensive insights (*e.g.*, Sahle *et al*. 2012: table 2; Fig. 6.1).

6.2 Inter-assemblage comparisons

Table 6.1 provides a summary of cost (SPW/SPT) and benefit (FSA/T) values and ratios for the sites studied here. Comparisons of cost and benefit values here are conducted between sites from older *versus* younger contexts within their respective site-complexes. Such intra-regional comparison was conducted in order to account for the potential influence of paleoecological distinctions between the three different regions. However, an inter-regional comparison is also conducted to see what pattern can be discerned.

At first glance, the cost and benefit values at the Gademotta sites appear to be low at GDM7, high at GDM10, and high cost, low benefit at ETH-72-6 (Table 6.1; Fig. 6.1). Statistical comparisons were carried out using non-parametric tests of Mann-Whitney for pair-wise and Kruskal-Wallis for multi-group comparisons; F-test results show that for all sites compared here variances are unequal. Differences in both cost and benefit values between the Gademotta sites are not statistically significant (p= 0.087 for cost; p= 0.187 for benefit). Furthermore, comparisons between the

combined GDM7 and GDM10 data *versus* data from the much younger site ETH-72-6 for cost (p=0.132) and benefit (p=0.837) are also not statistically significant. Cost-to-benefit ratios are more or less similar for all of these sites and differences in these ratios are not statistically significant (H=3.457 and P=0.178). These results may be taken as strong indications that the hominin populations that repeatedly occupied the Gademotta area across the later Middle- and earlier Upper Pleistocene possessed substantially similar technological behaviors. Results are interesting considering these hominins occupied the same geographical area with similar contexts, such as raw material availability (within ~2.5 km for all sites) and paleoecological settings (an ecotonal, near-shore habitat) (Vogel *et al*. 2006; Negash *et al*. 2010; Basell 2008; Trauth *et al*. 2010; Fig 1.1.b).

Comparison between Herto and Aduma show that differences in both cost and benefit between these two sites are not statistically significant (p=0.879 for cost; p=0.149 for benefit) (Sahle & Beyene *forthcoming*). Cost-to-benefit ratios for these two sites are also not significantly different (p=0.26). Interestingly, these two sites show the most similar values for average cost and benefit as well as variation out of all assemblages compared here (Table 6.1). Given that these humans occupied the same region within a relatively small temporal span, during which the ecology remained relatively constant (e.g., Negash *et al*. 2011; Fig. 2.3), the statistically indistinguishable artifactual patterns indicate the presence of comparable behavioral capacities among the earliest Herto and the much

younger Aduma humans.

For the Kibish assemblages, Shea (2008) has shown that comparisons of costs and benefits provide a complex picture, one where the only statistically significant difference is observed when comparing benefit at AHS and BNS. Variation in benefit is higher for the older sites of AHS and KHS *versus* BNS. Benefit values are, however, generally small for all of the Kibish assemblages and are comparable to similar values documented for much older contexts in the Levant (Shea 2011: 27). Differences between cost-benefit ratios for the Kibish sites not are statistically significant (p=0.158).

The intra-regional comparisons summarized above are far from providing clear-cut pictures of cutting edge production and core exploitation patterns across time. For instance, GDM7 shows cost and benefit values that are closer to ETH-72-6 than does the relatively younger GDM10 assemblage (Table 6.1). Differences between GDM7 and GDM10 are not statistically significant (p=0.145 for cost; p=0.078 for benefit). Assemblages from GDM10 have been shown, in Chapter Four, to contain more extensively retouched and utilized tools. Provided occupations in the Gademotta area relied on the nearby Worja obsidian source, the presence of higher benefit and more utilized retouched tools at GDM10 remains intriguing.

Table 6.1 Summary statistics of cost and benefit values for selected MSA sites from the Omo Valley, Main Ethiopian Rift and Afar Rift

	GDM7 (*N*=54)	GDM10 (*N*=27)	ETH-72-6 (*N*=42)	AHS (*N*=144)	KHS (*N*=22)	BNS (*N*=76)	HERTO (*N*=59)	ADUMA (*N*=31)
COST (SPW/SPT)								
Mean	2.66	3.29	3.09	4.1	3.4	3.9	3.13	3.22
StDev*	0.78	1.73	0.98	2.1	1.5	1.8	1.03	1.41
Variance	0.62	3.00	0.96	4.2	2.18	3.25	1.07	2.00
CoVariance†	29.56	52.67	31.67	49.98	43.07	45.91	33.1	43.99
BENEFIT (FSA/T)								
Mean	150.52	197.95	156.38	201	171.4	159.6	207.72	185.41
StDev	43.46	99.06	58.95	98.2	109	54.3	95.91	91.17
Variance	1,880.6	9,813.1	3,475	9,636.2	11,884.6	2,944	9,198.4	8,313.4
CoVariance	28.81	50.04	37.69	48.83	63.59	33.99	46.17	49.17
COST : BENEFIT								
Mean	0.0187	0.0227	0.02798	0.02335	0.02	0.03	0.0196	0.0197
StDev	0.0065	0.0232	0.044	0.1377	0.014	0.01	0.021	0.1
Variance	0.00004	0.0005	0.0019	0.00018	0.00019	0.0002	0.0004	0.0001
CoVariance	34.99	102.04	157.56	56.83	56.88	55.3	105.87	51.69

*StDev= Standard deviation; †CoVariance= Coefficient of variance

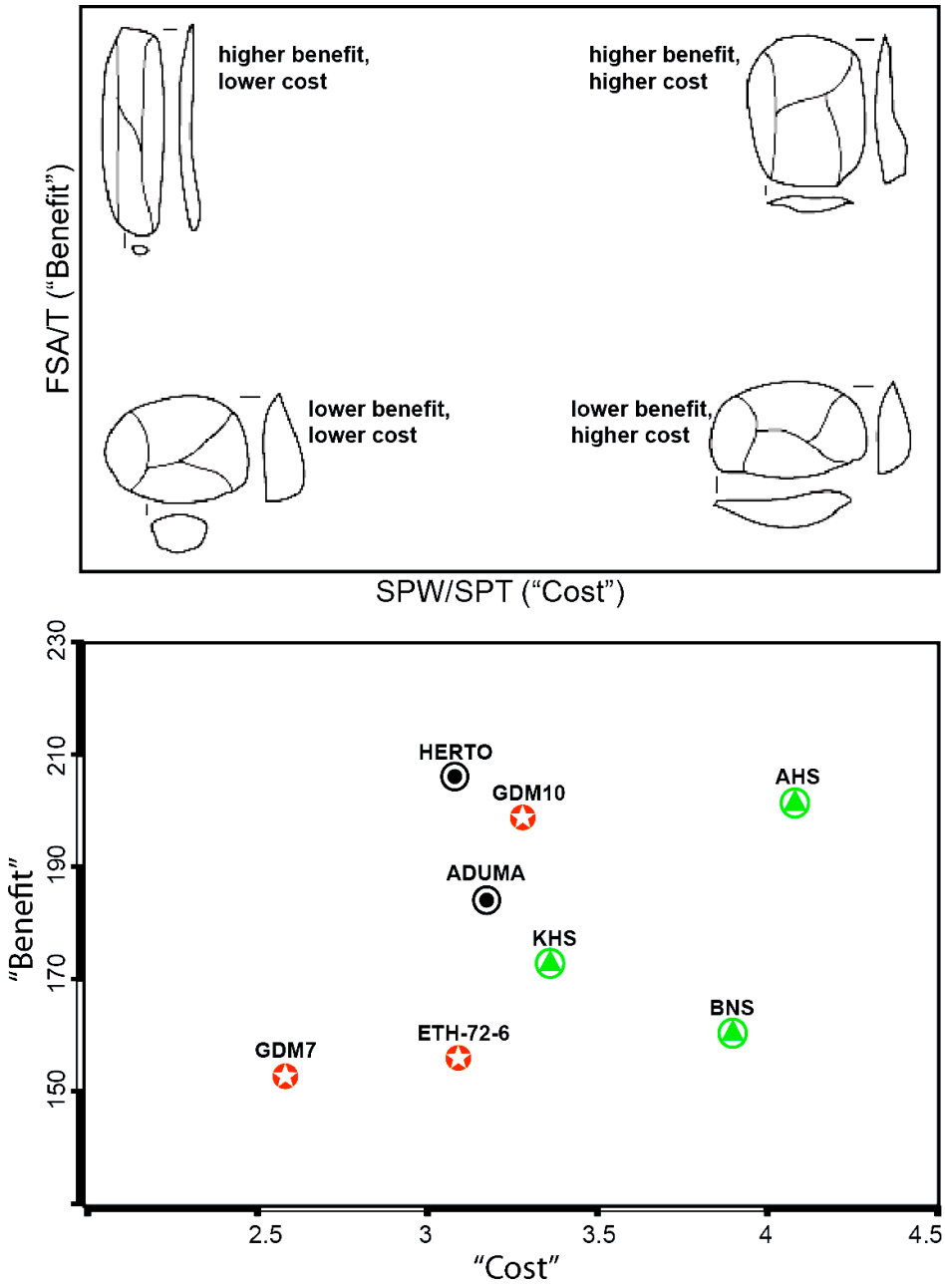

Figure 6.1 A schematic representation of a flake with various hypothetical cost and benefit values (above), adapted from Shea (*pers. comm.*); sites plotted against their respective cost and benefit values (below). Sites represented by the red symbols are from the Gademotta Fm.; those in black are from the Middle Awash region; green ones are from the Kibish Fm. of the Omo Valley

Inter-regional comparisons between the Kibish and Herto sites show that differences in both cost and benefit between the Herto and BNS assemblages are statistically significant (p=0.0078 for cost; p=0.0026 for benefit). However, difference in benefit for Herto *versus* the combined data from AHS and KHS does not rise to the level of statistical significance (p=0.2677). These are interesting results, especially taking into account differences in geographical location (Fig. 1.1a) and ecological settings of these sites. For instance, although there is no exclusive reliance on high-quality material such as obsidian in both regions, raw material types exploited by the Herto *versus* the Kibish humans are different. The Herto assemblages are primarily made on fine-grained basalt whereas cryptocrystalline silicates, mainly chert, make up the most commonly utilized raw material type in the Kibish assemblages (Clark *et al*. 2003; Beyene 2010; Shea 2008: 467).

More comprehensive inter-site comparisons of costs and benefits provide interesting results as all of the site-complexes under discussion are located several hundred kilometers away from each other and cover different time periods (Fig. 1.1a). In general, BNS and AHS yield the highest cost values while BNS, ETH-72-6, and GDM7 yield the lowest benefit values among the sites compared (Table 6.1). Differences between the combined GDM7 and GDM10 data *versus* KHS (cost: p=0.125; benefit: p=0.387); *versus* BNS (cost: p=0.22; benefit: p=0.82); and *versus* Aduma (cost: p=0.23; benefit: p=0.528) are not statistically significant. These

results provide valuable insights into the technological knowhow of hominin populations across time and space. In terms of cost-benefit ratio, the GDM7 assemblage shows the lowest ratio. The low cost value exhibited by this assemblage is also paralleled by the lowest benefit value it retains (Table 6.1). The Middle Awash sites of Herto and Aduma also show relatively smaller cost-benefit ratios due to their relatively medium cost and higher benefit values (Table 6.1). The Kibish sites display the highest cost values of all assemblages compared here. However, since they also retain relatively higher benefits, the older sites of AHS and KHS have medium cost-benefit ratios. BNS retains one of the highest costs and one of the lowest benefits, hence showing the highest cost-benefit ratio (Table 6.1).

6.3 Summary and Discussion

The comparisons of costs and benefits, intra- and inter-regionally, are difficult to interpret. Some of the lowest cost and highest benefit values are collected on assemblages from the oldest sites studied (i.e. GDM7 and GDM10). Some of the highest cost and lowest benefit values come from one of the youngest sites (i.e. BNS). In addition, as opposed to the pattern seen in other assemblages, GDM7 exhibits the lowest variation in both cost and benefit (*cf*. Shea 2008: 27). Statistical comparisons generally show that assemblages from different periods within the three regions are substantially similar in terms of cutting edge production and core exploitation patterns.

Raw material sources and other paleoecological settings were

substantially similar within a region through time (Vogel *et al*. 2006; Shea 2008: 468; Clark *et al*. 2003; Beyene 2010; Yellen *et al*. 2005). As a result, it remains difficult to parse out what specific factors governed some of the complex patterns of tool production behavior observed in the present analysis. What factors contributed to the lowest cost in the GDM7 assemblage? Why are benefit values so small for ETH-72-8B and BNS? Why is the cost for BNS so high and benefit values for all of these sites as small as that documented for much older Acheulean sites (Shea 2011: 27)? Considering a largely similar paleoecological setting for the respective sites, it will be difficult to answer these questions with the data at hand.

Inter-regionally, comparisons provide interesting insights that may be used to hypothesize similar behavioral capacities among hominin populations from the different regions of the broader rift valley in Ethiopia. This is particularly so, taking into account the similarities and differences in contexts and evidence among the different site-complexes. In general, the Kibish and Middle Awash sites show stronger similarities along technological, temporal and paleoecological lines than they do with those from Gademotta (Shea 2008: 479). Both at Kibish and in the Middle Awash, the early MSA is interstratified with layers containing tools attributed to the Acheulean tradition, as is the case in the Kapthurin Fm. of Kenya (Fig. 2.4). In contrast, no trace of a final Acheulean occupation has been identified at Gademotta (Wendorf & Schild 1974: fig 7; Wendorf *et al*. 1975: 740). Regarding raw material exploitation, the Middle Awash and Kibish sites

show a pattern where different types of material are used in different proportions (Shea 2008; Clark *et al.* 2003). The pattern in the Gademotta Fm. stands in sharp contrast in that obsidian proves to be almost the only raw material exploited. Finally, while the time range that sites in the Kibish Fm. and the Middle Awash area cover are largely comparable (~195-105 ka for Kibish; 160-80 ka for the Middle Awash), the Gademotta sites span the period from as early as 279 ka to as late as 105 ka (Fig. 2.4; McDougall *et al*. 2005; Clark *et al*. 2003; Morgan & Renne 2008; Sahle *et al*. 2013; F. Brown *et al*. 2012).

More comparisons using other parameters, such as tool reduction intensity (*cf*. Sahle *et al.* 2012; Bousman 2005; Eren *et al.* 2005; Kuhn 1991), are needed to better interpret these patterns and infer the technological behavior of hominins across the critical time period when our species emerged. The measurement of tool reduction intensity as a proxy for curation behavior could not be incorporated in the present study due to the low frequency of suitable retouched tools, such as end/transverse scrapers (Shea 2008; Table 4.2).

Based on the present cost-benefit data, it can be concluded that hominin populations that occupied discrete regions within the rift valley in Ethiopia possessed substantially similar behavior in terms of technological strategies pertaining to flake utilization and core exploitation.

Shea (2008: 480) suggests that the typological similarities between the Kibish assemblages and those from other Ethiopian MSA sites (such as

Gademotta-Kulkuletti, Aduma and Porc Epic [Pleurdeau 2005]) may be indicative of cultural continuity and demographic stability in this particular part of east Africa. Results of the present comparisons empirically substantiate this suggestion, using direct technological comparisons, in that cutting edge production and core exploitation patterns across the various sites in the Omo Valley, the Main Ethiopia Rift and the Afar Rift remained essentially similar across the later Middle- and earlier Upper Pleistocene.

CHAPTER SEVEN

7. SUMMARY, DISCUSSION AND CONCLUSIONS

7.1 Summary

The emergence of *H. sapiens* and the transition to cultures that are widely accepted as characterizing modern human cognition rank among the important evolutionary phenomena that render the African later Middle- and earlier Upper Pleistocene the focus of special research attention. In spite of the presence of a multitude of evidence that strongly supports an African origin of our species (McDougall *et al.* 2005; Clark *et al.* 2003; White *et al.* 2003; Ingman *et al*. 2000; Yotova *et al.* 2007), the behavioral capacities of the first *H. sapiens* and how these compare with their immediate predecessors, penecontemporaries as well as Upper Pleistocene descendents remain largely unaddressed (Shea 2011).

The paucity of well-dated sites from the later Middle Pleistocene, and greater research focus on the Upper Pleistocene portion of the MSA have long limited our understanding of the behavioral context across our species' evolutionary origin. Differences in the theoretical and methodological approaches applied to the archaeological records of these periods as well as the overall interpretation of the various evolutionary dynamics marking this critical timescale account for the current lack of comprehensive knowledge (Shea 2011, 2012). The accumulation of paleoanthropological and geochronological data over the past decade has contributed greatly to our

knowledge of hominin lifeways and evolutionary trajectories across the period under discussion. However, comparable methodological frameworks are lacking and a comprehensive picture of the behavioral context of hominins during this period across the continent is yet to come (Shea 2011 *and comments therein*, 2012; Lombard 2012).

Through the analysis of multiple occupation horizons within the Gademotta Fm. of the Main Ethiopian Rift, the present research has documented the technological behavior of hominin populations that inhabited the area through much of the MSA. Renewed geochronological and stratigraphic investigations have not only contributed to refining the contexts of the various occupation horizons, but also enabled more meaningful comparisons of technological behavior across the later Middle- and earlier Upper Pleistocene. $^{40}Ar/^{39}Ar$ geochronology, conducted as part of this dissertation research, now confirms that the cultural horizon represented by sites ETH-72-8B and GDM7 directly underlies the Unit 10 bedded tuff dated to 279 ± 2 ka, making it the world's oldest-dated MSA occupation (Sahle *et al*. 2013; Morgan & Renne 2008; *cf*. Deino & McBrearty 2002). New dating of localized cemented ash in the Unit 12 bedded sandstone also provides a combined $^{40}Ar/^{39}Ar$ isochron age of 260 ± 7 ka, further constraining occupations represented by ETH-72-7B and GDM10 at Gademotta and ETH-72-1 at Kulkuletti. The minimum age for these sites thus far came from Unit D, which was recently dated to 185 ± 5 ka* (Morgan & Renne 2008). Dating of Unit 15, the uppermost tephra bed

in the entire Gademotta sequence, is currently in progress. This unit overlies two important sites, ETH-72-6 and 72-9 (Laury & Albritton 1975; Wendorf & Schild 1974). A recent geochemical correlation has determined that the Unit 15 ash matches with the Aliyo Tuff (105 ± 1 ka) in the Kibish Fm., thus providing a tentative minimum age for the aforementioned occupations (F. Brown *et al*. 2012).

Renewed excavations in the Gademotta area have recovered assemblages from occupation horizons previously represented by ETH-72-8B and 72-7B of Wendorf and Schild (1974). Generally, debitage classes dominate the non-debris assemblages of the newly excavated sites of GDM7 and GDM10. The Levallois technique is well represented, as are retouched tools. Obsidian proves by far the most extensively exploited raw material type. However, rhyolite was also used at GDM7. The exploitation of obsidian is obviously attributable to its superior flaking qualities (i.e. homogeneity and isotropy) and availability in a nearby source (Vogel *et al*. 2006; Negash *et al*. 2010). The use of the relatively poor-quality rhyolite, albeit in a limited amount, remains intriguing.

Previous research suggested there was technological stasis across occupations at ETH-72-8B *versus* those at ETH-72-7B and 72-1. The new geochronological data on Unit 12 help to explain this because the two occupations can be separated by a mere 19 ± 8 ka. Modern excavation and data recovery mechanisms employed in the new round of research provide insights into the artifact distribution patterns at GDM7, which are not

consistent with claims of a circular "hut" at the adjoining site of ETH-72-8B (Wendorf & Schild 1974: 150-151).

A comparison of the capacities of hominins for behavioral variability across the later Middle- and earlier Upper Pleistocene has been conducted in two different ways: i) through an assessment of the capacity for projectile weapon use; ii) through the measurement of costs and benefits involved in flake production. To investigate the capacity of the Gademotta hominins to make and use projectile technologies, the present research conducted analyses on an assemblage of retouched pointed tools, identifying and measuring velocity-dependent microfracture features, documenting macrofracture patterns, and studying morphometrics. Cost and benefit analyses measured the technological behavior involved in the production of tool cutting edge and the exploitation of cores as inferred from the dimensions of whole-flake debitage classes.

Velocity-dependent microfracture features were documented and measured on a total of 16 pointed pieces from several sites at Gademotta and in the Kulkuletti area. Most instantaneous fracture velocities on these pieces fall within the rapid precursory loading rate regime, meaning that fractures could be attributed to impact from hard-hammer percussion, thrusting spears, javelins, arrows and/or darts. Additional micro- and macroscopic analyses found that the majority of the measured microfracture features are indicative of impact from use of the tips of the pointed forms in a longitudinal fashion. Similarly, macrofracture analysis showed that the

location and morphology of damage is by and large diagnostic of impact fractures from use of the pieces as the tips of hunting weapons. Most damage occured on the distal and distolateral tips of the pointed forms. In a few pieces, bending fractures snapped the medial-basal portion of the pieces, a pattern that occurs in projectile weapons (Hayens 1980).

Morphometric analysis of pointed pieces from several sites within the Gademotta Fm. indicate that TCSA and TCSP (*as defined by* Shea 2006; Sisk & Shea 2011), of points from this formation are statistically indistinguishable from other assemblages experimentally established as effective spear tips (Shea *et al.* 2001; Shea 2006), or recovered in association with hunted fauna from a much younger archaeological context at Klasies River, South Africa (Wurz 2002; Milo 1998).

Taken as a whole, the multiple lines of evidence support the conclusion that Gademotta hominins incorporated javelins in their technological repertoire as early as >279 ka and continued this technology until perhaps as late as 105 ka. It is certainly possible that some of the pointed pieces at Gademotta were employed as thrusting spears. However, fracture velocity data on the majority of the pointed forms were higher than the threshold experimentally established for thrusting spears. Moreover, although a single specimen records a fracture velocity value in the dynamic loading range (attributed only to arrow/dart impact), its morphological features are closer to spear points than to arrows/darts. Therefore, the most parsimonious interpretation of the Gademotta points is that the majority of

them were used as tips for javelins.

Costs and benefits in flake production were calculated on whole flake assemblages from sites in the Gademotta, Kibish and Middle Awash regions. Comparisons of cost, benefit and cost-benefit ratio values were conducted between sites from older *versus* younger contexts within the respective site-complexes. Results show that for most variables, differences between the later Middle- and earlier Upper Pleistocene sites were not statistically significant. Inter-regional comparisons also yielded results that confirm that cutting edge production and core exploitation patterns across the timescale of >279 ka-80 ka remained substantially similar.

7.2 Discussion and Conclusions

A long-standing question in paleoanthopology has been how later Middle Pleistocene behavioral contexts compare with Upper Pleistocene ones. In particular, behaviors across the broader time marked by the emergence of *H. sapiens* have long attracted enormous research attention. The currently most widely applied approach to studying behavioral modernity is problematic. This approach focuses on the first appearance datums for certain behavioral traits believed to be indicative of modern cognition. Unfortunately the hallmarks of modern cognition continue to be based on concepts that draw from the archaeological record marking the transition into the Upper Paleolithic in Europe, and there is widespread discontent with the application of this approach to the Stone Age of sub-

Saharan Africa (Minichillo 2005; Shea 2011).

The short-chronology-to-behavioral modernity approach (Klein 2000; Klein & Edgar 2002) has been strongly criticized in the face of multiple lines of evidence that show that hominin populations in the later Middle- and earlier Upper Pleistocene were capable advanced behaviors that were common by *ca*. 50 ka (*e.g.,* Minichillo 2005; Marean *et al*. 2007; K. Brown *et al*. 2009, 2012; McBrearty & Tryon 2006; Van Peer *et al*. 2003; Henshilwood *et al*. 2011; Wadley *et al*. 2011; Krause *et al*. 2007). The long chronology approach, too, has been criticized as merely adopting the trait-based approach to modern behaviors. The coupling of behavioral with anatomical modernity (*e.g.*, Nowell 2010, *and references therein*), and the stochastic appearance of certain so-called traits of modern behavior (Hovers & Belfer-Cohen 2006) further complicate how the African Paleolithic record has to be studied and interpreted. Despite dissatisfaction with the behavioral modernity approach, it is still widely applied.

In this dissertation, I have taken a different approach comparing the range of behavioral expressions among hominin populations across the later Middle- and earlier Upper Pleistocene in the Omo Valley, the Main Ethiopian Rift and the Afar Rift. This approach also has the advantage of drawing on those archaeological remains that are the most abundant and have the fewest taphonomic biases – i.e. lithics (Shea 2011, *and comments therein*; Minichillo 2005).

Currently, no strong evidence has been presented for modern behavior

amongst the earliest known *H. sapiens* (Shea 2008; Clark *et al*. 2003; Beyene 2010). In a recent review, Shea (2011: 10-11) tries to show how far-fetched interpretations can become dogma in the attempt to fit certain behavioral patterns into the trait-list of modern/symbolic behaviors. In his examples, Shea suggests that certain evidence, such as the potentially non-utilitarian transport of opal, can be interpreted as indicative of the capacity of the Kibish early *H. sapiens* populations for symbolic behavior. It has been argued that independent evidence from Herto can be used to make an even stronger case for the capacity of *H. sapiens idaltu* populations for symbolic thinking (Sahle & Beyene *forthcoming*). In the most common interpretation, the defleshing cutmarks on the Herto crania, together with the exploitation of lithic raw material sources *ca* 290km away from home bases, make a strong case for the behavioral modernity of the Herto humans (McBrearty & Brooks 2000 *and references therein*). The location and patterns of the cranial cutmarks provide strong evidence that these were the result of intentional defleshing while the absence of post-cranial remains in an otherwise very good depositional context supports the assumption that the crania were curated, most likely as part of a post-mortem ritual (Clark *et al*. 2003; White *et al*. 2003; Sahle & Beyene *forthcoming*). The presence of lithic raw material quarried from a remote source (Negash *et al*. 2011) is indicative of the presence of knowledge and exploitation of distant resources and/or a trade/exchange practice (McBrearty & Brooks 2000).

The analysis of costs and benefits involved in the behavioral responses

of hominins to ecological circumstances has been used as an important tool to measure their behavioral capacities (Shea 2011; Potts 1998; Braun *et al.* 2005). Costs and benefits calculated from whole flake metric data from the Gademotta, Kibish and Middle Awash assemblages show that hominins possessed significantly similar technological capacities across the later Middle- and earlier Upper Pleistocene. Further comparisons show that Middle- and Upper Pleistocene hominin populations inhabiting different sites within the rift valley in Ethiopia had substantially similar technological behavior as far as flake production and core exploitation patterns are concerned.

Projectile technologies are believed to have significantly improved hominin subsistence strategies by way of providing safer, more efficient hunting strategies and broader niche/diet (*e.g.*, Churchill 1993; Brooks *et al*. 2006; Shea & Sisk 2010). As a result, the presence of such technologies has been considered strong evidence for behavioral modernity (*e.g.*, McBrearty & Brooks 2000; Lombard & Phillipson 2010; Lombard 2011).

Velocity-dependent microfracture features documented on an assemblage of pointed pieces from several sites within the Gademotta Fm. show that nearly three-fourths of the pieces record fracture velocity values beyond the threshold experimentally established for thrusting spears. One specimen records a fracture velocity value within the dynamic precursory loading rate. Macrofracture studies confirm that most of these pointed pieces retain fractures that are diagnostic of impact from weapon use.

Morphometric data strongly suggest that the Gademotta pieces fit well within the range experimentally documented for spear tips. Spear points may have been used for both thrusting and throwing (*e.g.*, Villa & Lenoir 2006). As a result, it can be securely concluded from the various lines of evidence that at least the majority of the Gademotta pointed pieces were used as javelin tips. This makes them the world's earliest stone-tipped projectile armatures (*cf.* Thieme 1997; Lombard & Phillipson 2010; Lombard 2011).

A confident identification of prehistoric armatures needs the incorporation of more than one method as each method has its own strengths and weaknesses. Although one could accept or reject the hypothesis that the Gademotta pointed pieces were used as the tips of hunting weapons based solely on any one of the approaches employed here, the picture derived from the combination of results from all methods provides sound and compelling interpretations.

The dominance of antelopes (possibly *A. buselaphus* and *C. taurinus*) and the representation of an aquatic species (*H. ampibius* Linne) in the faunal assemblage recovered from a wadi fill tentatively considered contemporaneous with the occupation at ETH-72-8B (Gautier 1974: 165) has raised the question of whether the makers of the earliest MSA tools hunted those animals. The absence of cultural modification marks and any faunal remains directly associated with the excavated occupation horizons rendered this hypothesis difficult to investigate (*see also* Brandt 1986).

Renewed attempts to establish the stratigraphic relationship of this fossil-bearing secondary deposit with the other units in the Gademotta area proved that this is by no means straightforward.

Later Middle Pleistocene paleoclimatic and paleoenvironmental data for the rift valley in Ethiopia are particularly meager (Gasse *et al*. 1980; Gasse & Street 1978; Brandt & Brook 1984; Revel *et al*. 2010). Evidence suggests that certain regions within and along the margins of the Omo Valley, the Main Ethiopian Rift and the Afar Rift provided favorable contexts that supported occupations during severe and dramatically fluctuating paleoclimatic/ paleoenvironmental phases of the Middle- and Upper Pleistocene (*e.g*. Blome *et al*. 2012; Basell 2008; Brandt *et al*. 2012). In the Gademotta region extreme paleoclimatic conditions of the Middle- and Upper Pleistocene were ameliorated by local conditions such as the location of the area at eco-zonal boundaries between woodland and "savannah" environments (Basell 2008: 2491; *also see* Trauth *et al*. 2010) and its relatively high altitude (~1900m *asl* where the sites are). Together with a near-lake paleoecology, and a nearby obsidian flow (Vogel *et al*. 2006; Negash *et al*. 2010), these must have encouraged the repeated occupation of sites in the region across the later Middle- and Upper Pleistocene (Wendorf & Schild 1974; Sahle *et al*. 2013). At Herto and Aduma, sedimentological and faunal evidence shows that Middle- and Upper Pleistocene occupations were in near-lake/river habitats (Clark 2003: 750-751; Yellen *et al*. 2005: 37). The faunal evidence from the Kibish sites

indicates the paleoenvironment of the area ranged from riverine and closed woodland habitats to grassland (Assefa 2008). In all of these site-complexes in the rift valley in Ethiopia, local situations likely ameliorated regional/continental scale paleoclimatic conditions, creating microenvironmental conditions with relatively stable habitat (Blome *et al*. 2012).

The multitude of evidence presented from the Gademotta and other MSA sites within the rift valley in Ethiopia afford a strong case that the behavior of later Middle Pleistocene hominin populations that lived there was not dramatically different from those of Upper Pleitocene ones. As indicated already, interpretation of the evidence in light of the presence/absence of traits of modernity alone does not contribute to the more important goal of reconstructing behavioral context using evolutionarily important dimensions. Instead, a comparison of the technological behavior of hominin population across the critical time period when our lineage emerged promises a more comprehensive picture (Minichillo 2005; Shea 2008, 2011; Wurz 2012).

Shea (2008: 478-480; *see also* Clark 1988) suggests that typological similarities among sites in the east African region may be indicative of population isolation, continuity and/or periodic dispersals (*e.g.* Brandt *et al*. 2012; Beyin 2006). Specific models, within the "lengthy process to modern human origins" (Weaver 2012) framework, hypothesize that changes in the adaptive strategies of hominins are brought about partly by environmental

changes (Lahr & Foley 1998). Specifically, the restoration of new ecological equilibrium in a given area introduces behavioral changes to hominin populations inhabiting the area (Lahr & Foley 1998: 148). The present dissertation has empirically tested these assumptions using archaeological data.

The emergence of a distinctly MSA occupation by >279 ka and the repeated occupation of the region across the later Middle- and earlier Upper Pleistocene indicate that there were stable adaptations at Gademotta. The enormous variability witnessed in the metric attributes of assemblages from GDM7 and GDM10 as well as the presence of evolutionarily crucial innovations such as stone-tipped projectile weapons in these later Middle Pleistocene occupations suggest that environmental conditions were sufficiently favorable to supporting stable demographic patterns evidenced in the stability of technological adaptations across this time period. The Gademotta later MP populations, and those from the broader rift valley in Ethiopia (Shea 2008; Clark *et al.* 2003), must have represented populations with successful adaptive strategies in a relatively stable sub-region. These later Middle Pleistocene populations/species must have expanded in the sub-region and been ancestral to *H. sapiens*. Closer to the Middle-Upper Pleistocene divide, the presence of the Nubian Techno-complex at ETH-72-6 provides a stronger evidence for some form of cultural/demographic exchange between this particular region, the Nile Valley, and Arabia (Van Peer *et al*. 2003; Rose *et al*. 2011). Such a pattern is also consistent with the

available evidence that, by 125 ka, humans occupied the Red Sea coast north of the Afar Rift and exploited marine food resources (Walter *et al.* 2000; Beyin 2006). At Porc Epic, on the southeastern margins of the Southern Afar Rift, later MSA humans transported and used perforated terrestrial gastropod opercula for symbolic purposes (Assefa *et al*. 2008). Interestingly, these beads show notable similarity in their shape with the ostrich eggshell beads from the northern Kenyan site of Enkapune Ya Muto, again suggesting demographic exchange/contact (Assefa *et al*. 2008: 754; Ambrose 1998).

Recently, there is an increasing tendency to depict the South African coastal regions as important crucible of modern humans based heavily on archaeological evidence for what are commonly accepted as markers of sophisticated behavior (Marean *et al*. 2007; Henshilwood *et al*. 2011; K. Brown *et al*. 2012). While the strength of the behavioral evidence from these contexts is an issue in itself (*see, for example, the strength of the evidence used to support the claim for the presence of projectile weapons at Pinnacle Point* [K. Brown *et al*. 2012] *in light of discussions provided in Chapter Five of this dissertation regarding a sound identification of such technologies*), the claims for South Africa as a uniquely important crucible of modern humans are poorly-grounded. Such claims downplay the rich data on technological, fossil, genetic, and paleoenvironmental records elsewhere on the continent spanning the later Middle- and earlier Upper Pleistocene.

First, the richness of the behavioral evidence in sites from coastal

South Africa might be the result of many factors, ranging from greater research attention to taphonomic biases and context of occupation (*e.g.* costal/near-coast caves *versus* open-air sites) (Shea 2012). Second, while Marean and colleagues (Marean *et al*. 2007) have agued that there is likely to be a close relation between climatic changes and the development of sophisticated behavior in the southern coastal regions of South Africa, other authors dispute this (Blome *et al*. 2012). In contrast, east Africa exhibits a pattern whereby microenvironmental conditions and high reliefs may have supported relatively persistent hominin occupations regardless of climatic changes marking this period (Blome *et al*. 2012). Third, based on genetic evidence, east Africa is the region where the first *H. sapiens* are most likely to have originated, with southern Africa peripheral at best (Ray *et al*. 2005). It is reasonable to assume that different regions on the African continent were more suitable for hominins at different periods, and that the origin of modern humans was a more complex process. However, data from various fields of study suggest that east Africa is the most likely source place for the earliest *H. sapiens* (White *et al*. 2003; McDougall *et al*. 2005; Pearson *et al*. 2008; Sahle *et al*. 2013; McBrearty & Tryon 2006; Shea 2008, 2011; Ray *et al*. 2005; Soares *et al*. 2012; Blome *et al.* 2012).

To sum up, based on the data presented in this dissertation, we can conclude that later Middle- and earlier Upper Pleistocene hominin populations in the Omo Valley, the Main Ethiopian Rift and the Afar Rift shared comparable capacities for behavioral variability. In addition, the rich

genetic, fossil and paleoenvironmental data strongly suggest that microenvironmental and ecological conditions in different areas within this region must have allowed stable habitats that supported continuous/repeated occupations. This is consistent with such strong models that suggest the presence of successful hominin populations during the later Middle Pleistocene that must have been ancestral to modern humans (Lahr & Foley 1998). Hominin populations within the rift system in Ethiopia produced and used projectile weapons from as early as >279 ka; exploited resources from distant sources, and practiced post-mortem manipulation and curation of human remains by 154 ka; inhabited coastal areas and exploited marine resources by 125 ka; and shared a regional technological tradition in the Upper Pleistocene across MIS 5. This evidence for behavioral variability strongly indicates the presence of hominin populations during the later Middle Pleistocene with behavioral capacities comparable to earlier Upper Pleistocene hominin populations. The earliest *H. sapiens* appeared in this part of the continent in a context where evolutionarily stable adaptations may have provided the crucible for the development of behavioral patterns that exist in all populations today.

BIBLIOGRAPHY

Ambrose, S.H. (1998). Chronology of the Later Stone Age and food production in East Africa. *Journal of Archaeological Science* 25, 377-392.

Asfaw, B., White, T.D., Lovejoy, O., Latimer, B., Simpson, S., Suwa, G. (1999). *Australopithecus garhi*: A new species of early hominid from Ethiopia. *Science* 284**,** 629-635.

Assefa, Z. (2008). The large-mammal fauna from the Kibish Formation. *Journal of Human Evolution* 55, 501-512.

Assefa, Z., Lam, Y.M., Mienis, H.K. (2008). Symbolic use of terrestrial gastropod opercula during the Middle Stone Age at Porc-Epic Cave, Ethiopia. *Current Anthropology* 49, 746-756.

Barham, L. (2002). Systematic pigment use in the Middle Pleistocene of south-central Africa. *Current Anthropology* 43(1), 181-190.

Barham, L., Mitchell, P. (2008). *The first Africans: African archaeology from the earliest tool-makers to most recent foragers*. Cambridge: Cambridge University Press.

Bar-Yosef, O. (1998). On the nature of transitions: The Middle to Upper Palaeolithic and the Neolithic revolution. *Cambridge Archaeological Journal* 8, 141–163.

Basell, L.S. (2008). Middle Stone Age (MSA) site distributions in eastern Africa and their relationship to Quaternary environmental change, refugia and the evolution of *Homo sapiens*. *Quaternary Science Reviews* 27, 2484-2498.

Berger, L.R., de Ruiter, D.J., Churchill, S.E., Schmid, P., Carlson, K.J., Dirks, P.H.G.M., Kibii, J.M. (2010). *Australopithecus sediba*: A new species of *Homo*-like Australopith from South Africa. *Science* 328, 195-204.

Bergman, C.A., Newcomer, M.H. (1983). Flint arrowhead breakage: Examples from Ksar Akil, Lebanon. *Journal of Field Archaeology* 10, 238-243.

Beyene, Y. (2010) Herto brains and minds: Behaviour of early *Homo Sapiens* from the Middle Awash, Ethiopia. In: Dunbar, R., Gamble, C., Gowlett, J. (Eds.), *Social brain, distributed mind*. Proceedings of the British Academy 158. Oxford: Oxford University Press, pp. 43-54.

Beyin, A. (2006). The Bab al Mandeb vs the Nile-Levant: An appraisal of two dispersal routes for early modern humans out of Africa. *African Archaeological Review* 23, 5-30.

Bird, D.W., O'Connell, J.F. (2006). Behavioral ecology and archaeology. *Journal of Archaeological Research* 14, 143-188.

Blome, M.W., Cohen, A.S., Tryon, C.A., Brooks, A.S., Russell, J. (2012). The environmental context for the origins of modern human diversity: A synthesis of regional variability in African climate 150,000-30,000 years ago. *Journal of Human Evolution* 62, 563-592.

Blumenschine, R., Masao, F.T., Tactikos, J., Ebert, J. (2008). Effects of distance from stone source on landscape-scale variation in Oldowan artifact assemblages in the Paleo-Olduvai Basin, Tanzania. *Journal of Archaeological Science* 35, 76-86.

Bordes, F. (1961). *Typologie du Paléolithique ancien et moyen*. Bordeaux: Delmas.

Bousman, C.B. (2005). Coping with risk: Later Stone Age technological strategies at Blydefontein rock shelter, South Africa. *Journal of Anthropological Archaeology* 24, 193-226.

Bouzouggar, A., Barton, N., Vanhaeren, M., d'Errico, F., Collcutt, S., Higham, T., Hodge, E., Parfitt, S., Rhodes, E., Schwenninger, J.-L., Stringer, C., Turner, E., Ward, S., Moutmir, A., Stambouli, A. (2007). 82,000-year-old shell beads from North Africa and implications for the origins of modern human behavior. *Proceedings of the National Academy of Sciences (PNAS) USA* 24, 9964-9969.

Brandt, S.A. (1986). The Upper Pleistocene and Early Holocene prehistory of the Horn of Africa. *African Archaeological Review* 4, 41-82.

Brandt, S.A., Brook, G.A. (1984). Archaeological and paleoenvironmental research in northern Somalia. *Current Anthropology* 25, 119-121.

Brandt, S.A., Fisher, E.C., Hildebrand, E.A., Vogelsang, R., Ambrose, S.H., Lesur, J., Wang, H. (2012). Early MIS 3 occupation of Mochena Borago Rockshelter, Southwest Ethiopian Highlands: Implications for Late Pleistocene archaeology, paleoenvironments and modern human dispersals. *Quaternary International* 274, 38-54.

Braun, D.R., Tactikos, J.C., Ferraro, J.V., Harris, J.W.K. (2005). Flake recovery rates and inferences of Oldowan hominin behavior: A response to Kimura 1999, 2002. *Journal of Human Evolution* 48, 525–531.

Braun, D.R., Plummer, T., Ditchfield, P., Ferraro, J.V., Maina, D., Bishop, L.C., Potts, R. (2008). Oldowan behavior and raw material transport: Perspectives from the Kanjera Formation. *Journal of Archaeological Science* 35, 2329–2345.

Brooks, A.S., Nevell, L., Yellen, J.E., Hartman, G. (2006). Projectile technologies of the African MSA: Implications for modern human origins. In: Hovers, E., Kuhn, S. (Eds.), *Transitions before the transition*. New York: Springer, pp. 233–255.

Brooks, A., Yellen, J.E., Tappen, M., Helgren, D.M. (2002). Middle Stone Age adaptations at Aduma, Middle Awash Region, Ethiopia. Abstracts for the Paleoanthropology Society Meetings. *Journal of Human Evolution* 42(3), A8–A9.

Broom, R. (1938). The Pleistocene anthropoid apes of South Africa. *Nature* 142**,** 377-379.

Brown, F.H., Reid, C., Negash, A. (2009). Possible isotopic fractionation of argon in source obsidians and archaeological artifacts from Kulkuletti, Ethiopia. *Journal of Archaeological Science* 36, 2119-2124.

Brown, F.H., McDougall, I., Fleagle, J.G. (2012). Correlation of the KHS tuff of the Kibish Formation to volcanic ash layers at other sites, and the age of early *Homo sapiens* (Omo I and Omo II). *Journal of Human Evolution* 63(4), 577-585.

Brown, K.S., Marean, C.W., Herries, A.I.R., Jacobs, Z., Tribolo, C., Braun, D.R., Roberts, D.L., Meyer, M.C., Bernatchez, J. (2009). Fire as an engineering tool of early modern humans. *Science* 325, 859-862.

Brown, K.S., Marean, C.W., Jacobs, Z., Schoville, B.J., Oestmo, S., Fisher, E., Bernatchez, J., Karkanas, P., Matthews, T. (2012). An early and enduring advanced technology originating 71,000 years ago in South Africa. *Nature* 491, 590-593.

Bruggemann, J.H., Buffler, R.T., Guillaume, M.M.M., Walter, R.C., Von Cosel, R., Ghebretensae, B.N., Berhe, S.M. (2004). Stratigraphy, palaeoenvironments and model for the deposition of the Abdur Reef Limestone: Context for an important archaeological site from the last interglacial on the Red Sea coast of Eritrea. *Palaeogeography, Palaeoclimatology, Palaeoecology* 203, 179-206.

Brunet, M., Guy, F., Pilbeam, D., Mackaye, H.T., Likius, A., Ahounta, D., Beauvilain, A., Blondel, C., Bocherens, H., Boisserie, J.-R., De Bonis, L., Coppens, Y., Dejax, J., Denys, C., Duringerq, P., Eisenmann, V., Fanone, G., Fronty, P., Geraads, D., Lehmann, T., Lihoreau, F., Louchart, A., Mahamat, A., Merceron, G., Mouchelin, G., Otero, O., Campomanes, P.P., De Leon, M.P., Rage, J.-C., Sapanetkk, M., Schusterq, M., Sudrek, J., Tassy, P., Valentin, X., Vignaud, P., Viriot, L., Zazzo**,** A., Zollikofer, C. (2002). A new hominid from the Upper Miocene of Chad, Central Africa. *Nature* 418, 145-151.

Caron, F., d'Errico, F., Moral, P.D., Santos, F., Zilhão, J. (2011). The Reality of Neandertal Symbolic Behavior at the Grotte du Renne, Arcy-sur-Cure, France. *Public Library of Science (PLoS) One* 6(6) *doi:10.1371/journal.pone.0021545*

Chase, P.G. (2003). Comment on "The origin of modern behavior: A review and critique of models and test implications" by Henshilwood, C.S., Marean, C.W. *Current Anthropology* 44(5), 637.

Churchill, S.E. (1993). Weapon technology, prey size selection, and hunting methods in modern hunter-gatherers: Implications for hunting in the Palaeolithic and Mesolithic. In: Peterkin, G.L., Bricker, H.M., Mellars, P.A. (Eds.), *Hunting and Animal Exploitation in the Later Palaeolithic and Mesolithic of Europe*. Archaeological Papers of the American Anthropological Association 4, pp. 11-24.

Churchill, S.E., Rhodes, J.A. (2009). The Evolution of the human capacity for "killing at a distance": The human fossil evidence for the evolution of projectile weaponry. In: Hublin, J.-J., Richards, M.P. (Eds.), *The Evolution of Hominin Diets: Integrating Approaches to the Study of Paleolithic Subsistence*. Dordrecht: Springer, pp. 201-210.

Clark, J.D. (1982). The transition from Lower to Middle Paleolithic in the African continent. In: Ronen, A. (Ed.), *The transition from the Lower to Middle Paleolithic and the origin of modern man*. Oxford: B.A.R International Series 151, pp. 235-255.

Clark, J.D. (1988). The Middle Stone Age of East Africa and the beginning of regional identity. *Journal of World Prehistory* 2, 235-305.

Clark, J.D., Beyene, Y., WoldeGabriel, G., Hart, W.K., Renne, P.R., Gilbert, H., Defleur, A., Suwa, G., Katoh, S., Ludwig, K.R., Boisserie, J.R., Asfaw, B., White, T.D. (2003). Stratigraphic, chronological and behavioural contexts of Pleistocene *Homo sapiens* from Middle Awash, Ethiopia. *Nature* 423, 747-752.

Clark, J.D., de Heinzelin, J., Schick, K.D., Hart, W.K., White, T.D., WoldeGabriel, G., Walter, R.C., Suwa, G., Asfaw, B., Vrba, E., Haile-Selassie, Y. (1994). African *Homo erectus*: Old radiometric ages and young Oldowan assemblages in the Middle Awash Valley, Ethiopia. *Science* 264, 1907-1910.

Clarkson, C. (2002). Holocene scraper reduction, technological organization and land use at Ingaladdi Rockshelter, Northern Australia. *Archaeology in Oceania* 37(2), 79-86.

Conard, N.J., Bolus, M. (2003) Radiocarbon dating the appearance of modern humans and timing of cultural innovations in Europe: New results and new challenges. *Journal of Human Evolution* 44(3), 331-371.

Cotterell, B., Kamminga, J. (1987). The formation of flakes. *American Antiquity* 52, 675–708.

Dainelli, N., Benvenuti, M., Sagri, M., (2001). *Geological Map of the Ziway-Shala lakes basin (Ethiopia)*. Firenze: European Commission (EC) STD3 Project-Contract TS3*- CT92-0076.

Dart, R. (1925). *Australopithecus africanus*. The man-ape of South Africa. *Nature* 115, 195-199.

Davidson, I. (2003). Comment on "The origin of modern behavior: A review and critique of models and test implications" by Henshilwood, C.S., Marean, C.W. *Current Anthropology* 44(5), 637-638.

Davis, Z. J., Shea, J.J. (1998). Quantifying lithic curation: an experimental test of Dibble and Pelcin's original flake-tool mass predictor. *Journal of Archaeological Science* 25, 603-610.

Day M.H., Stringer C.B. (1991). Les restes crâniens d'Omo-Kibish et leur classification à l'intéreur du genre *Homo*. *L'Anthropologie* 95, 573-594.

Deacon, H.J., Deacon, J. (1999) *Human beginnings in South Africa*. Cape Town: David Philip.

Deacon H.J., Wurz, S. (2001). Middle Pleistocene populations of southern Africa and the emergence of modern behavior. In: Barham, L., Robson-Brown, K. (Eds.), *Human roots: Africa and Asia in the Middle Pleistocene*. Bristol: Western Academic & Specialist Press, pp. 55-63.

d'Errico, F. (2003). The invisible frontier. A multiple species model for the origin of behavioral modernity. *Evolutionary Anthropol*ogy 12, 188-202.

d'Errico, F. (2007). The origin of humanity and modern cultures: Archaeology's view. *Diogenes* 54(2), 122-133.

d'Errico, F., García Moreno, R., Rifkin, R. (2012). Technological, elemental and colorimetric analysis of an engraved ochre fragment from the Middle Stone Age levels of Klasies River Cave 1, South Africa. *Journal of Archaeological Science* 39, 942-952.

d'Errico, F., Stringer, C.B. (2011). Evolution, revolution or saltation scenario for the emergence of modern cultures? *Philosophical Transactions of the Royal Society B* 366, 1060-1069.

Deino, A.L., McBrearty, S. (2002). $^{40}Ar/^{39}Ar$ dating of the Kapthurin Formation, Baringo, Kenya. *Journal of Human Evolution* 42, 185-210.

Dibble, H.L. (1995). Middle Paleolithic scraper reduction: Background, clarification, and review of the evidence to date. *Journal of Archaeological Method and Theory* 2(4), 299-386.

Dibble, H.L. (1997). Platform variability and flake morphology: A comparison of experimental and archaeological data and implications for interpreting prehistoric lithic technological strategies. *Lithic Technology* 22(2), 150-170.

Dibble, H.L, Rezek, Z. (2009). Introducing a new experimental design for controlled studies of flake formation: Results for exterior platform angle, platform depth, angle of blow, velocity, and force. *Journal of Acraheological Science* 36, 1945-1954.

Dominguez-Rodrigo, M., Mabulla , A., Luque, L., Thompson, J.W., Rink, J., Bushozi, P., Dı´ez-Martin, F., Alcala, L. (2008). A new archaic *Homo sapiens* fossil from Lake Eyasi, Tanzania. *Journal of Human Evolution* 54, 899-903.

Douze, K. (2010). The "tranchet blow" technique at Gademotta and Kulkuletti Early Middle Stone Age sites (Ethiopia). *The 20th Meeting of the Society of Africanist Archaeologists (SAfA)* [Abstract]. Dakar: IFAN-Cheikh Anta Diop & Université Cheikh Anta Diop de Dakar, pp. 110-112.

Eren, M.I., Dominguez-Rodrigo, M., Kuhn, S.L., Adler, D.S., Le, I., Bar-Yosef, O. (2005). Defining and measuring reduction in unifacial stone tools. *Journal of Archaeological Science* 32, 1190-1201.

Fischer, A., Hansen, P.V., Rasmussen, P. (1984). Macro and micro wear traces on lithic projectile points: Experimental results and prehistoric examples. *Journal of Danish Archaeology* 3, 19-46.

Gabunia, L., Vekua, A., Lordkipanidze, D., Swisher III, C.C., Ferring, R., Justus, A., Nioradze, M., Tvalchrelidze, M., Antón, S.C., Bosinski, G., Jöris, O., de Lumley, M.-A., Maisuradze, G., Mouskhelishvili, A. (2000): Earliest Pleistocene hominid cranial remains from Dmanisi, Republic of Georgia: Taxonomy, geological setting, and age. *Science* 288(5468), 1019-1025.

Gamble, C. (2007). *Origins and revolutions: Human identity in earliest prehistory*. New York: Cambridge University Press.

Gasse, F., Rognon, R., Street, F.A. (1980). Quaternary history of the Afar and Ethiopian Rift lakes. In: Williams, M.A.J., Faure, H. (Eds.), *The Sahara and the Nile*. Rotterdam: A.A. Balkema, pp. 361-400.

Gasse, F., Street, F.A. (1978). Late Quaternary lake-level fluctuations and environments of the Northern Rift Valley and Afar Region (Ethiopia and Djibouti). *Palaeogeography, Palaeoclimatology, Palaeoecology* 24, 279-325.

Gautier, A. (1974). Some mammalian remains from a fossil wadi near the base of the Gademotta Formation. In: Wendorf, F., Schild, R. (Eds.), *A Middle Stone Age Sequence from the Central Rift Valley, Ethiopia* Warsaw: Ossolineum, pp. 160-165.

Goodwin, A.J.H., Van Riet Lowe, C. (1929). The Stone Age cultures of South Africa. *Annals of the South African Museum* 27, 1-146.

Gossa, T., Sahle, Y., Negash, A. (2012). A reassessment of the Middle and Later Stone Age assemblages from Aladi Spring, Southern Afar Rift, Ethiopia. *Azania: Archaeological research in Africa* 47(2), 210-222.

Groves, C., Throne, A. (2000). The affinities of the Klasies River Mouth remains. *Perspectives in Human Biology* 5, 43-53.

Grün, R., Beaumont, p., Tobias, P.V., Eggins, S. (2003). On the age of Border Cave 5 human mandible. *Journal of Human Evolution* 45, 155-167.

Grün, R., Brink, J.S., Spooner, N.A., Taylor, L., Stringer, C.B., Franciscus, R.G., Murray, A.S. (1996). Direct dating of Florisbad hominid. *Nature* 382, 500-501.

Haile-Selasssie, Y., Asfaw, B., White, T.D. (2004a). Hominid cranial remains from Upper Pleistocene deposits at Aduma, Middle Awash, Ethiopia. *American Journal of Physical Anthropology* 123, 1-10.

Haile-Selassie, Y., Suwa, G., White, T.D. (2004b). Late Miocene teeth from Middle Awash, Ethiopia, and early hominid dental evolution. *Science* 303, 1503-1505.

Haynes, C.V., Jr. (1980). The Clovis culture. *Canadian Journal of Anthropology* 1, 115-121.

Henshilwood, C.S., d'Errico, F., van Niekerk, K.L., Coquinot, Y., Jacobs, Z., Lauritzen, S.-E., Menu, M., García-Moreno, R., (2011). A 100,000-year-old ochre-processing workshop at Blombos Cave, South Africa. *Science* 334, 219-222.

Henshilwood, C.S., d'Errico, F., Watts, I. (2009). Engraved ochres from the Middle Stone Age levels at Blombos Cave, South Africa. *Journal of Human Evolution* 57, 27-47.

Henshilwood, C.S., Marean, C.W. (2003). The origin of modern human behavior: Critique of the models and their test implications. *Current Anthropology* 44(5), 627-651.

Herries, A. (2011). A chronological perspective on the Acheulian and its transition to the Middle Stone Age in southern Africa: The question of the Fauresmith. *International Journal of Evolutionary Biology* doi:10.4061/2011/961401

Holdaway, S. (1989). Were there hafted projectile points in the Mousterian? *Journal of Field Archaeology* 16, 79-86.

Hovers, E., Belfer-Cohen, A. (2006). "Now you see it, now you don't" – Modern human behavior in the Middle Paleolithic. In: Hovers, E., Kuhn, S.L. (Eds.), *Transitions before the transition: Evolution and stability in the Middle Plaeolithic and Middle Stone Age*. New York: Springer, pp. 295-304.

Ho Ho Committee (1979). The Ho Ho classification and nomenclature committee report. In: Hayden, B. (Ed.), *Lithic use-wear analysis*. New York: Academic Press.

Hutchings, W.K. (1997). *The Paleoindian fluted point: dart or spear armature? The identification of Paleoindian delivery technology through analysis of lithic fracture velocity*. Unpublished Ph.D. dissertation. Simon Fraser University.

Hutchings, W.K. (1999). Quantification of fracture propagation velocity employing a sample of Clovis channel flakes. *Journal of Archaeological Science 26*, 1437-1447.

Hutchings, W.K. (2011). Measuring use-related fracture velocity in lithic armatures to identify spears, javelins, darts, and arrows. *Journal of Archaeological Science* 37, 1749-1765.

Ingman, M., Kaessmann, H., Pääbo, S., Gyllensten, U. (2000). Mitochondrial genome variation and the origin of modern humans. *Nature* 408, 708–713.

Ivita, R. (2011). Shape variation in Aterian tanged tools and the origins of projectile technology: A morphometric perspective on stone tool function. *Public Library of Science (PLoS) One* 6(12) doi:10.1371/journal.pone.0029029

Johanson, D.C., White, T.D., Coppens, Y. (1978). A new species of the genus *Australopithecus* (Primates: Hominidae) from the Pliocene of Eastern Africa. *Kirtlandia* 28, 2-14.

Johnson, C.R., McBrearty, S. (2010). 500,000 year old blades from the Kapthurin Formation, Kenya. *Journal of Human Evolution* 58, 198-200.

Klein, R. G. (1999). *The Human Career*. 2nd Edition. Chicago: Chicago University Press.

Klein, R.G. (2000). Archaeology and the evolution of human behavior. *Evolutionary Anthropology* 9, 17–36.

Klein, R.G. (2008). Out of Africa and the evolution of human behavior. *Evolutionary Anthropology* 17, 267–281.

Klein, R.G., Cruz-Uribe, K. (1996). Exploitation of large bovids and seals at Middle and Later Stone Age sites in South Africa. *Journal of Human Evolution* 31, 315-334.

Klein, R.G., Edgar, B. (2002). *The dawn of human culture*. New York: Wiley and Sons.

Krause, J., Lalueza-Fox, C., Orlando. L., Enard, W., Green, R.E., Burbano, H.A., Hublin, J.-J., Hänni, C., Fortea, J., de la Rasilla, M., Bertranpetit, J., Rosas, A., Pääbo, S. (2007). The derived *FOXP2* variant of modern humans was shared with Neandertals. *Current Biology* 17, 1-5.

Kuhn, S.L. (1991). "Unpacking" reduction: Lithic raw material economy in the Mousterian of west-central Italy. *Journal of Anthropological Archaeology* 10(1), 76-106.

Kuhn, S.L. (1992). Blank form and reduction as determinants of Mousterian scraper morphology. *American Antiquity* 57(1), 115-128.

Kurashina, H. (1978). *An examination of prehistoric lithic technology in east-central Ethiopia*. Unpublished Ph.D. dissertation. University of California, Berkeley.

Lahr, M.M., Foley, R.A. (1998). Towards a theory of modern human origins: Geography, demography and diversity in recent human evolution. *Yearbook of Physical Anthropology* 41, 137-176.

Laury, R.B., Albritton, C.C. (1975). Geology of Middle Stone Age archaeological sites in the Main Ethiopian Rift Valley. *Geological Society of America Bulettin,* 86, 999-1011.

Leakey, L.S.B. (1959). A new fossil from Olduvai. *Nature* 184, 491-494.

Leakey, L.S.B., Tobias, P.V., Napier, J.R. (1964). A new species of the genus *Homo* from Olduvai Gorge. *Nature* 202, 7-9.

Leakey, M.G., Feibel, C.S., McDougall, I., Walker, A. (1995). New four-million-year-old hominid species from Kanapoi and Allia Bay, Kenya. *Nature* 376, 565-571.

Leakey, M.G., Feibel, C.S., McDougall, I., Ward, C., Walker, A. (1998). New specimens and confirmation of an early age for *Australopithecus anamensis. Nature* 393, 62-66.

Lombard, M. (2005). A method for identifying Stone Age hunting tools. *The South African Archaeological Bulletin* 60, 115-120.

Lombard, M. (2007). The gripping nature of ochre: The association of ochre with Howiesons Poort adhesive and Later Stone Age mastics from South Africa. *Journal of Human Evolution* 53, 406-419.

Lombard, M. (2011). Quartz-tipped arrows older than 60 ka: Further use-trace evidence from Sibudu, KwaZulu-Natal, South Africa. *Journal of Archaeological Science* 38, 1918-1930.

Lombard, M. (2012). Thinking through the Middle Stone Age of sub-Saharan Africa. *Quaternary International* 270, 140-155.

Lombard, M., Phillipson, L. (2010). Indications of bow and stone-tipped arrow use 64,000 years ago in KwaZulu-Natal, South Africa. *Antiquity* 84, 1-14.

Marean, C.W., Assefa, Z. (1999). Zooarcheological evidence for the faunal exploitation behavior of Neandertals and early modern humans. *Evolutionary Anthropology* 8, 22-37.

Marean, C.W., Bar-Matthews, M., Bernatchez, J., Fisher, E., Goldberg, P., Herries, A.I., Jacobs, Z., Jerardino, A., Karkanas, P., Minichillo, T., Nilssen, P.J., Thompson, E., Watts, I., Williams, H. (2007). Early human use of marine resources and pigment in South Africa during the Middle Pleistocene. *Nature* 449, 905-908.

McBrearty, S., Brooks, A.S. (2000). The revolution that wasn't: A new interpretation of the origin of modern human behavior. *Journal of Human Evolution,* 39, 453-563.

McBrearty, S., Tryon, C.A. (2006). From Acheulian to Middle Stone Age in the Kapthurin Formation, Kenya. In: Hovers, E., Kuhn, S.L. (Eds.), *Transitions before the transition: Evolution and stability in the Middle Plaeolithic and Middle Stone Age.* New York: Springer, pp. 257-277.

McDougall, I., Brown, F.H., Fleagle, J.G. (2005). Stratigraphic placement and age of modern humans from Kibish, Ethiopia. *Nature* 433, 733-736.

McDougall, I., Brown, F.H., Fleagle, J.G. (2008). Sapropels and the age of hominins Omo I and II, Kibish, Ethiopia. *Journal of Human Evolution* 55, 409-420.

McPherron, S.J.P., Dibble, H.L. (2002). Using computers in adverse field conditions: Tales from the Egyptian desert. *The SAA Archaeological Record* 3, 28-32.

Mellars P. (1996). *The Neanderthal legacy: An archaeological perspective from western Europe*. Princeton: Princeton University Press.

Mellars P. (2005). The impossible coincidence: A single species model for the origins of modern human behavior in Europe. *Evolutionary Anthropol*ogy14, 12-27.

Mellars, P.A. (2006). Why did modern human populations disperse from Africa ca. 60,000 years ago? A new model. *Proceedings of the National Academy of Sciences of the USA* 103, 9381-9386.

Mellars, P.A. (2007). Rethinking the human revolution: Eurasian and African perspectives. In: Mellars, P., Boyle, K., Bar-Yosef, O., Stringer, C.B. (Eds.) *Rethinking the human revolution*. Cambridge: McDonald Institute for Archaeological Research, pp. 1-14.

Mercader, J. (2009). Mozambican grass seed consumption during the Middle Stone Age. *Science* 326, 1680-1683.

Mercader, J., Bennett, T., Raja, M. (2008). Middle Stone Age starch acquisition in the Niassa Rift, Mozambique. *Quaternary Research* 70, 283-300.

Merrick, H.V., Brown, F.H., Nash, W.P. (1994) Use and movement of obsidian in the Early and Middle Stone Ages of Kenya and northern Tanzania. In: Childs, S.T (Ed.) *Society, culture, and technology in Africa*, pp. 29-44.

Milo, R.G. (1998). Evidence for hominid predation at Klasies River Mouth, South Africa, and its implications for the behaviour of early modern humans. *Journal of Archaeological Science* 25, 99-133.

Minichillo, T.J. (2005). *Middle Stone Age lithic study, South Africa: An examination of modern human origins*. Unpublished Ph.D. Dissertation. University of Washington.

Morgan, L.E., Renne, P.R. (2008). Diachronous dawn of Africa's Middle Stone Age: New $^{40}Ar/^{39}Ar$ ages from the Ethiopian Rift. *Geology* 36 (12), 967-970.

Negash, A., Brown, F.H., Alene, M., Nash, B. (2010). Provenance of Middle Stone Age obsidian artifacts from the central sector of the Main Ethiopian Rift Valley. *SINET: Ethiopian Journal of Science* 33(1), 21-30.

Negash, A., Brown, F.H., Nash, B., (2011). Varieties and sources of artifactual obsidian in the Middle Stone Age of the Middle Awash, Ethiopia. *Archaeometry* 53(4), 661-673.

Negash, A., Shackley, M.S. (2006). Geochemical provenance of obsidian artefacts from the MSA site of Porc Epic, Ethiopia. *Archaeometry* 48(1), 1-12.

Neuhäuser, M., Ruxton, G.D. (2009). Distribution-free two-sample comparisons in the case of heterogeneous variances. *Behavioral Ecology and Sociobiology* 63, 617-623.

Nomade, S., Renne, P.R., Vogel, N., Deino, A.L., Sharp, W.D., Becker, T.A., Jaouni, A.R., Mundil, R. (2005). Alder Creek sanidine (ACs-2): A Quaternary Ar-40/Ar-39 dating standard tied to the Cobb Mountain geomagnetic event. *Chemical Geology* 218, 315-338.

Nowell, A. (2010). Defining behavioral modernity in the context of Neandertal and anatomically modern human populations. *Annual Review of Anthropology* 39, 437-452.

O'Connell, J.F. (2006). How did modern humans displace Neanderthals? Insights from hunter-gatherer ethnography and archaeology. In: Conard, N. (Ed.), *Neanderthals and modern humans meet?* Tübingen: Kerns Verlag, pp. 43-64.

Odell, G.H., Cowan, F. (1986). Experiments with spears and arrows on animal targets. *Journal of Field Archaeology* 13, 195-212.

Pearson, O.M., Royer, D.F., Grine, F.E., Fleagle, J.G. (2008). A description of the Omo I postcranial skeleton, including newly discovered fossils. *Journal of Human Evolution* 55, 421-437.

Pickford, M., Senut, B. (2001). 'Millennium Ancestor', a 6-million-year-old bipedal hominid from Kenya - Recent discoveries push back human origins by 1.5 million years. *South African Journal of Science* 97**,** 22-22.

Pleurdeau, D. (2005). Human technical behavior in the African Middle Stone Age: The lithic assemblage of Porc-Epic Cave (Dire Dawa, Ethiopia). *African Archaeological Review* 22(4), 177-197.

Porat, N., Chazan, M., Grün, R., Aubert, M., Eisenmann, V., Horwitz, L.K. (2010). New radiometric ages for the Fauresmith industry from Kathu Pan, southern Africa: Implications for the Earlier to Middle Stone Age transition. *Journal of Human Evolution* 37, 269-283.

Potts, R. (1998). Variability selection and hominid evolution. *Evolutionary Anthropology* 7, 81-96.

Powell, A., Shennan, S., Thomas, M.G. (2009). Late Pleistocene demography and the appearance of modern human behavior. *Science* 324, 1298-1301.

Ravi-Chandar, K. (2004) *Dynamic fracture*. Amsterdam: Elsevier.

Ray, N., Currat, M., Berthier, P., Excoffier, L. (2005). Recovering the geographic origin of early modern humans by realistic and spatially explicit simulations. *Genome Research* 15, 1161-1167.

Renne, P.R., Balco, G., Ludwig, K.R., Mundil, R., Min, K. (2011). Response to the comment by W.H. Schwarz *et al*. on "Joint determination of ^{40}K decay constants and $^{40}Ar^*/^{40}K$ for the Fish Canyon sanidine standard, and improved accuracy for $^{40}Ar/^{39}Ar$ geochronology" by P.R. Renne *et al*. (2010). *Geochimica et Cosmochimica Acta* 75 (17), 5097-5100.

Renne, P.R., Knight, K.B., Nomade, S., Leung, K.N., Lou, T.P. (2005). Application of deuterondeuteron (D-D) fusion neutrons to Ar-40/Ar-39 geochronology: *Applied Radiation and Isotopes* 62, 25-32.

Renne, P.R., Swisher, C.C., III, Deino, A.L., Karner, D.B., Owens, T., DePaolo, D.J., (1998). Intercalibration of standards, absolute ages and uncertainties in $^{40}Ar/^{39}Ar$ dating. *Chemical Geolology* 145(1-2), 117-152.

Revel, M., Ducassou, E., Grousset, F.E., Bernasconi, S.M., Migeon, S., Revillon, S., Mascle, J., Murat, A., Zaragosi, S., Bosch, D. (2010). 100,000 years of African monsoon variability recorded in sediments of the Nile margin. *Quaternary Science Reviews* 29, 1342-1362.

Richerson, P.J., Boyd, R., Bettinger, R.L. (2009). Cultural innovations and demographic change. *Human Biology* 81, 211-235.

Rightmire, G.P. (1991). The Dispersal of *Homo erectus* from Africa and the emergence of more modern humans. *Journal of Anthropological Research* 47(2), 177-191.

Rightmire, G.P. (2008). Homo in the middle Pleistocene: Hypodigms, variation, and species recognition. *Evolutionary Anthropology* 17, 8-21.

Rose, J.I., Usik, V.I., Marks, A.E., Hilbert, Y.H., Galletti, C.S., Parton, A., Geiling, J.M., Cerny, V., Morley, M.W., Roberts, R.G. (2011). The Nubian Complex of Dhofar, Oman: An African Middle Stone Age industry in southern Arabia. *Public Library of Science (PLoS) One* 6 (11) doi:10.1371/journal.pone.0028239

Rots, V. (2012). Insights into early Middle Palaeolithic tool use and hafting in Western Europe. The functional analysis of level IIa of the early Middle Palaeolithic site of *Biache-Saint-Vaast* (France). *Journal of Archaeological Science* 40(1), 497-506.

Rots, V., Van Peer, P., Vermeersch, P.M. (2011). Aspects of tool production, use, and hafting in Palaeolithic assemblages from Northeast Africa. *Journal of Human Evolution* 60, 637-664.

Sahle, Y., Beyene, Y. (*forthcoming*). Behavioral capacities of the earliest *Homo sapiens*: Inferences from Middle Awash, Ethiopia. (*A contribution in an upcoming monograph on Herto*).

Sahle, Y., Morgan, L.E., Braun D.R., Atnafu, B., Hutchings, W.K. (2013). Chronological and behavioral contexts of the earliest Middle Stone Age in the Gademotta Formation, Main Ethiopian Rift. *Quaternary International*. doi.org/10.1016/j.quaint.2013.03.010

Sahle, Y., Negash, A. (2010). An ethnoarchaeology of lithic site-formation patterns amongst the Hadiya of Ethiopia: Some intial results. *Nyame Akuma* 74, 36-41.

Sahle, Y., Negash, A., Braun, D.R. (2012). Variability in ethnographic hidescraper use among the Hadiya of Ethiopia: Implications for reduction analysis. *African Archaeological review* 29(4), 383-397.

Sano, K. (2009). Hunting evidence from stone artefacts from the Magdalenian cave site Bois Laiterie, Belgium: a fracture analysis. *Quartär* 56, 67-86.

Schild, R., Wendorf, F. (2005). Gademotta and Kulkuletti and the ages for the beginning of the Middle Paleolithic in Africa. *Journal of the Israel Prehistoric Society* 35, 117-142.

Schmitt, D.O., Churchill, S.E., Hylander, W.L. (2003). Experimental evidence concerning spear use in Neandertals and early modern humans. *Journal of Archaeological Science* 30, 103-114.

Shea, J. J. (1988). Spear points from the Middle Paleolithic of the Levant. *Journal of Field Archaeology* 15, 441-450.

Shea, J.J. (2006). The origins of lithic projectile point technology: Evidence from Africa, the Levant, and Europe. *Journal of Archaeological Science* 33, 823-846.

Shea, J.J. (2008). The Middle Stone Age archaeology of the Lower Omo Valley Kibish Formation: Excavations, lithic assemblages and inferred patterns of early *Homo sapiens* behavior. *Journal of Human Evolution* 55, 448-485.

Shea, J.J. (2009). The impact of projectile weaponry on Late Pleistocene human evolution. In: Hublin, J.-J., Richards, M. (Eds.), *The evolution of diets: Integrating approaches to the study of Paleolithic subsistence*. Dordrecht: Springer, pp. 187-197.

Shea, J.J. (2011) *Homo sapiens* is as *Homo sapiens* was: Behavioral variability versus "behavioral modernity" in Paleolithic Archaeology. *Current Anthropology* 52(1), 1-35.

Shea, J.J. (2012) "Early" symbolic material culture in South Africa: A comment on Henshilwood and Dubreuil. *Current Anthropology* 53(1), 130-131.

Shea, J.J., Davis, Z., Brown, K. (2001). Experimental tests of Middle Paleolithic spear points using a calibrated crossbow. *Journal of Archaeological Science* 28, 807-816.

Shea, J.J., Sisk, M.L. (2010) Projectile technology and *Homo sapiens* dispersal from Africa to Western Eurasia. *PaleoAnthropology*, 100-122.

Shott, M.J. (1989). On tool-class use lives and the formation of archaeological assemblages. *American Antiquity,* 54(1), 9-30.

Shott, M.J. (1996). An exegesis of the curation concept. *Journal of Anthropological Research,* 52(3), 259-280.

Shott, M.J., Bradbury, A.P., Carr, P.J. (2000). Flake size from platform attributes: Predictive and empirical approaches. *Journal of Archaeological Science* 27, 877-894.

Shott, M.J., Weedman, K.J. (2007). Measuring reduction in stone tools: An ethnoarchaeological study of Gamo hidescrapers from Ethiopia. *Journal of Archaeological Science* 34, 1016-1035.

Sisk, M.L., Shea, J.J. (2008). Intrasite spatial variation of the Omo Kibish Middle Stone Age assemblages: Artifact refitting and distribution patterns. *Journal of Human Evolution* 55, 486-500.

Sisk, M.L., Shea, J.J. (2010). Defining complex projectile technology: A reply to Whittaker. *PaleoAnthropology*, L08-L09.

Sisk, M.L., Shea, J.J. (2011). The African origin of complex projectile technology: An analysis using tip cross-sectional area and perimeter. *International Journal of Evolutionary Biology* doi:10.4061/2011/968012

Soares, P., Alshamali, F., Pereira, J.B., Fernandes, V., Silva, N.M., Afonso, C., Costa, M.D., Musilová, E., Macaulay, V., Richards, M.B., Cerny, V., Pereira, L. (2012). The expansion of mtDNA Haplogroup L3 within and out of Africa. *Molecular and Biological Evolution* 29, 915-927.

Steiger, R.H., Jäger, E. (1977). Subcommission on geochronology: Convention on the use of decay constants in geo- and cosmochemistry. *Earth and Planetary Science Letters* 36, 359-362.

Stringer, C.B. (2007). The origin and dispersal of *Homo sapiens*: Our current state of knowledge. In: Mellars, P., Boyle, K., Bar-Yosef, O., Stringer, C.B. (Eds.), *Rethinking the human revolution: New behavioural and biological and perspectives on the origins and dispersal of modern humans*. Cambridge: McDonald Institute, pp. 15-20.

Suwa, G., Asfaw, B., Beyene, Y., White, T.D., Katoh, S., Nagaoka, S., Nakaya, H., Uzawa, K., Renne, P., WoldeGabriel, G. (1997). The first skull of *Australopithecus boisei. Nature* 389, 489-492.

Tattersall, I., Schwartz, J.H. (2008). The morphological distinctiveness of *Homo sapiens* and its recognition in the fossil record: Clarifying the problem. *Evolutionary Anthropology* 17, 49-54.

Texier, P.-J. Poraz, G., Parkington, J., Rigaud, J.-P., Poggenpoel, C., Miller, C., Tribolo, C., Cartwrite, C., Coudenneau, A., Klein, R., Steele, T., Verna, C. (2010). A Howiesons Poort tradition of engraved ostrich eggshell containters dated to 60,000 years ago at Diepkloof Rock Shelter, South Africa. *Proceedings of the National Academy of Sciences (PNAS) USA* 107, 6180-6185).

Thieme, H. (1997). Lower Paleolithic hunting spears from Germany. *Nature* 385, 807-810.

Trauth, M.H., Maslin, M.A., Deino, A.L., Junginger, A., Lesoloyia, M., Odada, E.O., Olago, D.O., Olaka, L.A., Strecker, M.R., Tiedemann, R. (2010). Human evolution in a variable environment: The amplifier lakes of Eastern Africa. *Quaternary Science reviews* 29, 2981-2988.

Tryon, C.A. (2011). Comment on "*Homo sapiens* is as *Homo sapiens* was: Behavioral variability versus "behavioral modernity" in Paleolithic Archaeology" by Shea, J.J. *Current Anthropology* 52(1), 22-23.

Tryon, C.A., McBrearty, S. (2002). Tephrostratigraphy and the Acheulian to Middle Stone Age transition in the Kapthurin Formation, Baringo, Kenya. *Journal of Human Evolution* 42, 211-235.

Tryon, C.A., McBrearty, S. (2006) Tephrostratigraphy of the Bedded Tuff Member (Kapthurin Formation, Kenya) and the nature of archaeological change in the later Middle Pleistocene. *Quaternary Research* 65, 492-507.

Tryon C.A., McBrearty, S., Texier, P.-J. (2005). Levallois lithic technology from the Kapthurin Formation, Kenya: Acheulean origin and Middle Stone Age diversity. *African Archaeological Review* 22 (4), 199-229.

Tryon, C.A., Roach, N.T., Logan, M.A.V. (2008). The Middle Stone Age of the northern Kenyan Rift: Age and context of new archaeological sites from the Kapedo Tuffs. *Journal of Human Evolution* 55, 652-664.

Tryon, C.A., Potts, R. (2011). Approaches for Understanding Flake Production in the African Acheulean. *PlaeoAnthropology*, 376-389.

Van Peer, P. (1992). The Levallois reduction strategy. *Monographs in World Archaeology 13*. Madison: Prehistory Press.

Van Peer, P., Fullagar, R., Stokes, S., Bailey, R. M., Moeyersons, J., Steenhudt, F., Geerts, A., Vanderbeken, T., De Dapper, M., Geus, F. (2003). The Early to Middle Stone Age transition and the emergence of modern human behavior at site 8-B-11, Sai Island, Sudan. *Journal of Human Evolution* 45, 187-194.

Van Peer, P., Vermeersch, P. (2007). The place of northeast Africa in the early history of modern humans: New data and interpretations on the Middle Stone Age. In: Mellars, P., Boyle, K., Bar-Yosef, O., Stringer. C.B., (Eds.), *Rethinking the Human Revolution*. Cambridge: McDonald Institute for Archaeological Research, pp 187-198.

Vekua, A., Lordkipanidze, D., Rightmire, G.P., Agusti, J., Ferring, R., Maisuradze, G., Mouskhelishvili, A., Nioradze, A., de Leon, M.P., Tappen, M., Tvalchrelidze, M., Zollikofer, C. (2002). A new skull of early *Homo* from Dmanisi, Georgia. *Science* 297(5578), 85-89.

Villa, P., Lenoir, M. (2006). Hunting weapons of the Middle Stone Age and the Middle Palaeolithic: Spear points from Sibudu, Rose Cottage and Bouheben. *South African Humanities* 18, 89-122.

Villa, P., Soressi, M., Henshilwood, C., Mourre, V. (2009). The Still Bay points of Blombos Cave (South Africa). *Journal of Archaeological Science* 36, 441-460.

Vogel, N., Nomade, S., Negash, A., Renne, P.R. (2006). Forensic $^{40}Ar/^{39}Ar$ dating: A provenance study of Middle Stone Age obsidian artifacts from Ethiopia. *Journal of Archaeological Science* 33, 1749-1765.

Wadley, L. 2001. What Is Cultural Modernity? A General View and A SouthAfrican Perspective From Rose Cottage Cave. *Cambridge Archaeological Journal* 11, 201-221.

Wadley, L., Hodgskiss, T., Grant, M. (2009). Implications for complex cognition from the hafting of tools with compound adhesives in the Middle Stone Age, South Africa. *Proceedings of the National Academy of Sciences (PNAS) USA* 106(24), 9590-9594.

Wadley, L., Sievers, C., Bamford, M., Goldberg, P., Berna, F., Miller, C. (2011). Middle Stone Age bedding construction and settlement patterns at Sibudu, South Africa. *Science* 334, 1388-1391.

Wallner, H. (1939). Linienstrukturen an Bruchflachen. *Zeitschrift fur Physik* 114, 368-378.

Walter, R., Buffler, R.T., Bruggemann, J.H., Guillaume, M.M.M., Berhe, S.M., Negassi, B., Libeskal, Y., Cheng, H., Edwards, R.L., Von Cosel, R., Néraudeau, D., Gagnon, M. (2000). Early human occupation of the Red Sea coast of Eritrea during the last interglacial. *Nature* 405, 65-69.

Watts, I. (2010). The pigments from Pinnacle Point Cave 13B, Western Cape, South Africa. *Journal of Human Evolution* 59, 392-411.

Weaver, T.D. (2012). Did a discrete event 200,000-100,000 years ago produce modern humans? *Journal of Human Evolution* doi:10.1016/j.jhevol.2012.04.003

Wendorf F., Close A.E., and Schild, R. (1994). Africa in the period of *Homo sapiens neandertalensis* and contemporaries. In: De Laet ,S.J., Dani, A.H., Lorenzo, J.L., Nunoo, R.B. (Eds.), *History of Humanity. Volume 1, Prehistory and the Beginnings of Civilization*. New York: UNESCO/Routledge, pp. 117-131.

Wendorf, F., Laury, R.L., Albritton, C.C., Schild, R., Haynes, C.V., Damon, P.E., Shafiqullah, M., Scarborough, R. (1975). Dates for the Middle Stone Age of East Africa. *Science* 187, 740-742.

Wendorf, F., Schild, R. (1974) *A Middle Stone Age sequence from the Central Rift Valley, Ethiopia*. Wroclaw: Ossolineum.

Wendorf, F., Schild, R. (1993). Probable functions of Mousterian points and convergent sidescrapers in the Middle Stone Age of Ethiopia. *Quaternaria Nova,* 3, 39–51.

White, T.D. (2000). Cutmarks on the Bodo cranium: A case of prehistoric defleshing. *American Journal of Physical Anthropology* 69, 503–550.

White, T.D., Asfaw, B., Beyene, Y., Hailie-Selassie, Y., Lovejoy, C.O., Suwa, G., Woldegabriel, G. (2009). *Ardipithecus ramidus* and the paleobiology of early hominids. *Science* 326, 75-86.

White, T.D., Asfaw, B., DeGusta, D., Gilbert, H., Richards, G.D., Suwa, G., Howell, F.C. (2003). Pleistocene *Homo sapiens* from Middle Awash, Ethiopia. *Nature* 423, 742–747.

White, T.D., Suwa, G., Asfaw, B. (1994). *Australopithecus ramidus*, a new species of early hominid from Aramis, Ethiopia. *Nature* 371, 306-312.

White, T.D, WoldeGabriel, G., Asfaw,B., Ambrose, S., Beyene, Y., Bernor, R.L., Boisserie, J.-R., Currie, B., Gilbert, H., Haile-Selassie, Y., Hart, W.K., Hlusko, L.J., Howell, F.C., Kono, R.T., Lehmann, T., Louchart, A., Lovejoy, C.O., Renne, P.R., Saegusa, H., Vrba, E.S., Wesselman, H., Suwa, G. (2006). Asa Issie, Aramis and the origin of *Australopithecus. Nature* 440, 883-889.

Wilkins, J., Schoville, B.J., Brown, K.S., Chazan, M. (2012). Evidence for early hafted stone technology. *Science* 338, 942-946.

Williams, M.A.J., Bishop, P.M., Dakin, F.M., Gillespie, R. (1977). Late Quaternary lake levels in southern Afar and the adjacent Ethiopian Rift. *Nature* 267, 690-693.

Willoughby, P. (2007). The evolution of modern humans in Africa: A comprehensive guide. Maryland: AltaMira Press.

Wurz, S. (2002). Variability in the Middle Stone Age Lithic Sequence, 115,000–60,000 Years Ago at Klasies River, South Africa. *Journal of Archaeological Science* 29, 1001-1015.

Wurz, S. (2012). The transition to modern behavior. *Nature Education Knowledge* 3(10), 15.

Wynn, T. (2009). Hafted spears and the archaeology of mind. *Proceedings of the National Academy of Science, USA* 106(24), 9544-9545.

Yellen, J., Brooks, A., Helgren, D., Tappen, M., Ambrose, S., Bonnefille, R., Feathers, J., Goodfriend, G., Ludwig, K., Renne, P., Stewart, K. (2005). The archaeology of Aduma Middle Stone Age sites in the Awash Valley, Ethiopia. *PaleoAnthropology,* 10, 25-100.

Yotova, V., Lefebvre, J.F., Kohany, O., Jurka J., Michalski, R., Modiano, D., Utermann, G., Williams, S.M., Labuda, D. (2007). Tracing genetic history of modern humans using X-chromosome lineages. *Annals of Human Genetics* 122, 431-443.

Zilhão J. (2006). Neandertals and moderns mixed, and it matters. *Evolutionary Anthropology* 15, 183–195.

Zilhão, J. (2011). Aliens from outer time? Why the "Human Revolution" is wrong, and where do we go from here? In: Condemi, S., Weniger, G.-C. (Eds.), *Continuity and discontinuity in the peopling of Europe: One hundred fifty years of Neanderthal study*. Dordrecht: Springer, pp. 331-366.

Zilhão, J. Angelucci D, Badal-García E, d'Errico F, Daniel F, Dayet, L., Douka, K., Higham, T.F.G., Martínez-Sánchez, M.J., Montes-Bernárdez, R., Murcia-Mascarós, S., Pérez-Sirvent, C., Roldán-García, C., Pérez-Sirvent, C., Vanhaeren, M., Villaverde, V., Wood, R., Zapata, J. (2010). Symbolic use of marine shells and mineral pigments by Iberian Neandertals. *Proceedings of the National Academy of Science, USA* 107(3), 1023–1028.

Appendix-1

LITHIC ANALYSIS FRAMEWORK

(*modified from* Shea 2008: appendix)

RAW MATERIALS

Raw material type and color was recorded for all artifacts, including debris from both renewed excavations. All identifications were made by myself and Dr. Braun, based on visual and hand lens inspection. Raw material types are by and large dominated by obsidian, for which only the different color types (black, gray, and green) were recorded. Rhyolite made up the largest, single, non-obsidian raw material type. This varied in color from shades of gray to green. The identification of rhyolite was mostly conducted using a hand lens, which enabled to see phenocryst inclusions. Other raw material types varied from ignimbrite to basalt and were mostly noted in the debris class, hence were not specifically documented.

ARTIFACT CLASSIFICATION

Flaked stone artifacts were divided into five main artifact categories: cores, debitage, debris, retouched tools, and hammerstones. More specific classifications and measurements differed among these artifact categories. Each is discussed below.

All artifact measurements were made in millimeters using digital calipers. Classifications and measurements were recorded in the laboratory in the NME. Representative samples of artifacts were sketched in the lab and by myself. A selection of these have been included in this dissertation.

Cores/flaked pieces

Cores include most of the artifacts from which flakes longer than 1 cm have been struck. Cores were classified into the following artifact categories:

***Bifacial chopper*:** a pebble core that has two series of continuous flake scars detached on opposite faces of the same portion of its circumference, but not for more than 50% of its circumference.

***Partial discoid*:** a pebble core that has bifacial flake scars on more than 50% of its circumference.

***Discoid*:** a pebble core, roughly circular in planform aspect and lenticular cross section, whose entire circumference has bifacial flake scars, but whose flake scars do not extend past the midpoint of the core.

***Core scraper*:** essentially a discoid with one flat, non-cortical surface and another highly convex surface covered by flake scars indicating the working edge.

***Asymmetrical discoid*:** a core on which invasive flake removals are predominantly on one side and platform preparation flake scars are on the other. Flake scars on the former surface do not generally extend beyond the midpoint of the core surface. Usually, there is a residual cortical surface at the center of the less invasively flaked surface. Yellen *et al*. (2005) coined the term ‘‘Aduma cores’’ for similar artifacts from the Middle Awash Valley.

***Levallois core*:** cores with a hierarchy of flake removal surfaces, a flake removal surface on which flake scars extend past the midpoint of the core, and a platform preparation surface with less invasive flake scars.

***Core-on-flake*:** a flake that has a flake detachment scar longer than 30 mm somewhere on its surface and no other sign of edge-modification or retouch.

***Other core type*:** this category encompasses cores that do not fit into one of the above categories (e.g., pebbles with a single flake removal, prismatic blade cores).

***Core fragment*:** fragment of a pebble, flake, or angular rock fragment with visible flake scars greater than 20 mm, but for which no precise typological assignment could be made.

The principal measurements made on cores included the following:

***Length*:** the core's longest dimension.

***Width*:** the longest dimension perpendicular to length.

***Thickness*:** the distance between the upper and lower surfaces of the core measured at the intersection of length and width and perpendicular to the plane defined by the length and width dimensions.

Debitage/unretouched flakes and flake fragments

Debitage includes all unretouched flakes and flake fragments larger than 1 cm. The debitage types recognized by this study include the following:

***Cobble fragment*:** hemispherical fragment of a cobble or pebble split by a shear fracture.

***Initial cortical flake*:** flake with more than half of its dorsal surface covered by cortex.

***Residual cortical flake*:** flake with less than half of its dorsal surface covered by cortex.

***Levallois flake*:** symmetrical, non-cortical flake with facetted and projecting striking platform.

***Levallois blade*:** symmetrical, non-cortical blade (an elongated rectangular flake) with facetted and projecting striking platform.

***Levallois point*:** symmetrical, non-cortical triangular flake with facetted and projecting striking platform.

***Atypical Levallois flake*:** asymmetrical, non-cortical, or partly cortical flake with facetted and projecting striking platform.

***Atypical Levallois blade*:** asymmetrical, non-cortical, or partly cortical blade with facetted and projecting striking platform.

***Atypical Levallois point*:** asymmetrical, noncortical, or partly cortical triangular flake with facetted and projecting striking platform.

***Pseudo-Levallois point*:** triangular or trapezoidal flake with facetted striking platform and whose technological and morphological long axes diverge from each other.

***Kombewa flake*:** a flakewhose dorsal surface preserves the former ventral bulbar surface of the flake/core from which it was struck.

***Prismatic blade*:** flakes whose length is at least twice that of their width, which feature parallel lateral edges and distal– proximally aligned dorsal flake scars.

***Non-cortical flake*:** any non-Levallois, non-cortical flake >30mm in any dimension and not subsumed by other debitage types.

***Biface-thinning flake*:** a flake with a facetted striking platform, low external platform-dorsal surface angle, and multidirectional flake scars on its dorsal surface.

***Core-trimming element*:** flakes whose lateral or distal edges contain substantial amounts of residual core edge (i.e., for more than one third of the flake's circumference).

Angular fragment: flake fragment that cannot be definitively assigned to a flake fragment subtype.

***Flake fragment, proximal*:** incomplete flake retaining the striking platform and bulbar eminence.

***Flake fragment, other*:** incomplete flake lacking the striking platform and/or bulbar eminence.

More specific notations about the kind of flake fragment (distal, medial, lateral, etc.) were noted in cataloging the artifacts, but this aspect of flake fragment variation is not presented in this study.

Five metric variables were measured on all whole flakes >30mm. These measurements, based on definitions in Dibble (1997), were selected because they can be related to cost-benefit models of lithic production strategies. Values for the following variables were measured on all whole flakes from the Gademotta, Herto and Aduma MSA assemblages >30mm. Similar values were measured on Kibish MSA assemblages >30mm by Dr. Shea:

***Technological length*:** the distance from the point of percussion on the flake striking platform to the most distant point on the distal end of the flake perpendicular to the plane of striking platform width.

***Midpoint width*:** flake width measured perpendicularly to technological length at the midpoint of technological length.

***Midpoint thickness*:** the distance between the dorsal and ventral surfaces at the mid point of technological length.

***Striking platform Width*:** the distance between the two most lateral points on the striking platform.

***Striking platform thickness*:** the distance between the point of percussion and the nearest point on the opposite edge of the striking platform.

Debris/small debitage

Debris included flakes or flake fragments <30mm in any dimension. Debris was cataloged by raw material type and as either 'cortical' or 'non-cortical'.

Retouched tools

Retouched tools from the Kibish MSA assemblages were classified in terms of the following numbered types:

***Point*:** triangular/convergent flake with retouch restricted to its distolateral edges (e.g., Mousterian point, retouched Levallois point).

***Side scraper*:** flake with invasive retouch along one lateral edge.

***Double scraper*:** flake with invasive retouch along both lateral edges and whose edges do not converge to a point at the distal end of the flake.

***Convergent side scraper*:** flake with invasive retouch along both lateral edges and whose edges converge symmetrically to a point at the distal end of the flake

***Transverse scraper*:** flake with invasive retouch on its distal edge.

***Borer/awl*:** flake with sharp projection formed by two sets of concave flake removals.

***Notch*:** flake with either a single or a small cluster of flake removals creating a marked concavity on its edge.

***Denticulate*:** flake with a series of deep concavities along its edge.

***Bipolar flake*:** a flake with symmetrical patterns of crushing and/or invasive flake scars on opposite sides of the circumference.

***Other retouched flake*:** retouched flake not subsumed by the other categories.

***Foliate point*:** bifacially flaked artifact with convergent lateral edges that is less than 10 cm in length. Fragments of foliate points were differentiated from whole pieces.

Measurements of the retouched tools are largely the same as those made for debitage (i.e., length, width, thickness, platform width, platform thickness). The extent of retouch on each tool was measured by placing the artifact on an eight-point polar coordinate grid and recording the number of whole segments of the tool's circumference that intersected with retouched edges.

Hammerstones/pounded pieces

Pebbles/cobbles with discrete patches of pitting and crushing of the sort resulting from hard-hammer percussion were identified as hammerstones. Hammerstones were classified as either whole or fragmentary, and their

length, width, and thickness were measured in the same way as for cores. Cores with signs of percussion damage on them were classified as cores, but a note reporting their visible damage was made in the ‘‘Remarks’’ section of the database.

Appendix-2

RELATIVE ABUNDANCE AND ISOCHRON DATA FOR $^{40}Ar/^{39}Ar$ GEOCHRONOLOGY

Complete Ar data, corrected for backgrounds, mass discrimination, and radioactive decay. Relative abundances of Ar isotopes are given in nanoAmperes (nA) of amplified ionbeam current. The average sensitivity of the source/detector system, determined from air pipette analyses interspersed with the samples, is 7.39 x 1013 nA/mol.

Relative abundances (Samples Trench1Step1 and Trench1Step2 of Unit 12)

Run ID	Sample	^{40}Ar	$\pm\ ^{40}Ar$ (1σ)	^{39}Ar	$\pm\ ^{39}Ar$ (1σ)	^{38}Ar
61114-01A	T1S1	0.1599242	0.0002860	0.0121835	0.0000595	0.0001628
61114-03A	T1S1	0.0210457	0.0002550	0.0068338	0.0000497	0.0000987
61114-04A	T1S1	0.0164226	0.0002140	0.0067762	0.0000743	0.0001113
61114-05A	T1S1	0.0257079	0.0002267	0.0046874	0.0000375	0.0000675
61114-06A	T1S1	0.0290698	0.0002404	0.0055416	0.0000430	0.0000904
61114-08A	T1S1	0.0204238	0.0002404	0.0057869	0.0000669	0.0001009
61114-10A	T1S1	0.0171103	0.0001943	0.0049595	0.0000430	0.0000475
61114-11A	T1S1	0.0326892	0.0002550	0.0038691	0.0000391	0.0000834
61114-12A	T1S1	0.0227993	0.0001928	0.0061611	0.0000734	0.0000909
61114-13A	T1S1	0.0421797	0.0002550	0.0085764	0.0000819	0.0001618
61114-14A	T1S1	0.0458690	0.0002550	0.0058192	0.0000422	0.0001216
61114-15A	T1S1	0.0236133	0.0002404	0.0099134	0.0000532	0.0000844
61114-17A	T1S1	0.0210016	0.0002550	0.0057398	0.0000659	0.0000694
61114-19A	T1S1	0.0159731	0.0002550	0.0035685	0.0000632	0.0000629
61114-20A	T1S1	0.0203766	0.0002202	0.0057964	0.0000696	0.0000438
61114-22A	T1S1	0.0252922	0.0002476	0.0037781	0.0000354	0.0000519
61114-23A	T1S1	0.0222905	0.0002404	0.0068360	0.0000472	0.0001048
61114-25A	T1S1	0.0218339	0.0002404	0.0039197	0.0000422	0.0000898
61114-26A	T1S1	0.0249515	0.0002476	0.0072667	0.0000455	0.0000914
61114-27A	T1S1	0.0295541	0.0002550	0.0070012	0.0000463	0.0000859
61114-28A	T1S1	0.0490523	0.0002860	0.0034583	0.0000447	0.0001304
61114-29A	T1S1	0.1049711	0.0002404	0.0051580	0.0000706	0.0001265
61114-31A	T1S1	0.0184699	0.0002140	0.0042365	0.0000406	0.0000322
61114-32A	T1S1	0.0590149	0.0002860	0.0062400	0.0000472	0.0000952
61114-33A	T1S1	0.0208764	0.0002476	0.0060377	0.0000472	0.0000841
61114-35A	T1S1	0.0187388	0.0002550	0.0049379	0.0000414	0.0000495
61114-36A	T1S1	0.0142532	0.0002267	0.0034467	0.0000375	0.0000381
61114-37A	T1S1	0.0178090	0.0002404	0.0040603	0.0000422	0.0000868
61114-39A	T1S1	0.0857972	0.0002267	0.0140255	0.0000848	0.0002282
61114-40A	T1S1	0.0275653	0.0002267	0.0046949	0.0000568	0.0000619
61114-41A	T1S1	0.0163354	0.0002025	0.0079661	0.0000414	0.0001004

61114-42A	T1S1	0.0184361	0.0002267	0.0045547	0.0000422	0.0000705
61114-43A	T1S1	0.0366176	0.0002476	0.0080824	0.0000463	0.0000663
61114-44A	T1S1	0.0250542	0.0002267	0.0032228	0.0000524	0.0000354
61114-47A	T1S1	0.0641398	0.0003748	0.0029487	0.0000333	0.0000828
61114-48A	T1S1	0.0282744	0.0003002	0.0046635	0.0000455	0.0000634
61114-49A	T1S1	0.0334722	0.0003342	0.0044221	0.0000398	0.0000880
61114-50A	T1S1	0.0260478	0.0002786	0.0055090	0.0000398	0.0001020
61114-51A	T1S1	0.0482591	0.0002823	0.0060445	0.0000463	0.0001183
61114-52A	T1S1	0.0254718	0.0003053	0.0035526	0.0000383	0.0000597
61114-53A	T1S1	0.0339474	0.0002864	0.0065615	0.0000463	0.0000669
61114-54A	T1S1	0.0749808	0.0004280	0.0072932	0.0000781	0.0001524
61114-55A	T1S1	0.0215116	0.0003002	0.0032562	0.0000368	0.0000780
61114-56A	T1S1	0.0568259	0.0003406	0.0090564	0.0000613	0.0001999
61114-57A	T1S1	0.0313315	0.0003106	0.0088513	0.0000506	0.0001243
61114-58A	T1S1	0.0918796	0.0003106	0.0040712	0.0000398	0.0000995
61114-59A	T1S1	0.0750763	0.0003002	0.0113251	0.0000982	0.0002006
61114-60A	T1S1	0.0232911	0.0003106	0.0052429	0.0000641	0.0000839
61115-01A	T1S2	0.1155504	0.0003106	0.0059765	0.0000715	0.0001672
61115-02A	T1S2	0.0452533	0.0003220	0.0071589	0.0000455	0.0000974
61115-03A	T1S2	0.0342665	0.0002823	0.0063665	0.0000669	0.0001072
61115-04A	T1S2	0.0442188	0.0003106	0.0062705	0.0000422	0.0001328
61115-05A	T1S2	0.0472913	0.0003342	0.0082928	0.0000559	0.0001237
61115-06A	T1S2	0.0284099	0.0003053	0.0047986	0.0000541	0.0000419
61115-07A	T1S2	0.0260752	0.0002953	0.0064999	0.0000696	0.0000958
61115-08A	T1S2	0.0349397	0.0003280	0.0050195	0.0000595	0.0000781
61115-09A	T1S2	0.0205593	0.0002864	0.0073813	0.0000455	0.0000683
61115-10A	T1S2	0.0496896	0.0003280	0.0071166	0.0000743	0.0000907
61115-11A	T1S2	0.0217980	0.0003106	0.0034368	0.0000354	0.0001127
61115-12A	T1S2	0.0520017	0.0002864	0.0092889	0.0000515	0.0001345
61115-13A	T1S2	0.0363292	0.0003280	0.0044096	0.0000383	0.0000980
61115-14A	T1S2	0.0463318	0.0002907	0.0083262	0.0000724	0.0000710
61115-15A	T1S2	0.0171943	0.0003002	0.0057884	0.0000447	0.0000860
61115-16A	T1S2	0.0421961	0.0003162	0.0076989	0.0000489	0.0000942
61115-17A	T1S2	0.0860732	0.0003895	0.0039620	0.0000604	0.0000978
61115-18A	T1S2	0.0426169	0.0003280	0.0051355	0.0000375	0.0001039
61115-19A	T1S2	0.0335708	0.0003106	0.0034848	0.0000463	0.0000716
61115-20A	T1S2	0.0843892	0.0003106	0.0070984	0.0000455	0.0001222
61115-21A	T1S2	0.0381908	0.0003280	0.0072873	0.0000438	0.0001223
61115-22A	T1S2	0.0300991	0.0003280	0.0079939	0.0000463	0.0000980
61115-23A	T1S2	0.0240136	0.0003220	0.0073247	0.0000430	0.0001060
61115-24A	T1S2	0.0225902	0.0003106	0.0064626	0.0000604	0.0000333
61115-25A	T1S2	0.0643964	0.0003406	0.0079357	0.0000613	0.0001328
61115-26A	T1S2	0.0392704	0.0003162	0.0042196	0.0000622	0.0000595
61115-27A	T1S2	0.0875766	0.0003748	0.0060149	0.0000715	0.0000905
61115-28A	T1S2	0.0609596	0.0003538	0.0044874	0.0000391	0.0000633
61115-29A	T1S2	0.0483483	0.0003220	0.0059542	0.0000447	0.0000979
61115-30A	T1S2	0.0366566	0.0003162	0.0076334	0.0000724	0.0001332

61115-31A	T1S2	0.0241408	0.0003053	0.0044940	0.0000375	0.0000766
61115-32A	T1S2	0.0184761	0.0003162	0.0063214	0.0000447	0.0000936
61115-33A	T1S2	0.0971636	0.0003748	0.0064615	0.0000724	0.0001452
61115-34A	T1S2	0.0531059	0.0003471	0.0073543	0.0000715	0.0000731
61115-35A	T1S2	0.0194202	0.0003002	0.0042737	0.0000383	0.0000382
61115-36A	T1S2	0.0268418	0.0003002	0.0084596	0.0000463	0.0001283
61115-37A	T1S2	0.0358531	0.0003002	0.0051972	0.0000406	0.0001375
61115-38A	T1S2	0.0206188	0.0003106	0.0067325	0.0000406	0.0000773
61115-39A	T1S2	0.0416800	0.0002864	0.0071457	0.0000489	0.0001060
61115-40A	T1S2	0.0375463	0.0003053	0.0060742	0.0000678	0.0000833
61115-41A	T1S2	0.0407430	0.0003220	0.0060511	0.0000706	0.0001097
61115-42A	T1S2	0.0566094	0.0003538	0.0069780	0.0000506	0.0001146
61115-44A	T1S2	0.0321956	0.0003053	0.0096313	0.0000532	0.0001526
61115-45A	T1S2	0.0339043	0.0003406	0.0048873	0.0000406	0.0001108
61115-46A	T1S2	0.0330423	0.0003162	0.0060071	0.0000422	0.0000532
61115-47A	T1S2	0.0169080	0.0003002	0.0052973	0.0000604	0.0000661
61115-48A	T1S2	0.0451763	0.0003342	0.0041005	0.0000398	0.0000593
61115-50A	T1S2	0.0536621	0.0002702	0.0053321	0.0000398	0.0000834
61115-51A	T1S2	0.0294187	0.0002476	0.0058969	0.0000507	0.0000725
61115-52A	T1S2	0.0258300	0.0002335	0.0083316	0.0000774	0.0000780
61115-53A	T1S2	0.0248705	0.0002335	0.0071207	0.0000330	0.0000640
61115-54A	T1S2	0.0243007	0.0001910	0.0082692	0.0000425	0.0000828
61115-55A	T1S2	0.0147981	0.0002941	0.0055318	0.0000591	0.0000742
61115-56A	T1S2	0.0307415	0.0002335	0.0079482	0.0000706	0.0001174
61115-57A	T1S2	0.0244158	0.0002202	0.0046066	0.0000372	0.0000732
61115-58A	T1S2	0.0257900	0.0002335	0.0062093	0.0000452	0.0000791
61115-60A	T1S2	0.0320694	0.0002550	0.0076611	0.0000479	0.0000825

***Omitted Analyses**:*

61114-02A	T1S1	0.0114793	0.0002267	0.0026588	0.0000375	0.0000709
61114-07A	T1S1	0.0083326	0.0001933	0.0045732	0.0000422	0.0000816
61114-09A	T1S1	0.0132793	0.0002404	0.0039339	0.0000430	0.0000512
61114-16A	T1S1	0.0129232	0.0002335	0.0048048	0.0000422	0.0000833
61114-18A	T1S1	0.0113603	0.0002267	0.0029762	0.0000340	0.0000227
61114-21A	T1S1	0.0118539	0.0002140	0.0042133	0.0000398	0.0000728
61114-24A	T1S1	0.0089610	0.0002081	0.0035742	0.0000559	0.0000175
61114-30A	T1S1	0.0127323	0.0002335	0.0027371	0.0000347	0.0000345
61114-34A	T1S1	0.0118067	0.0002202	0.0035388	0.0000375	0.0000552
61114-38A	T1S1	0.0128134	0.0002476	0.0022557	0.0000506	0.0000547
61114-45A	T1S1	0.0098630	0.0002025	0.0024049	0.0000347	0.0000817
61114-46A	T1S1	0.0073159	0.0002140	0.0019696	0.0000326	0.0000617
61114-40aB	T1S1	0.0041747	0.0002025	0.0007338	0.0000287	-0.0000102
61114-41aB	T1S1	0.0012797	0.0002025	0.0003652	0.0000277	0.0000000
61114-42aB	T1S1	0.0010477	0.0001972	0.0003465	0.0000277	0.0000116
61115-43A	T1S2	0.0053179	0.0002823	0.0038519	0.0000383	-0.0000090
61115-49A	T1S2	0.0077962	0.0002081	0.0004592	0.0000225	0.0000126
61115-59A	T1S2	0.0011058	0.0001972	0.0002512	0.0000220	0.0000002

Run ID	Sample	± ^{38}Ar (1σ)	^{37}Ar	± ^{37}Ar (1σ)	^{36}Ar	± ^{36}Ar (1σ)
61114-01A	T1S1	0.0000264	0.0000410	0.0000349	0.0001760	0.0000063
61114-03A	T1S1	0.0000264	0.0000159	0.0000362	0.0000266	0.0000056
61114-04A	T1S1	0.0000280	-0.0000231	0.0000377	0.0000130	0.0000066
61114-05A	T1S1	0.0000280	-0.0000271	0.0000372	0.0000530	0.0000065
61114-06A	T1S1	0.0000264	0.0000049	0.0000358	0.0000479	0.0000056
61114-08A	T1S1	0.0000269	-0.0000557	0.0000377	0.0000283	0.0000056
61114-10A	T1S1	0.0000259	0.0000247	0.0000383	0.0000259	0.0000067
61114-11A	T1S1	0.0000286	0.0000109	0.0000377	0.0000371	0.0000055
61114-12A	T1S1	0.0000269	-0.0000113	0.0000377	0.0000419	0.0000069
61114-13A	T1S1	0.0000298	0.0000090	0.0000377	0.0000801	0.0000058
61114-14A	T1S1	0.0000280	-0.0000289	0.0000383	0.0001173	0.0000063
61114-15A	T1S1	0.0000286	0.0000265	0.0000394	0.0000126	0.0000054
61114-17A	T1S1	0.0000269	0.0000496	0.0000367	0.0000274	0.0000052
61114-19A	T1S1	0.0000264	-0.0000038	0.0000394	0.0000262	0.0000056
61114-20A	T1S1	0.0000259	-0.0000251	0.0000412	0.0000303	0.0000065
61114-22A	T1S1	0.0000264	-0.0000271	0.0000372	0.0000113	0.0000055
61114-23A	T1S1	0.0000280	0.0000258	0.0000394	0.0000264	0.0000055
61114-25A	T1S1	0.0000298	-0.0000216	0.0000367	0.0000472	0.0000067
61114-26A	T1S1	0.0000264	-0.0000248	0.0000394	0.0000325	0.0000055
61114-27A	T1S1	0.0000275	-0.0000323	0.0000388	0.0000451	0.0000056
61114-28A	T1S1	0.0000292	-0.0000109	0.0000400	0.0001402	0.0000060
61114-29A	T1S1	0.0000264	-0.0000175	0.0000372	0.0002962	0.0000069
61114-31A	T1S1	0.0000269	-0.0000047	0.0000358	0.0000322	0.0000055
61114-32A	T1S1	0.0000269	-0.0000436	0.0000372	0.0001591	0.0000062
61114-33A	T1S1	0.0000286	0.0000193	0.0000367	0.0000272	0.0000066
61114-35A	T1S1	0.0000269	-0.0000151	0.0000372	0.0000282	0.0000054
61114-36A	T1S1	0.0000269	-0.0000270	0.0000383	0.0000151	0.0000054
61114-37A	T1S1	0.0000286	-0.0000345	0.0000383	0.0000321	0.0000066
61114-39A	T1S1	0.0000318	-0.0000196	0.0000372	0.0001796	0.0000064
61114-40A	T1S1	0.0000269	-0.0000316	0.0000383	0.0000065	0.0000060
61114-41A	T1S1	0.0000280	-0.0000021	0.0000372	0.0000145	0.0000063
61114-42A	T1S1	0.0000255	-0.0000134	0.0000377	0.0000292	0.0000054
61114-43A	T1S1	0.0000264	-0.0000485	0.0000394	0.0000682	0.0000056
61114-44A	T1S1	0.0000259	-0.0000500	0.0000388	0.0000624	0.0000064
61114-47A	T1S1	0.0000275	-0.0000188	0.0000338	0.0001684	0.0000057
61114-48A	T1S1	0.0000269	0.0000199	0.0000338	0.0000600	0.0000064
61114-49A	T1S1	0.0000269	-0.0000181	0.0000333	0.0000828	0.0000058
61114-50A	T1S1	0.0000264	0.0000541	0.0000350	0.0000559	0.0000065
61114-51A	T1S1	0.0000280	0.0000316	0.0000333	0.0001252	0.0000056
61114-52A	T1S1	0.0000269	0.0000264	0.0000350	0.0000646	0.0000062
61114-53A	T1S1	0.0000286	0.0000356	0.0000338	0.0000798	0.0000053
61114-54A	T1S1	0.0000280	0.0000230	0.0000338	0.0001890	0.0000058
61114-55A	T1S1	0.0000255	-0.0000385	0.0000333	0.0000629	0.0000053
61114-56A	T1S1	0.0000370	-0.0000253	0.0000350	0.0001088	0.0000056
61114-57A	T1S1	0.0000264	-0.0000022	0.0000350	0.0000410	0.0000052
61114-58A	T1S1	0.0000259	0.0000171	0.0000369	0.0002664	0.0000063

61114-59A	T1S1	0.0000259	0.0000177	0.0000344	0.0001750	0.0000074
61114-60A	T1S1	0.0000269	-0.0000414	0.0000362	0.0000274	0.0000051
61115-01A	T1S2	0.0000259	0.0000485	0.0000333	0.0003438	0.0000068
61115-02A	T1S2	0.0000340	0.0000309	0.0000338	0.0000915	0.0000068
61115-03A	T1S2	0.0000269	-0.0000249	0.0000356	0.0000884	0.0000069
61115-04A	T1S2	0.0000264	-0.0000023	0.0000350	0.0001065	0.0000057
61115-05A	T1S2	0.0000269	0.0000325	0.0000333	0.0001008	0.0000072
61115-06A	T1S2	0.0000269	-0.0000389	0.0000350	0.0000644	0.0000065
61115-07A	T1S2	0.0000264	0.0000069	0.0000333	0.0000557	0.0000065
61115-08A	T1S2	0.0000286	-0.0000254	0.0000350	0.0000923	0.0000055
61115-09A	T1S2	0.0000264	0.0000004	0.0000338	0.0000375	0.0000052
61115-10A	T1S2	0.0000255	-0.0000417	0.0000328	0.0001231	0.0000073
61115-11A	T1S2	0.0000298	-0.0000152	0.0000309	0.0000559	0.0000054
61115-12A	T1S2	0.0000264	0.0000352	0.0000322	0.0001051	0.0000057
61115-13A	T1S2	0.0000280	0.0000525	0.0000328	0.0000907	0.0000057
61115-14A	T1S2	0.0000311	0.0000097	0.0000369	0.0000824	0.0000068
61115-15A	T1S2	0.0000269	-0.0000026	0.0000328	0.0000147	0.0000050
61115-16A	T1S2	0.0000259	0.0000451	0.0000318	0.0000935	0.0000068
61115-17A	T1S2	0.0000280	-0.0000334	0.0000322	0.0002590	0.0000062
61115-18A	T1S2	0.0000251	0.0000416	0.0000344	0.0001088	0.0000055
61115-19A	T1S2	0.0000275	0.0000507	0.0000328	0.0000607	0.0000068
61115-20A	T1S2	0.0000264	0.0000314	0.0000322	0.0001934	0.0000077
61115-21A	T1S2	0.0000264	0.0000256	0.0000313	0.0000819	0.0000071
61115-22A	T1S2	0.0000255	-0.0000124	0.0000350	0.0000549	0.0000053
61115-23A	T1S2	0.0000255	0.0000137	0.0000350	0.0000276	0.0000053
61115-24A	T1S2	0.0000332	0.0000270	0.0000350	0.0000413	0.0000054
61115-25A	T1S2	0.0000280	0.0000153	0.0000338	0.0001627	0.0000061
61115-26A	T1S2	0.0000292	0.0000019	0.0000328	0.0000966	0.0000055
61115-27A	T1S2	0.0000325	-0.0000262	0.0000350	0.0002658	0.0000066
61115-28A	T1S2	0.0000269	0.0000308	0.0000369	0.0001264	0.0000057
61115-29A	T1S2	0.0000255	0.0000371	0.0000338	0.0001193	0.0000065
61115-30A	T1S2	0.0000259	0.0000154	0.0000333	0.0000772	0.0000065
61115-31A	T1S2	0.0000264	-0.0000446	0.0000318	0.0000389	0.0000053
61115-32A	T1S2	0.0000264	0.0000250	0.0000333	0.0000241	0.0000052
61115-33A	T1S2	0.0000275	-0.0000003	0.0000338	0.0002770	0.0000063
61115-34A	T1S2	0.0000347	-0.0000147	0.0000328	0.0001305	0.0000059
61115-35A	T1S2	0.0000259	0.0000020	0.0000356	0.0000304	0.0000051
61115-36A	T1S2	0.0000275	-0.0000138	0.0000313	0.0000308	0.0000052
61115-37A	T1S2	0.0000264	0.0000235	0.0000322	0.0001044	0.0000055
61115-38A	T1S2	0.0000264	-0.0000280	0.0000338	0.0000284	0.0000052
61115-39A	T1S2	0.0000275	0.0000058	0.0000350	0.0000906	0.0000055
61115-40A	T1S2	0.0000264	-0.0000395	0.0000333	0.0000947	0.0000055
61115-41A	T1S2	0.0000264	0.0000098	0.0000328	0.0000940	0.0000053
61115-42A	T1S2	0.0000280	0.0000897	0.0000350	0.0001394	0.0000057
61115-44A	T1S2	0.0000292	-0.0000028	0.0000350	0.0000514	0.0000050
61115-45A	T1S2	0.0000275	-0.0000216	0.0000356	0.0000905	0.0000067
61115-46A	T1S2	0.0000264	-0.0000126	0.0000344	0.0000743	0.0000055

61115-47A	T1S2	0.0000292	0.0000293	0.0000338	0.0000199	0.0000062
61115-48A	T1S2	0.0000275	0.0000454	0.0000333	0.0001145	0.0000056
61115-50A	T1S2	0.0000214	-0.0000237	0.0000311	0.0001451	0.0000063
61115-51A	T1S2	0.0000227	-0.0000117	0.0000334	0.0000604	0.0000059
61115-52A	T1S2	0.0000202	0.0000289	0.0000311	0.0000405	0.0000057
61115-53A	T1S2	0.0000220	0.0000179	0.0000341	0.0000225	0.0000059
61115-54A	T1S2	0.0000208	-0.0000012	0.0000334	0.0000476	0.0000059
61115-55A	T1S2	0.0000208	0.0000507	0.0000311	0.0000277	0.0000056
61115-56A	T1S2	0.0000220	-0.0000289	0.0000334	0.0000402	0.0000057
61115-57A	T1S2	0.0000214	-0.0000242	0.0000322	0.0000417	0.0000067
61115-58A	T1S2	0.0000220	-0.0000333	0.0000300	0.0000441	0.0000065
61115-60A	T1S2	0.0000202	0.0000280	0.0000295	0.0000530	0.0000066

Omitted Analyses:

61114-02A	T1S1	0.0000255	-0.0000269	0.0000400	0.0000257	0.0000054
61114-07A	T1S1	0.0000259	0.0000350	0.0000377	0.0000163	0.0000054
61114-09A	T1S1	0.0000355	-0.0000172	0.0000383	0.0000176	0.0000054
61114-16A	T1S1	0.0000298	-0.0000216	0.0000388	0.0000200	0.0000053
61114-18A	T1S1	0.0000362	0.0000139	0.0000362	0.0000193	0.0000056
61114-21A	T1S1	0.0000264	-0.0000093	0.0000358	0.0000112	0.0000053
61114-24A	T1S1	0.0000259	-0.0000334	0.0000362	0.0000070	0.0000054
61114-30A	T1S1	0.0000275	0.0000199	0.0000367	0.0000208	0.0000054
61114-34A	T1S1	0.0000259	0.0000153	0.0000377	0.0000138	0.0000053
61114-38A	T1S1	0.0000259	-0.0000106	0.0000377	0.0000296	0.0000056
61114-45A	T1S1	0.0000259	-0.0000120	0.0000377	0.0000230	0.0000062
61114-46A	T1S1	0.0000264	-0.0001023	0.0000388	0.0000166	0.0000063
61114-40aB	T1S1	0.0000275	-0.0000617	0.0000362	0.0000098	0.0000055
61114-41aB	T1S1	0.0000259	-0.0000158	0.0000367	0.0000045	0.0000060
61114-42aB	T1S1	0.0000264	-0.0000043	0.0000377	0.0000000	0.0000053
61115-43A	T1S2	0.0000311	0.0000110	0.0000333	0.0000006	0.0000055
61115-49A	T1S2	0.0000196	-0.0000527	0.0000316	0.0000510	0.0000056
61115-59A	T1S2	0.0000202	0.0000090	0.0000311	-0.0000022	0.0000055

Run ID	Sample	$^{40}Ar^*/^{39}Ar$	$\pm^{40}Ar^*/^{39}Ar$ (1σ)	$\%^{40}Ar^*$	$\pm\%^{40}Ar^*$ (1σ)
61114-01A	T1S1	8.80758	0.17117	67.15	1.20
61114-03A	T1S1	1.91526	0.24744	62.25	8.05
61114-04A	T1S1	1.84876	0.29237	76.36	12.08
61114-05A	T1S1	2.10179	0.41879	38.36	7.62
61114-06A	T1S1	2.66464	0.30886	50.84	5.87
61114-08A	T1S1	2.06171	0.29234	58.48	8.28
61114-10A	T1S1	1.89186	0.40740	54.89	11.82
61114-11A	T1S1	5.57952	0.43647	66.09	5.13
61114-12A	T1S1	1.66888	0.33582	45.14	9.06
61114-13A	T1S1	2.12796	0.20578	43.31	4.14
61114-14A	T1S1	1.86044	0.33067	23.62	4.14
61114-15A	T1S1	2.00094	0.16358	84.09	6.91

61114-17A	T1S1	2.23611	0.27834	61.17	7.60
61114-19A	T1S1	2.28279	0.47959	51.05	10.70
61114-20A	T1S1	1.94716	0.33849	55.45	9.62
61114-22A	T1S1	5.78728	0.44067	86.53	6.58
61114-23A	T1S1	2.10636	0.24210	64.66	7.44
61114-25A	T1S1	1.97108	0.51192	35.42	9.18
61114-26A	T1S1	2.09368	0.22802	61.04	6.65
61114-27A	T1S1	2.29360	0.24215	54.39	5.73
61114-28A	T1S1	2.07589	0.53775	14.65	3.71
61114-29A	T1S1	3.19845	0.43077	15.73	1.97
61114-31A	T1S1	2.08848	0.38958	47.95	8.93
61114-32A	T1S1	1.83959	0.30926	19.47	3.19
61114-33A	T1S1	2.11455	0.32867	61.21	9.52
61114-35A	T1S1	2.08460	0.32882	54.99	8.68
61114-36A	T1S1	2.81803	0.46968	68.21	11.39
61114-37A	T1S1	2.01437	0.48834	45.97	11.14
61114-39A	T1S1	2.29136	0.14352	37.49	2.26
61114-40A	T1S1	5.44701	0.39192	92.86	6.62
61114-41A	T1S1	1.50510	0.23743	73.48	11.61
61114-42A	T1S1	2.12999	0.35558	52.67	8.79
61114-43A	T1S1	2.00448	0.21244	44.29	4.66
61114-44A	T1S1	1.97899	0.59681	25.48	7.65
61114-47A	T1S1	4.69415	0.61644	21.60	2.74
61114-48A	T1S1	2.22234	0.41563	36.69	6.84
61114-49A	T1S1	1.97120	0.40264	26.07	5.28
61114-50A	T1S1	1.70530	0.35886	36.10	7.58
61114-51A	T1S1	1.80328	0.28632	22.61	3.52
61114-52A	T1S1	1.74526	0.53319	24.36	7.41
61114-53A	T1S1	1.54227	0.24685	29.84	4.73
61114-54A	T1S1	2.54534	0.25634	24.78	2.39
61114-55A	T1S1	0.83302	0.50109	12.62	7.55
61114-56A	T1S1	2.68169	0.19270	42.78	3.02
61114-57A	T1S1	2.15491	0.17886	60.94	5.06
61114-58A	T1S1	3.03335	0.49990	13.45	2.08
61114-59A	T1S1	2.01549	0.20248	30.43	2.98
61114-60A	T1S1	2.87382	0.29952	64.76	6.74
61115-01A	T1S2	2.16431	0.37766	11.20	1.79
61115-02A	T1S3	2.50616	0.28851	39.68	4.53
61115-03A	T1S4	1.23176	0.32990	22.91	6.09
61115-04A	T1S5	1.97975	0.27860	28.10	3.90
61115-05A	T1S6	2.07425	0.26652	36.41	4.64
61115-06A	T1S7	1.90430	0.41353	32.20	6.96
61115-07A	T1S8	1.45306	0.30132	36.26	7.49
61115-08A	T1S9	1.46745	0.33967	21.10	4.83
61115-09A	T1S10	1.26498	0.21544	45.46	7.74
61115-10A	T1S11	1.81023	0.31486	25.95	4.46
61115-11A	T1S12	1.47953	0.48047	23.35	7.55

61115-12A	T1S13	2.22185	0.19015	39.72	3.35
61115-13A	T1S14	2.10399	0.39527	25.56	4.75
61115-14A	T1S15	2.60909	0.25069	46.93	4.47
61115-15A	T1S16	2.20955	0.26637	74.46	9.04
61115-16A	T1S17	1.85624	0.27093	33.90	4.91
61115-17A	T1S18	2.19634	0.50498	10.12	2.19
61115-18A	T1S19	1.97963	0.32975	23.88	3.92
61115-19A	T1S20	4.44036	0.59169	46.13	6.10
61115-20A	T1S21	3.75205	0.33471	31.59	2.74
61115-21A	T1S22	1.88464	0.29554	35.99	5.61
61115-22A	T1S23	1.71184	0.20286	45.51	5.38
61115-23A	T1S24	2.15331	0.22059	65.75	6.77
61115-24A	T1S25	1.58827	0.25551	45.48	7.31
61115-25A	T1S26	1.99468	0.24004	24.60	2.88
61115-26A	T1S27	2.46916	0.40088	26.55	4.24
61115-27A	T1S28	1.36103	0.35335	9.36	2.30
61115-28A	T1S29	5.17520	0.40079	38.13	2.88
61115-29A	T1S30	2.14090	0.33312	26.39	4.05
61115-30A	T1S31	1.78381	0.26097	37.18	5.40
61115-31A	T1S32	2.77431	0.35925	51.70	6.69
61115-32A	T1S33	1.78739	0.25236	61.22	8.68
61115-33A	T1S34	2.23441	0.31886	14.87	1.98
61115-34A	T1S35	1.91866	0.24859	26.59	3.37
61115-35A	T1S36	2.41573	0.36495	53.21	8.05
61115-36A	T1S37	2.08276	0.18650	65.71	5.90
61115-37A	T1S38	0.90143	0.32739	13.08	4.69
61115-38A	T1S39	1.79899	0.23683	58.80	7.77
61115-39A	T1S40	2.04613	0.23783	35.11	4.03
61115-40A	T1S41	1.51952	0.27728	24.61	4.43
61115-41A	T1S42	2.09667	0.27362	31.17	4.01
61115-42A	T1S43	2.15748	0.25424	26.62	3.06
61115-44A	T1S44	1.74818	0.16095	52.35	4.81
61115-45A	T1S45	1.40317	0.41741	20.25	5.98
61115-46A	T1S46	1.80558	0.27937	32.86	5.05
61115-47A	T1S47	2.07440	0.35672	65.06	11.21
61115-48A	T1S48	2.68458	0.42355	24.39	3.78
61115-50A	T1S49	1.93171	0.36535	19.21	3.56
61115-51A	T1S50	1.92829	0.30394	38.69	6.07
61115-52A	T1S51	1.65086	0.20711	53.30	6.67
61115-53A	T1S52	2.54998	0.25046	73.08	7.19
61115-54A	T1S53	1.21914	0.21524	41.53	7.31
61115-55A	T1S54	1.18524	0.30730	44.35	11.51
61115-56A	T1S55	2.35215	0.21952	60.88	5.65
61115-57A	T1S56	2.59184	0.43509	48.95	8.20
61115-58A	T1S57	2.02812	0.31673	48.88	7.62
61115-60A	T1S58	2.12127	0.26001	50.72	6.20

Omitted Analyses:

61114-02A	T1S1	1.42028	0.60806	32.93	14.09
61114-07A	T1S1	0.76134	0.35222	41.83	19.36
61114-09A	T1S1	2.03687	0.41588	60.40	12.35
61114-16A	T1S1	1.44348	0.33341	53.72	12.43
61114-18A	T1S1	1.88164	0.56568	49.34	14.85
61114-21A	T1S1	2.01343	0.37959	71.64	13.54
61114-24A	T1S1	1.91588	0.45199	76.50	18.09
61114-30A	T1S1	2.38858	0.59144	51.39	12.73
61114-34A	T1S1	2.17363	0.45227	65.21	13.60
61114-38A	T1S1	1.76316	0.75646	31.07	13.31
61114-45A	T1S1	1.24050	0.77767	30.28	18.97
61114-46A	T1S1	1.16126	0.96012	31.30	25.88
61114-40aB	T1S1	1.65961	2.24000	29.21	39.43
61114-41aB	T1S1	-0.24680	4.89679	-7.05	139.93
61114-42aB	T1S1	2.98731	4.60781	98.90	153.46
61115-43A	T1S2	1.33676	0.43526	96.95	31.97
61115-49A	T1S2	-16.23921	3.75788	-95.82	21.75
61115-59A	T1S2	7.02705	6.66790	159.77	153.60

		(Renne *et al*. 1998; Steiger & Jager 1977)			(Renne *et al*. 2010, 2011)	
Run ID	**Sample**	**Age (Ma)**	**± Age w/o J (1σ)**	**± w/ J (1σ)**	**Age (Ma)**	**± (1σ), full systematics**
61114-01A	T1S1	1.2012	0.0233	0.0235	1.2130	0.0238
61114-03A	T1S1	0.2613	0.0338	0.0338	0.2648	0.0344
61114-04A	T1S1	0.2522	0.0399	0.0399	0.2538	0.0413
61114-05A	T1S1	0.2867	0.0571	0.0571	0.2903	0.0566
61114-06A	T1S1	0.3635	0.0421	0.0421	0.3651	0.0430
61114-08A	T1S1	0.2813	0.0399	0.0399	0.2838	0.0382
61114-10A	T1S1	0.2581	0.0556	0.0556	0.2604	0.0572
61114-11A	T1S1	0.7611	0.0595	0.0595	0.7665	0.0604
61114-12A	T1S1	0.2277	0.0458	0.0458	0.2293	0.0471
61114-13A	T1S1	0.2903	0.0281	0.0281	0.2926	0.0295
61114-14A	T1S1	0.2538	0.0451	0.0451	0.2565	0.0448
61114-15A	T1S1	0.2730	0.0223	0.0223	0.2753	0.0224
61114-17A	T1S1	0.3051	0.0380	0.0380	0.3085	0.0396
61114-19A	T1S1	0.3114	0.0654	0.0654	0.3170	0.0640
61114-20A	T1S1	0.2656	0.0462	0.0462	0.2695	0.0461
61114-22A	T1S1	0.7894	0.0601	0.0601	0.7985	0.0605
61114-23A	T1S1	0.2874	0.0330	0.0330	0.2904	0.0340
61114-25A	T1S1	0.2689	0.0698	0.0698	0.2717	0.0742
61114-26A	T1S1	0.2856	0.0311	0.0311	0.2890	0.0317

61114-27A	T1S1	0.3129	0.0330	0.0330	0.3165	0.0335
61114-28A	T1S1	0.2832	0.0734	0.0734	0.2869	0.0742
61114-29A	T1S1	0.4363	0.0588	0.0588	0.4417	0.0571
61114-31A	T1S1	0.2849	0.0531	0.0531	0.2888	0.0506
61114-32A	T1S1	0.2510	0.0422	0.0422	0.2558	0.0437
61114-33A	T1S1	0.2885	0.0448	0.0448	0.2903	0.0454
61114-35A	T1S1	0.2844	0.0449	0.0449	0.2824	0.0450
61114-36A	T1S1	0.3844	0.0641	0.0641	0.3894	0.0667
61114-37A	T1S1	0.2748	0.0666	0.0666	0.2783	0.0645
61114-39A	T1S1	0.3126	0.0196	0.0196	0.3169	0.0194
61114-40A	T1S1	0.7430	0.0534	0.0535	0.7480	0.0548
61114-41A	T1S1	0.2053	0.0324	0.0324	0.2087	0.0316
61114-42A	T1S1	0.2906	0.0485	0.0485	0.2937	0.0486
61114-43A	T1S1	0.2735	0.0290	0.0290	0.2756	0.0299
61114-44A	T1S1	0.2700	0.0814	0.0814	0.2733	0.0808
61114-47A	T1S1	0.6403	0.0841	0.0841	0.6501	0.0830
61114-48A	T1S1	0.3032	0.0567	0.0567	0.3077	0.0572
61114-49A	T1S1	0.2689	0.0549	0.0549	0.2707	0.0555
61114-50A	T1S1	0.2326	0.0490	0.0490	0.2352	0.0498
61114-51A	T1S1	0.2460	0.0391	0.0391	0.2443	0.0417
61114-52A	T1S1	0.2381	0.0727	0.0727	0.2432	0.0712
61114-53A	T1S1	0.2104	0.0337	0.0337	0.2128	0.0347
61114-54A	T1S1	0.3472	0.0350	0.0350	0.3517	0.0349
61114-55A	T1S1	0.1136	0.0684	0.0684	0.1150	0.0698
61114-56A	T1S1	0.3658	0.0263	0.0263	0.3700	0.0264
61114-57A	T1S1	0.2940	0.0244	0.0244	0.2968	0.0257
61114-58A	T1S1	0.4138	0.0682	0.0682	0.4150	0.0680
61114-59A	T1S1	0.2750	0.0276	0.0276	0.2791	0.0279
61114-60A	T1S1	0.3920	0.0409	0.0409	0.3953	0.0416
61115-01A	T1S2	0.2953	0.0515	0.0515	0.2977	0.0524
61115-02A	T1S2	0.3419	0.0394	0.0394	0.3449	0.0388
61115-03A	T1S2	0.1680	0.0450	0.0450	0.1689	0.0462
61115-04A	T1S2	0.2701	0.0380	0.0380	0.2760	0.0381
61115-05A	T1S2	0.2830	0.0364	0.0364	0.2858	0.0361
61115-06A	T1S2	0.2598	0.0564	0.0564	0.2640	0.0590
61115-07A	T1S2	0.1982	0.0411	0.0411	0.1976	0.0434
61115-08A	T1S2	0.2002	0.0463	0.0463	0.2018	0.0474
61115-09A	T1S2	0.1726	0.0294	0.0294	0.1733	0.0299
61115-10A	T1S2	0.2470	0.0430	0.0430	0.2501	0.0432
61115-11A	T1S2	0.2018	0.0655	0.0655	0.2042	0.0668
61115-12A	T1S2	0.3031	0.0259	0.0259	0.3051	0.0261

61115-13A	T1S2	0.2870	0.0539	0.0539	0.2891	0.0541
61115-14A	T1S2	0.3559	0.0342	0.0342	0.3578	0.0353
61115-15A	T1S2	0.3014	0.0363	0.0363	0.3043	0.0359
61115-16A	T1S2	0.2532	0.0370	0.0370	0.2585	0.0358
61115-17A	T1S2	0.2996	0.0689	0.0689	0.3036	0.0700
61115-18A	T1S2	0.2701	0.0450	0.0450	0.2718	0.0459
61115-19A	T1S2	0.6057	0.0807	0.0807	0.6089	0.0801
61115-20A	T1S2	0.5118	0.0457	0.0457	0.5157	0.0460
61115-21A	T1S2	0.2571	0.0403	0.0403	0.2597	0.0404
61115-22A	T1S2	0.2335	0.0277	0.0277	0.2363	0.0286
61115-23A	T1S2	0.2938	0.0301	0.0301	0.2964	0.0315
61115-24A	T1S2	0.2167	0.0349	0.0349	0.2194	0.0350
61115-25A	T1S2	0.2721	0.0327	0.0328	0.2746	0.0343
61115-26A	T1S2	0.3368	0.0547	0.0547	0.3400	0.0550
61115-27A	T1S2	0.1857	0.0482	0.0482	0.1869	0.0500
61115-28A	T1S2	0.7059	0.0547	0.0547	0.7141	0.0553
61115-29A	T1S2	0.2921	0.0454	0.0454	0.2947	0.0449
61115-30A	T1S2	0.2434	0.0356	0.0356	0.2476	0.0361
61115-31A	T1S2	0.3785	0.0490	0.0490	0.3792	0.0492
61115-32A	T1S2	0.2438	0.0344	0.0344	0.2477	0.0353
61115-33A	T1S2	0.3048	0.0435	0.0435	0.3085	0.0456
61115-34A	T1S2	0.2618	0.0339	0.0339	0.2664	0.0338
61115-35A	T1S2	0.3296	0.0498	0.0498	0.3356	0.0526
61115-36A	T1S2	0.2841	0.0254	0.0254	0.2867	0.0257
61115-37A	T1S2	0.1230	0.0447	0.0447	0.1238	0.0448
61115-38A	T1S2	0.2454	0.0323	0.0323	0.2486	0.0324
61115-39A	T1S2	0.2791	0.0324	0.0324	0.2818	0.0340
61115-40A	T1S2	0.2073	0.0378	0.0378	0.2108	0.0380
61115-41A	T1S2	0.2860	0.0373	0.0373	0.2900	0.0371
61115-42A	T1S2	0.2943	0.0347	0.0347	0.2972	0.0354
61115-44A	T1S2	0.2385	0.0220	0.0220	0.2407	0.0215
61115-45A	T1S2	0.1914	0.0569	0.0569	0.1961	0.0595
61115-46A	T1S2	0.2463	0.0381	0.0381	0.2491	0.0381
61115-47A	T1S2	0.2830	0.0487	0.0487	0.2879	0.0503
61115-48A	T1S2	0.3662	0.0578	0.0578	0.3676	0.0571
61115-50A	T1S2	0.2635	0.0498	0.0498	0.2655	0.0483
61115-51A	T1S2	0.2631	0.0415	0.0415	0.2645	0.0413
61115-52A	T1S2	0.2252	0.0283	0.0283	0.2267	0.0278
61115-53A	T1S2	0.3479	0.0342	0.0342	0.3508	0.0333
61115-54A	T1S2	0.1663	0.0294	0.0294	0.1697	0.0308
61115-55A	T1S2	0.1617	0.0419	0.0419	0.1650	0.0419
61115-56A	T1S2	0.3209	0.0299	0.0300	0.3244	0.0318

61115-57A	T1S2	0.3536	0.0593	0.0594	0.3566	0.0601
61115-58A	T1S2	0.2767	0.0432	0.0432	0.2779	0.0436
61115-60A	T1S2	0.2894	0.0355	0.0355	0.2955	0.0361
Omitted Analyses:						
61114-02A	T1S1	0.1937635	0.0829505	0.0829516	0.1951	0.0849
61114-07A	T1S1	0.1038696	0.0480515	0.048052	0.1054	0.0502
61114-09A	T1S1	0.2778761	0.0567306	0.0567341	0.2800	0.0584
61114-16A	T1S1	0.1969278	0.045483	0.0454851	0.1994	0.0470
61114-18A	T1S1	0.2566995	0.0771665	0.0771687	0.2601	0.0802
61114-21A	T1S1	0.274678	0.0517802	0.0517839	0.2778	0.0517
61114-24A	T1S1	0.261371	0.0616569	0.0616597	0.2647	0.0620
61114-30A	T1S1	0.3258525	0.0806777	0.080681	0.3240	0.0830
61114-34A	T1S1	0.2965314	0.0616939	0.0616976	0.2991	0.0635
61114-38A	T1S1	0.2405382	0.1031921	0.1031935	0.2419	0.1044
61114-45A	T1S1	0.1692379	0.1060898	0.1060904	0.1750	0.1092
61114-46A	T1S1	0.158428	0.1309803	0.1309808	0.1531	0.1335
61114-40aB	T1S1	0.2264119	0.3055726	0.305573	0.2403	0.3140
61114-41aB	T1S1	-0.0336715	0.6680982	0.6680982	0.0067	0.6611
61114-42aB	T1S1	0.4075225	0.6285173	0.628518	0.4135	0.6033
61115-43A	T1S2	0.1823693	0.0593782	0.0593796	0.1829	0.0593
61115-49A	T1S2	-2.216932	0.5133299	0.5133543	-2.2558	0.5113
61115-59A	T1S2	0.9584694	0.9092408	0.9092434	0.9520	0.9270

Isochron (Samples Trench1Step1 and Trench1Step2 of Unit 12)

Run ID	Sample	$^{36}Ar/^{40}Ar$	±% $^{36}Ar/^{40}Ar$ (1σ)	$^{39}Ar/^{40}Ar$	±% $^{39}Ar/^{40}Ar$ (1σ)
61114-01A	T1S1	0.0011002	3.680888	0.0762432	0.5714236
61114-03A	T1S1	0.0012643	21.03325	0.3250306	1.463619
61114-04A	T1S1	0.0007916	50.65436	0.4130591	1.756729
61114-05A	T1S1	0.0020646	12.32482	0.1825032	1.237327
61114-06A	T1S1	0.0016465	11.84769	0.1908032	1.17977
61114-08A	T1S1	0.0013908	19.70733	0.2836286	1.700775
61114-10A	T1S1	0.001511	26.06728	0.2901258	1.478269
61114-11A	T1S1	0.0011357	14.9231	0.1184581	1.320942
61114-12A	T1S1	0.0018374	16.46518	0.2704916	1.508033
61114-13A	T1S1	0.0018989	7.273258	0.2035136	1.173995
61114-14A	T1S1	0.0025582	5.460995	0.1269774	0.95766
61114-15A	T1S1	0.0005328	42.59241	0.4202643	1.198852
61114-17A	T1S1	0.0013006	19.2782	0.2735499	1.723277
61114-19A	T1S1	0.0016396	21.62055	0.2236155	2.446743

61114-20A	T1S1	0.0014923	21.45109	0.2847488	1.666387
61114-22A	T1S1	0.0004512	47.91535	0.1495162	1.401725
61114-23A	T1S1	0.0011837	20.76546	0.306975	1.328828
61114-25A	T1S1	0.0021631	14.16026	0.1796887	1.589823
61114-26A	T1S1	0.0013051	16.83938	0.2915239	1.22056
61114-27A	T1S1	0.0015278	12.42351	0.2371232	1.133205
61114-28A	T1S1	0.0028588	4.417706	0.070561	1.461638
61114-29A	T1S1	0.0028226	2.481986	0.0491774	1.430581
61114-31A	T1S1	0.0017434	17.03787	0.2295861	1.553966
61114-32A	T1S1	0.0026973	4.032187	0.1058292	0.9414577
61114-33A	T1S1	0.0012991	24.31316	0.2894882	1.470256
61114-35A	T1S1	0.0015077	19.02556	0.263772	1.651127
61114-36A	T1S1	0.0010647	35.33774	0.2420571	1.98593
61114-37A	T1S1	0.0018097	20.48563	0.2282136	1.757344
61114-39A	T1S1	0.0020937	3.691821	0.1636188	0.7058521
61114-40A	T1S1	0.0002392	91.35366	0.1704774	1.509735
61114-41A	T1S1	0.0008883	43.42258	0.4882077	1.39471
61114-42A	T1S1	0.0015852	18.38789	0.247292	1.5909
61114-43A	T1S1	0.0018661	8.328886	0.2209384	0.9317111
61114-44A	T1S1	0.002496	10.25634	0.1287554	1.910792
61114-47A	T1S1	0.002626	3.558101	0.0460128	1.315516
61114-48A	T1S1	0.0021206	10.72906	0.165082	1.490454
61114-49A	T1S1	0.0024764	7.124021	0.1322343	1.392244
61114-50A	T1S1	0.0021403	11.79768	0.2116836	1.339132
61114-51A	T1S1	0.0025923	4.594123	0.1253583	1.008011
61114-52A	T1S1	0.0025334	9.769766	0.1395904	1.663124
61114-53A	T1S1	0.0023501	6.730348	0.1934574	1.145781
61114-54A	T1S1	0.0025195	3.238858	0.0973502	1.257265
61114-55A	T1S1	0.0029267	8.647856	0.1515183	1.850314
61114-56A	T1S1	0.0019166	5.246108	0.1595197	0.9487108
61114-57A	T1S1	0.0013083	12.66533	0.2827877	1.191867
61114-58A	T1S1	0.0028989	2.53761	0.0443454	1.077107
61114-59A	T1S1	0.0023302	4.33765	0.1509839	0.9977919
61114-60A	T1S1	0.0011805	18.6398	0.2253313	1.863402
61115-01A	T1S2	0.0029742	2.180944	0.0517626	1.268733
61115-02A	T1S2	0.0020203	7.48236	0.1583374	0.9990363
61115-03A	T1S2	0.0025822	7.914094	0.185972	1.38073
61115-04A	T1S2	0.0024083	5.435078	0.1419335	1.017702
61115-05A	T1S2	0.00213	7.277215	0.1755146	1.021526
61115-06A	T1S2	0.002271	10.2183	0.1690693	1.607457
61115-07A	T1S2	0.002135	11.68471	0.2495167	1.609339
61115-08A	T1S2	0.0026426	6.128357	0.1437966	1.560333
61115-09A	T1S2	0.0018266	14.00519	0.359407	1.576099
61115-10A	T1S2	0.0024802	6.042061	0.1433568	1.279912
61115-11A	T1S2	0.0025674	9.805019	0.1578141	1.812386
61115-12A	T1S2	0.0020189	5.55486	0.1787887	0.8268314
61115-13A	T1S2	0.0024933	6.379034	0.1214768	1.299109

61115-14A	T1S2	0.0017775	8.376711	0.179874	1.116638
61115-15A	T1S2	0.0008554	34.39175	0.3369991	1.968535
61115-16A	T1S2	0.002214	7.41323	0.1826192	1.027443
61115-17A	T1S2	0.0030105	2.56456	0.0460713	1.636401
61115-18A	T1S2	0.0025497	5.164168	0.1206057	1.10655
61115-19A	T1S2	0.0018044	11.23827	0.1038859	1.668709
61115-20A	T1S2	0.0022914	4.066399	0.084185	0.7839013
61115-21A	T1S2	0.0021438	8.735773	0.1909887	1.094619
61115-22A	T1S2	0.0018251	9.717204	0.265854	1.282752
61115-23A	T1S2	0.0011472	19.24173	0.3053341	1.516015
61115-24A	T1S2	0.001826	13.20765	0.2863598	1.716464
61115-25A	T1S2	0.0025254	3.87401	0.1233404	0.9800428
61115-26A	T1S2	0.00246	5.78294	0.1075452	1.72923
61115-27A	T1S2	0.003036	2.661956	0.0687428	1.30666
61115-28A	T1S2	0.0020724	4.654458	0.0736722	1.089584
61115-29A	T1S2	0.0024656	5.523309	0.1232569	1.04738
61115-30A	T1S2	0.0021041	8.556829	0.2084365	1.328796
61115-31A	T1S2	0.0016178	13.61191	0.1863456	1.56685
61115-32A	T1S2	0.001299	21.84669	0.3424944	1.910675
61115-33A	T1S2	0.0028513	2.460001	0.0665585	1.2283
61115-34A	T1S2	0.0024586	4.624254	0.1386113	1.215766
61115-35A	T1S2	0.0015671	16.8728	0.2202753	1.842958
61115-36A	T1S2	0.0011485	16.80934	0.3154934	1.293986
61115-37A	T1S2	0.0029114	5.436432	0.1450871	1.190814
61115-38A	T1S2	0.0013798	18.44047	0.326875	1.677786
61115-39A	T1S2	0.0021734	6.206954	0.1716009	1.014204
61115-40A	T1S2	0.0025252	5.889014	0.1619353	1.426869
61115-41A	T1S2	0.0023055	5.807535	0.1486544	1.455152
61115-42A	T1S2	0.0024579	4.207951	0.1233653	1.001666
61115-44A	T1S2	0.001596	9.912061	0.2994569	1.144534
61115-45A	T1S2	0.0026713	7.501684	0.1442852	1.351193
61115-46A	T1S2	0.0022489	7.472952	0.1819744	1.234085
61115-47A	T1S2	0.0011704	31.55134	0.3136121	2.172256
61115-48A	T1S2	0.0025326	5.023704	0.0908403	1.265785
61115-50A	T1S2	0.0027059	4.468429	0.0994567	0.9443713
61115-51A	T1S2	0.0020535	9.856278	0.2006438	1.248835
61115-52A	T1S2	0.001564	14.15534	0.3228887	1.342585
61115-53A	T1S2	0.0009016	26.38796	0.2866024	1.093975
61115-54A	T1S2	0.0019584	12.4734	0.3406512	0.9849568
61115-55A	T1S2	0.0018639	20.41212	0.3742014	2.322972
61115-56A	T1S2	0.0013104	14.31422	0.2588188	1.213697
61115-57A	T1S2	0.0017099	15.98887	0.1888597	1.257221
61115-58A	T1S2	0.0017122	14.82109	0.2410136	1.207847
61115-60A	T1S2	0.0016504	12.50141	0.2391239	1.057224

Omitted Analyses:

61114-02A	T1S1	0.0022465	20.88255	0.2318472	2.495391
61114-07A	T1S1	0.0019483	33.09161	0.5494481	2.569661
61114-09A	T1S1	0.0013263	30.78704	0.2965429	2.177556
61114-16A	T1S1	0.0015499	26.54999	0.3721894	2.070279
61114-18A	T1S1	0.0016968	29.04463	0.2622282	2.365617
61114-21A	T1S1	0.0009499	47.13127	0.3558055	2.099709
61114-24A	T1S1	0.000787	75.98589	0.3993091	2.876064
61114-30A	T1S1	0.001628	25.91708	0.2151637	2.292156
61114-34A	T1S1	0.0011651	38.59885	0.3000201	2.209314
61114-38A	T1S1	0.0023088	19.19135	0.1762027	3.035147
61114-45A	T1S1	0.0023353	27.12632	0.2440734	2.57776
61114-46A	T1S1	0.0023009	37.53001	0.2695623	3.452119
61114-40aB	T1S1	0.0023709	55.45405	0.1760248	6.377171
61114-41aB	T1S1	0.0035856	130.8368	0.2857525	17.99363
61114-42aB	T1S1	0.0000369	13703.13	0.3310583	20.97894
61115-43A	T1S2	0.0001021	1019.747	0.7252789	5.548573
61115-49A	T1S2	0.0065586	11.31286	0.0590022	5.692841
61115-59A	T1S2	-0.0020021	-251.3123	0.2273712	20.36417

Run ID	Sample	±% $^{39}Ar/^{36}Ar$ (1σ)	ρ $^{40}Ar/^{39}Ar$	ρ $^{36}Ar/^{39}Ar$
61114-01A	T1S1	3.667357	0.9462024	0.1773031
61114-03A	T1S1	21.00205	0.9962985	0.0604954
61114-04A	T1S1	50.64588	0.9991785	0.0244712
61114-05A	T1S1	12.30583	0.9912335	0.0783085
61114-06A	T1S1	11.8304	0.9910099	0.0784293
61114-08A	T1S1	19.69744	0.9948207	0.0560469
61114-10A	T1S1	26.05013	0.9975599	0.0445287
61114-11A	T1S1	14.92651	0.9935497	0.0551621
61114-12A	T1S1	16.4775	0.9937294	0.0496681
61114-13A	T1S1	7.290343	0.9763718	0.0989395
61114-14A	T1S1	5.452487	0.9656741	0.1382075
61114-15A	T1S1	42.57937	0.9992924	0.0270778
61114-17A	T1S1	19.26527	0.9944828	0.0591287
61114-19A	T1S1	21.62639	0.992392	0.0596319
61114-20A	T1S1	21.44999	0.9957561	0.046842
61114-22A	T1S1	47.91095	0.9993262	0.020935
61114-23A	T1S1	20.74023	0.99664	0.0560623
61114-25A	T1S1	14.14655	0.990875	0.0750482
61114-26A	T1S1	16.81127	0.9953762	0.0657736
61114-27A	T1S1	12.39757	0.9921694	0.0797365
61114-28A	T1S1	4.536161	0.9189744	0.1392747
61114-29A	T1S1	2.781633	0.7772451	0.182578
61114-31A	T1S1	17.01508	0.9938893	0.0676369

61114-32A	T1S1	4.036236	0.9381877	0.174884
61114-33A	T1S1	24.28921	0.9972144	0.0507204
61114-35A	T1S1	18.98515	0.9946659	0.0724186
61114-36A	T1S1	35.3129	0.9979677	0.0429789
61114-37A	T1S1	20.45842	0.99497	0.0635853
61114-39A	T1S1	3.690794	0.9404047	0.1756662
61114-40A	T1S1	91.35628	0.9997958	0.0087019
61114-41A	T1S1	43.40351	0.9991844	0.031189
61114-42A	T1S1	18.36019	0.994581	0.0667531
61114-43A	T1S1	8.301557	0.985569	0.105033
61114-44A	T1S1	10.33233	0.9774801	0.0721211
61114-47A	T1S1	3.648561	0.8903911	0.1849523
61114-48A	T1S1	10.70511	0.9854202	0.098882
61114-49A	T1S1	7.087309	0.9696546	0.1446236
61114-50A	T1S1	11.75621	0.9894728	0.0971668
61114-51A	T1S1	4.587156	0.9491703	0.1656128
61114-52A	T1S1	9.737929	0.9795405	0.1176107
61114-53A	T1S1	6.689674	0.9729172	0.1429979
61114-54A	T1S1	3.320461	0.8746218	0.2055865
61114-55A	T1S1	8.587566	0.9693851	0.1520379
61114-56A	T1S1	5.2255	0.9630363	0.151554
61114-57A	T1S1	12.62536	0.9920337	0.0885403
61114-58A	T1S1	2.64575	0.8310138	0.2272722
61114-59A	T1S1	4.372078	0.9440908	0.145883
61114-60A	T1S1	18.62266	0.9933734	0.0657552
61115-01A	T1S2	2.419762	0.7470422	0.2292991
61115-02A	T1S2	7.453704	0.9809462	0.1180189
61115-03A	T1S2	7.921455	0.9758018	0.1065833
61115-04A	T1S2	5.40156	0.9631859	0.1593114
61115-05A	T1S2	7.251893	0.9794324	0.1193902
61115-06A	T1S2	10.20805	0.9822078	0.1001083
61115-07A	T1S2	11.66445	0.9863613	0.093462
61115-08A	T1S2	6.146105	0.9527324	0.1454401
61115-09A	T1S2	13.93487	0.9907567	0.1051462
61115-10A	T1S2	6.071846	0.9623255	0.1207214
61115-11A	T1S2	9.73569	0.9769135	0.1404858
61115-12A	T1S2	5.526505	0.9705149	0.1435644
61115-13A	T1S2	6.34843	0.9652571	0.150656
61115-14A	T1S2	8.380169	0.9830834	0.0905615
61115-15A	T1S2	34.3494	0.9978827	0.0515562
61115-16A	T1S2	7.38032	0.9800539	0.1228532
61115-17A	T1S2	2.909374	0.7536113	0.1933855
61115-18A	T1S2	5.126952	0.955627	0.1739322
61115-19A	T1S2	11.26581	0.9845501	0.0745119
61115-20A	T1S2	4.062751	0.9473172	0.1669667
61115-21A	T1S2	8.69473	0.9846963	0.1149387
61115-22A	T1S2	9.654385	0.9852378	0.1239359

61115-23A	T1S2	19.19353	0.995363	0.0743853
61115-24A	T1S2	13.15456	0.9882818	0.1030375
61115-25A	T1S2	3.875594	0.9305387	0.1871801
61115-26A	T1S2	5.891224	0.9397612	0.1224438
61115-27A	T1S2	2.837006	0.8148315	0.2108385
61115-28A	T1S2	4.667127	0.9467546	0.1565168
61115-29A	T1S2	5.505468	0.9634348	0.148217
61115-30A	T1S2	8.54735	0.9802184	0.105687
61115-31A	T1S2	13.56499	0.9903022	0.0946677
61115-32A	T1S2	21.78057	0.9949821	0.0804363
61115-33A	T1S2	2.624504	0.7985755	0.2274409
61115-34A	T1S2	4.647849	0.9394373	0.1612412
61115-35A	T1S2	16.81344	0.9920306	0.0911511
61115-36A	T1S2	16.76999	0.9950303	0.0736418
61115-37A	T1S2	5.397849	0.9566674	0.1719993
61115-38A	T1S2	18.3772	0.994187	0.0859246
61115-39A	T1S2	6.180702	0.9719077	0.1372721
61115-40A	T1S2	5.913028	0.9545992	0.1384603
61115-41A	T1S2	5.845429	0.9522419	0.1349597
61115-42A	T1S2	4.186649	0.9395841	0.1896191
61115-44A	T1S2	9.864305	0.9875421	0.1099549
61115-45A	T1S2	7.457564	0.9736229	0.1409362
61115-46A	T1S2	7.421497	0.9761272	0.1412755
61115-47A	T1S2	31.51506	0.9970602	0.0534233
61115-48A	T1S2	5.032629	0.946042	0.1602356
61115-50A	T1S2	4.468298	0.949462	0.1607163
61115-51A	T1S2	9.841411	0.9861461	0.092869
61115-52A	T1S2	14.14545	0.9926808	0.0666645
61115-53A	T1S2	26.3686	0.9983288	0.0418291
61115-54A	T1S2	12.44566	0.9932419	0.07778
61115-55A	T1S2	20.33133	0.9921466	0.0943129
61115-56A	T1S2	14.31063	0.9936495	0.0590091
61115-57A	T1S2	15.97341	0.9946962	0.0612463
61115-58A	T1S2	14.7999	0.9941026	0.067869
61115-60A	T1S2	12.47844	0.9928012	0.0758163

Omitted Analyses:

61114-02A	T1S1	20.82602	0.9915474	0.0858898
61114-07A	T1S1	33.01435	0.9964639	0.069853
61114-09A	T1S1	30.74591	0.9968999	0.0564215
61114-16A	T1S1	26.49428	0.9961532	0.0678824
61114-18A	T1S1	28.99014	0.9960083	0.0657372
61114-21A	T1S1	47.10125	0.9987529	0.0377769
61114-24A	T1S1	75.96304	0.9991858	0.0276347
61114-30A	T1S1	25.87468	0.9952423	0.065623
61114-34A	T1S1	38.56231	0.9979816	0.046722
61114-38A	T1S1	19.21682	0.9859827	0.075968
61114-45A	T1S1	27.07829	0.9947102	0.0686963

61114-46A	T1S1	37.44348	0.995361	0.0720845
61114-40aB	T1S1	55.36998	0.9931952	0.0712394
61114-41aB	T1S1	130.0531	0.9904711	0.1121833
61114-42aB	T1S1	13703.12	0.9999988	0.0013001
61115-43A	T1S2	1019.733	0.9999847	0.0052891
61115-49A	T1S2	12.04178	0.87889	0.1260442
61115-59A	T1S2	-250.8037	0.9967034	0.0655576

Relative abundances (Sample TerraceB' of Unit10)

Run #	Sample	^{40}Ar	± ^{40}Ar (1σ)	^{39}Ar	± ^{39}Ar (1σ)
61116-01A	TB'	0.0171553	0.0002140	0.0055426	0.0000372
61116-02A	TB'	0.0383827	0.0002025	0.0059704	0.0000407
61116-03A	TB'	0.0225184	0.0002335	0.0050585	0.0000735
61116-04A	TB'	0.0377865	0.0002550	0.0033846	0.0000355
61116-05A	TB'	0.0349438	0.0002404	0.0043160	0.0000355
61116-06A	TB'	0.0469342	0.0002625	0.0091647	0.0000526
61116-07A	TB'	0.0490051	0.0002625	0.0049001	0.0000355
61116-08A	TB'	0.0177772	0.0002202	0.0040444	0.0000355
61116-09B	TB'	0.0316497	0.0002404	0.0066761	0.0000425
61116-10A	TB'	0.0698477	0.0002860	0.0100004	0.0000498
61116-11A	TB'	0.0194541	0.0002202	0.0057250	0.0000398
61116-12A	TB'	0.0382616	0.0002550	0.0049187	0.0000563
61116-13A	TB'	0.0159064	0.0002202	0.0055817	0.0000407
61116-15A	TB'	0.0899903	0.0002335	0.0030445	0.0000498
61116-16A	TB'	0.0297204	0.0002404	0.0070958	0.0000470
61116-18A	TB'	0.0600544	0.0002140	0.0048340	0.0000364
61116-19A	TB'	0.0186321	0.0002202	0.0061832	0.0000389
61116-20A	TB'	0.0155955	0.0002202	0.0034565	0.0000322
61116-21A	TB'	0.0262671	0.0002335	0.0057359	0.0000389
61116-22A	TB'	0.0280127	0.0002335	0.0048545	0.0000347
61116-23A	TB'	0.0342789	0.0002476	0.0058052	0.0000347
61116-24A	TB'	0.0426641	0.0002335	0.0134491	0.0000610
61116-25A	TB'	0.0200575	0.0002476	0.0061382	0.0000443
61116-26A	TB'	0.0926154	0.0002267	0.0326001	0.0001008
61116-27A	TB'	0.0272667	0.0002404	0.0052621	0.0000338
61116-28A	TB'	0.0234748	0.0002404	0.0068924	0.0000434
61116-29A	TB'	0.0289764	0.0002476	0.0061932	0.0000416
61116-30A	TB'	0.0216584	0.0002335	0.0056371	0.0000398
61116-31A	TB'	0.1582730	0.0003801	0.0057626	0.0000582

61116-32A	TB'	0.0315953	0.0002025	0.0102967	0.0000507
61116-33A	TB'	0.0312022	0.0002202	0.0048336	0.0000563
61116-35A	TB'	0.0291200	0.0002476	0.0059417	0.0000416
61116-36A	TB'	0.0653815	0.0002140	0.0115861	0.0000563
61116-37A	TB'	0.0232593	0.0002335	0.0069070	0.0000347
61116-38A	TB'	0.0179445	0.0002267	0.0048868	0.0000330
61116-39A	TB'	0.0269065	0.0002335	0.0065443	0.0000425
61116-40A	TB'	0.0203448	0.0002267	0.0050925	0.0000372
61116-41A	TB'	0.0281143	0.0002267	0.0065320	0.0000443
61116-42A	TB'	0.0215157	0.0002404	0.0062937	0.0000425
61116-43A	TB'	0.0291765	0.0002202	0.0051707	0.0000398
61116-44A	TB'	0.0193894	0.0002267	0.0058277	0.0000398
61116-45A	TB'	0.0166710	0.0002335	0.0060015	0.0000407
61116-46A	TB'	0.0207666	0.0002476	0.0038344	0.0000355
61116-47A	TB'	0.0283340	0.0002550	0.0064698	0.0000461
61116-48A	TB'	0.0212376	0.0002335	0.0054720	0.0000364
61116-49A	TB'	0.0233527	0.0002267	0.0064648	0.0000407
61116-50A	TB'	0.0242090	0.0001972	0.0059895	0.0000372
61116-51A	TB'	0.0191216	0.0002267	0.0052901	0.0000372
61116-52A	TB'	0.0280092	0.0001914	0.0088219	0.0000498
61116-53A	TB'	0.0297676	0.0002267	0.0079412	0.0000461
61116-54A	TB'	0.1009719	0.0003191	0.0080831	0.0000754
61116-55A	TB'	0.0655057	0.0002702	0.0039321	0.0000610
61116-56A	TB'	0.0301175	0.0002404	0.0058812	0.0000407
61116-57A	TB'	0.0218934	0.0002267	0.0051426	0.0000347
61116-58A	TB'	0.0340777	0.0002476	0.0109214	0.0000582
61116-59A	TB'	0.0248592	0.0002404	0.0064774	0.0000407
61116-60A	TB'	0.0314814	0.0002267	0.0047349	0.0000381
Omitted Analyses:					
61116-09A	TB'	0.0008261	0.0002025	0.0000025	0.0000212
61116-14A	TB'	0.0018710	0.0001972	0.0008319	0.0000262
61116-17A	TB'	0.0112186	0.0002025	0.0053179	0.0000434
61116-34A	TB'	0.0099051	0.0002202	0.0043589	0.0000347

Run #	Sample	^{38}Ar	± ^{38}Ar (1σ)	^{37}Ar	± ^{37}Ar (1σ)
61116-01A	TB'	0.0000411	0.0000208	-0.0000187	0.0000286
61116-02A	TB'	0.0000873	0.0000220	0.0000346	0.0000316
61116-03A	TB'	0.0000785	0.0000227	0.0000371	0.0000334
61116-04A	TB'	0.0000443	0.0000202	0.0000303	0.0000334

61116-05A	TB'	0.0000660	0.0000214	-0.0000176	0.0000328
61116-06A	TB'	0.0001719	0.0000227	0.0000504	0.0000311
61116-07A	TB'	0.0000950	0.0000240	0.0000204	0.0000300
61116-08A	TB'	0.0000783	0.0000220	0.0000139	0.0000328
61116-09B	TB'	0.0001216	0.0000214	0.0000333	0.0000316
61116-10A	TB'	0.0001704	0.0000227	-0.0000280	0.0000305
61116-11A	TB'	0.0000705	0.0000202	0.0000058	0.0000328
61116-12A	TB'	0.0000597	0.0000233	0.0000045	0.0000305
61116-13A	TB'	0.0000658	0.0000227	0.0000225	0.0000295
61116-15A	TB'	0.0000692	0.0000227	0.0000248	0.0000311
61116-16A	TB'	0.0000736	0.0000208	0.0000098	0.0000322
61116-18A	TB'	0.0001045	0.0000208	0.0000136	0.0000316
61116-19A	TB'	0.0000561	0.0000208	0.0000442	0.0000322
61116-20A	TB'	0.0000314	0.0000233	-0.0000414	0.0000311
61116-21A	TB'	0.0000723	0.0000214	-0.0000306	0.0000316
61116-22A	TB'	0.0000763	0.0000220	0.0000060	0.0000311
61116-23A	TB'	0.0000854	0.0000227	0.0000459	0.0000300
61116-24A	TB'	0.0002200	0.0000248	-0.0000443	0.0000322
61116-25A	TB'	0.0000910	0.0000214	-0.0000057	0.0000322
61116-26A	TB'	0.0004212	0.0000255	-0.0000058	0.0000328
61116-27A	TB'	0.0000755	0.0000214	0.0000122	0.0000316
61116-28A	TB'	0.0001050	0.0000220	0.0000083	0.0000291
61116-29A	TB'	0.0000697	0.0000214	-0.0000316	0.0000305
61116-30A	TB'	0.0000548	0.0000214	0.0000744	0.0000316
61116-31A	TB'	0.0001375	0.0000214	0.0000254	0.0000295
61116-32A	TB'	0.0001347	0.0000227	-0.0000270	0.0000328
61116-33A	TB'	0.0000896	0.0000220	0.0000112	0.0000341
61116-35A	TB'	0.0000660	0.0000202	-0.0000003	0.0000316
61116-36A	TB'	0.0001727	0.0000220	0.0000353	0.0000316
61116-37A	TB'	0.0000721	0.0000214	-0.0000132	0.0000316
61116-38A	TB'	0.0000695	0.0000214	-0.0000769	0.0000328
61116-39A	TB'	0.0000734	0.0000196	0.0000348	0.0000311
61116-40A	TB'	0.0000648	0.0000202	-0.0000453	0.0000322
61116-41A	TB'	0.0000937	0.0000214	-0.0000078	0.0000347
61116-42A	TB'	0.0000787	0.0000220	-0.0000335	0.0000311
61116-43A	TB'	0.0000913	0.0000202	-0.0000239	0.0000328
61116-44A	TB'	0.0000863	0.0000220	0.0000272	0.0000305
61116-45A	TB'	0.0000636	0.0000214	-0.0000247	0.0000311
61116-46A	TB'	0.0000617	0.0000202	0.0000002	0.0000334
61116-47A	TB'	0.0001062	0.0000208	-0.0000256	0.0000305
61116-48A	TB'	0.0000560	0.0000197	-0.0000056	0.0000316
61116-49A	TB'	0.0000941	0.0000202	0.0000251	0.0000291

61116-50A	TB'	0.0000720	0.0000193	-0.0000332	0.0000322
61116-51A	TB'	0.0000419	0.0000227	-0.0000243	0.0000311
61116-52A	TB'	0.0000997	0.0000208	0.0000032	0.0000322
61116-53A	TB'	0.0001322	0.0000227	0.0000098	0.0000295
61116-54A	TB'	0.0001808	0.0000240	0.0000070	0.0000328
61116-55A	TB'	0.0000966	0.0000208	0.0000001	0.0000322
61116-56A	TB'	0.0001043	0.0000220	-0.0000473	0.0000311
61116-57A	TB'	0.0000644	0.0000214	0.0000080	0.0000300
61116-58A	TB'	0.0001290	0.0000208	-0.0000166	0.0000311
61116-59A	TB'	0.0001223	0.0000196	-0.0000139	0.0000328
61116-60A	TB'	0.0000463	0.0000240	0.0000463	0.0000305

Omitted Analyses:

61116-09A	TB'	0.0000262	0.0000202	0.0000072	0.0000300
61116-14A	TB'	0.0000041	0.0000195	0.0000244	0.0000322
61116-17A	TB'	0.0000496	0.0000208	0.0000205	0.0000334
61116-34A	TB'	0.0000296	0.0000220	0.0000326	0.0000334

Run #	Sample	^{36}Ar	$\pm\ ^{36}Ar$ (1σ)	$^{40}Ar^*/^{39}Ar$	$\pm^{40}Ar^*/^{39}Ar$ (1σ)
61116-01A	TB'	0.0000313	0.000006	1.4069	0.3124
61116-02A	TB'	0.0000904	0.000006	1.9086	0.3120
61116-03A	TB'	0.0000292	0.000006	2.7290	0.3422
61116-04A	TB'	0.0001101	0.000006	1.4528	0.5588
61116-05A	TB'	0.0000888	0.000006	1.9472	0.4127
61116-06A	TB'	0.0001096	0.000006	1.5528	0.2031
61116-07A	TB'	0.0001215	0.000007	2.5974	0.4149
61116-08A	TB'	0.0000283	0.000006	2.3062	0.4364
61116-09B	TB'	0.0000601	0.000006	2.0559	0.2659
61116-10A	TB'	0.0001580	0.000007	2.2629	0.2059
61116-11A	TB'	0.0000213	0.000006	2.2839	0.2950
61116-12A	TB'	0.0000482	0.000007	4.8484	0.4247
61116-13A	TB'	0.0000226	0.000006	1.6447	0.2974
61116-15A	TB'	0.0002724	0.000007	2.8506	0.7106
61116-16A	TB'	0.0000497	0.000006	2.0937	0.2455
61116-18A	TB'	0.0001685	0.000006	2.0189	0.3930
61116-19A	TB'	0.0000298	0.000006	1.5800	0.2778
61116-20A	TB'	0.0000239	0.000006	2.4363	0.4884
61116-21A	TB'	0.0000421	0.000006	2.3814	0.3058
61116-22A	TB'	0.0000726	0.000006	1.3071	0.3654
61116-23A	TB'	0.0000659	0.000006	2.5179	0.3238

61116-24A	TB'	0.0000524	0.000006	2.0036	0.1298
61116-25A	TB'	0.0000236	0.000006	2.1180	0.2882
61116-26A	TB'	0.0000842	0.000006	2.0675	0.0565
61116-27A	TB'	0.0000451	0.000006	2.6230	0.3429
61116-28A	TB'	0.0000323	0.000006	2.0063	0.2544
61116-29A	TB'	0.0000591	0.000006	1.8225	0.2815
61116-30A	TB'	0.0000334	0.000006	2.0815	0.3002
61116-31A	TB'	0.0004782	0.000008	2.6926	0.4575
61116-32A	TB'	0.0000295	0.000006	2.2081	0.1685
61116-33A	TB'	0.0000105	0.000006	5.8059	0.3996
61116-35A	TB'	0.0000614	0.000006	1.8137	0.3043
61116-36A	TB'	0.0001385	0.000006	2.0737	0.1711
61116-37A	TB'	0.0000211	0.000006	2.4492	0.2490
61116-38A	TB'	0.0000165	0.000006	2.6447	0.3547
61116-39A	TB'	0.0000494	0.000006	1.8593	0.2731
61116-40A	TB'	0.0000259	0.000006	2.4668	0.3468
61116-41A	TB'	0.0000532	0.000006	1.8710	0.2711
61116-42A	TB'	0.0000329	0.000006	1.8492	0.2760
61116-43A	TB'	0.0000704	0.000006	1.5696	0.3397
61116-44A	TB'	0.0000308	0.000006	1.7490	0.3030
61116-45A	TB'	0.0000070	0.000006	2.4232	0.2793
61116-46A	TB'	0.0000430	0.000006	2.0685	0.4576
61116-47A	TB'	0.0000419	0.000006	2.4413	0.2768
61116-48A	TB'	0.0000302	0.000006	2.2325	0.3172
61116-49A	TB'	0.0000387	0.000006	1.8257	0.2709
61116-50A	TB'	0.0000441	0.000006	1.8356	0.2919
61116-51A	TB'	0.0000290	0.000006	1.9713	0.3221
61116-52A	TB'	0.0000373	0.000006	1.9118	0.2000
61116-53A	TB'	0.0000528	0.000006	1.7632	0.2251
61116-54A	TB'	0.0002251	0.000008	4.1753	0.3243
61116-55A	TB'	0.0001804	0.000007	2.9571	0.5165
61116-56A	TB'	0.0000564	0.000006	2.2480	0.3044
61116-57A	TB'	0.0000392	0.000006	1.9821	0.3345
61116-58A	TB'	0.0000404	0.000006	2.0107	0.1610
61116-59A	TB'	0.0000411	0.000006	1.9400	0.2783
61116-60A	TB'	0.0000644	0.000006	2.5945	0.3853
Omitted Analyses:					
61116-09A	TB'	0.0000008	0.000006	237.3898	2176.2180
61116-14A	TB'	0.0000034	0.000006	1.0688	2.2162
61116-17A	TB'	0.0000094	0.000006	1.5828	0.3251
61116-34A	TB'	0.0000065	0.000006	1.8295	0.3901

		(Renne *et al*. 1998; Steiger & Jager 1977)			(Renne *et al*. 2010, 2011)	
Run #	**Sample**	**%^{40}Ar***	**±%^{40}Ar* (1σ)**	**Age (Ma)**	**± Age w/o J (1σ)**	**± w/ J (1σ)**
61116-01A	TB'	45.504	10.100	0.1928	0.0428	0.0428
61116-02A	TB'	29.715	4.810	0.2615	0.0427	0.0427
61116-03A	TB'	61.361	7.653	0.3739	0.0469	0.0469
61116-04A	TB'	13.024	4.950	0.1990	0.0766	0.0766
61116-05A	TB'	24.073	5.054	0.2668	0.0565	0.0565
61116-06A	TB'	30.349	3.915	0.2127	0.0278	0.0278
61116-07A	TB'	25.994	4.093	0.3558	0.0568	0.0568
61116-08A	TB'	52.518	9.935	0.3160	0.0598	0.0598
61116-09B	TB'	43.407	5.587	0.2817	0.0364	0.0364
61116-10A	TB'	32.430	2.878	0.3100	0.0282	0.0282
61116-11A	TB'	67.281	8.701	0.3129	0.0404	0.0404
61116-12A	TB'	62.386	5.413	0.6642	0.0582	0.0582
61116-13A	TB'	57.776	10.457	0.2253	0.0407	0.0407
61116-15A	TB'	9.652	2.269	0.3905	0.0973	0.0973
61116-16A	TB'	50.037	5.847	0.2868	0.0336	0.0336
61116-18A	TB'	16.265	3.075	0.2766	0.0538	0.0538
61116-19A	TB'	52.487	9.229	0.2165	0.0381	0.0381
61116-20A	TB'	54.054	10.838	0.3338	0.0669	0.0669
61116-21A	TB'	52.055	6.671	0.3262	0.0419	0.0419
61116-22A	TB'	22.674	6.300	0.1791	0.0501	0.0501
61116-23A	TB'	42.680	5.461	0.3450	0.0444	0.0444
61116-24A	TB'	63.230	4.076	0.2745	0.0178	0.0178
61116-25A	TB'	64.888	8.843	0.2902	0.0395	0.0395
61116-26A	TB'	72.855	1.948	0.2833	0.0077	0.0078
61116-27A	TB'	50.669	6.610	0.3594	0.0470	0.0470
61116-28A	TB'	58.969	7.476	0.2749	0.0348	0.0348
61116-29A	TB'	38.993	5.995	0.2497	0.0386	0.0386
61116-30A	TB'	54.227	7.816	0.2852	0.0411	0.0411
61116-31A	TB'	9.812	1.468	0.3689	0.0627	0.0627
61116-32A	TB'	72.038	5.490	0.3025	0.0231	0.0231
61116-33A	TB'	90.025	6.130	0.7953	0.0547	0.0547
61116-35A	TB'	37.045	6.187	0.2485	0.0417	0.0417
61116-36A	TB'	36.783	2.969	0.2841	0.0234	0.0234
61116-37A	TB'	72.807	7.420	0.3355	0.0341	0.0341
61116-38A	TB'	72.106	9.693	0.3623	0.0486	0.0486
61116-39A	TB'	45.268	6.629	0.2547	0.0374	0.0374
61116-40A	TB'	61.814	8.694	0.3380	0.0475	0.0475

61116-41A	TB'	43.515	6.282	0.2563	0.0371	0.0371
61116-42A	TB'	54.151	8.080	0.2533	0.0378	0.0378
61116-43A	TB'	27.845	5.989	0.2150	0.0465	0.0465
61116-44A	TB'	52.621	9.115	0.2396	0.0415	0.0415
61116-45A	TB'	87.333	10.116	0.3320	0.0383	0.0383
61116-46A	TB'	38.231	8.440	0.2834	0.0627	0.0627
61116-47A	TB'	55.802	6.315	0.3345	0.0379	0.0379
61116-48A	TB'	57.580	8.183	0.3058	0.0435	0.0435
61116-49A	TB'	50.592	7.498	0.2501	0.0371	0.0371
61116-50A	TB'	45.462	7.211	0.2515	0.0400	0.0400
61116-51A	TB'	54.596	8.922	0.2701	0.0441	0.0441
61116-52A	TB'	60.280	6.293	0.2619	0.0274	0.0274
61116-53A	TB'	47.085	5.989	0.2416	0.0308	0.0308
61116-54A	TB'	33.454	2.502	0.5720	0.0444	0.0444
61116-55A	TB'	17.767	3.003	0.4051	0.0707	0.0708
61116-56A	TB'	43.944	5.925	0.3080	0.0417	0.0417
61116-57A	TB'	46.604	7.854	0.2715	0.0458	0.0458
61116-58A	TB'	64.510	5.158	0.2755	0.0221	0.0221
61116-59A	TB'	50.603	7.250	0.2658	0.0381	0.0381
61116-60A	TB'	39.057	5.767	0.2554	0.0528	0.0528

Isochron (Sample Terrace B' of Unit 10)

Run #	Sample	$^{36}Ar/^{40}Ar$	±% $^{36}Ar/^{40}Ar$ (1σ)	$^{39}Ar/^{40}Ar$	±% $^{39}Ar/^{40}Ar$ (1σ)
61116-01A	TB'	0.001825	18.418650	0.323432	1.467487
61116-02A	TB'	0.002354	6.870810	0.155689	0.906314
61116-03A	TB'	0.001294	19.591250	0.224848	1.836554
61116-04A	TB'	0.002913	5.739389	0.089645	1.291927
61116-05A	TB'	0.002543	6.678771	0.123629	1.116836
61116-06A	TB'	0.002333	5.648108	0.195449	0.846354
61116-07A	TB'	0.002479	5.570094	0.100079	0.945050
61116-08A	TB'	0.001590	20.762800	0.227724	1.569546

61116-09B	TB'	0.001896	9.825622	0.211136	1.036294
61116-10A	TB'	0.002263	4.314239	0.143311	0.692078
61116-11A	TB'	0.001096	26.291380	0.294587	1.377822
61116-12A	TB'	0.001260	14.274180	0.128672	1.369312
61116-13A	TB'	0.001414	24.518920	0.351281	1.618015
61116-15A	TB'	0.003026	2.646810	0.033859	1.701291
61116-16A	TB'	0.001674	11.616260	0.238991	1.091200
61116-18A	TB'	0.002805	3.760977	0.080565	0.875684
61116-19A	TB'	0.001591	19.267480	0.332197	1.389134
61116-20A	TB'	0.001539	23.378450	0.221872	1.745924
61116-21A	TB'	0.001606	13.806380	0.218592	1.164686
61116-22A	TB'	0.002590	8.157869	0.173462	1.143188
61116-23A	TB'	0.001920	9.491362	0.169505	0.982506
61116-24A	TB'	0.001232	10.985630	0.315575	0.757958
61116-25A	TB'	0.001176	24.865960	0.306357	1.480428
61116-26A	TB'	0.000909	7.140374	0.352379	0.455437
61116-27A	TB'	0.001652	13.299730	0.193171	1.137489
61116-28A	TB'	0.001374	18.029710	0.293915	1.249808
61116-29A	TB'	0.002043	9.782664	0.213952	1.132705
61116-30A	TB'	0.001533	16.912200	0.260515	1.337200
61116-31A	TB'	0.003021	1.830632	0.036440	1.079695
61116-32A	TB'	0.000937	19.453550	0.326249	0.854234
61116-33A	TB'	0.000334	60.702670	0.155058	1.407315
61116-35A	TB'	0.002109	9.791533	0.204244	1.147170
61116-36A	TB'	0.002117	4.751094	0.177374	0.635023
61116-37A	TB'	0.000911	26.920770	0.297274	1.169757
61116-38A	TB'	0.000934	34.317190	0.272640	1.483679
61116-39A	TB'	0.001833	12.043620	0.243463	1.129731
61116-40A	TB'	0.001279	22.543360	0.250582	1.381501
61116-41A	TB'	0.001892	11.070050	0.232573	1.099053
61116-42A	TB'	0.001536	17.453360	0.292836	1.354365
61116-43A	TB'	0.002417	8.305079	0.177400	1.123327
61116-44A	TB'	0.001587	19.083700	0.300872	1.403970
61116-45A	TB'	0.000424	78.479440	0.360405	1.609269
61116-46A	TB'	0.002069	13.581540	0.184824	1.560194
61116-47A	TB'	0.001480	14.144290	0.228577	1.194055
61116-48A	TB'	0.001421	19.099310	0.257923	1.333074
61116-49A	TB'	0.001655	15.065440	0.277114	1.204265
61116-50A	TB'	0.001827	13.169810	0.247670	1.070339
61116-51A	TB'	0.001521	19.471020	0.276955	1.428526
61116-52A	TB'	0.001330	15.750240	0.315302	0.931682
61116-53A	TB'	0.001772	11.260430	0.267047	1.003216

61116-54A	TB'	0.002229	3.833517	0.080125	1.027367
61116-55A	TB'	0.002754	3.735779	0.060080	1.651955
61116-56A	TB'	0.001878	10.516540	0.195478	1.101941
61116-57A	TB'	0.001789	14.609640	0.235127	1.283475
61116-58A	TB'	0.001189	14.363590	0.320833	0.946724
61116-59A	TB'	0.001655	14.564140	0.260839	1.200412
61116-60A	TB'	0.002041	9.440053	0.150537	1.124180
Omitted Analyses:					
61116-09A	TB'	0.000963	692.111700	0.003002	872.82630
61116-14A	TB'	0.001756	187.258200	0.445045	11.289660
61116-17A	TB'	0.000834	61.510520	0.474573	2.042190
61116-34A	TB'	0.000650	87.755060	0.440554	2.431621

Appendix-3

MATERIAL PROPERTIES OF THE WORJA OBSIDIAN

Sample ID	P-Distance (cm)	Young's Modulus (*E*)	Poisson's Ratio (*v*)	Transit Time	Voltage (high/low)
KUL 1-1	5.4	12.92e+6 psi	0.17	11.2 µ sec	H
KUL 1-2	5.1	12.98e+6 psi	0.17	11.1 µ sec	H
KUL 1-3	5.4	12.76e+6 psi	0.17	11.9µ sec	H
KUL 1-4	5	13.32e+6 psi	0.17	11.4 µ sec	H
KUL 1-5	6.4	12.92e+6 psi	0.17	15.7 µ sec	H
KUL 2-1	6.2	12.99e+6 psi	0.17	11.7 µ sec	H
KUL 2-2	6.3	12.82e+6 psi	0.17	13.1 µ sec	H
KUL 2-3	6	13.2e+6 psi	0.17	11.3 µ sec	H
KUL 2-4	5.4	12.9e+6 psi	0.17	13.8 µ sec	H
KUL 2-5	5.5	12.89e+6 psi	0.17	10.7 µ sec	H
KUL 3-1	6.4	12.94e+6 psi	0.17	11.8 µ sec	H
KUL 3-2	6	12.74e+6 psi	0.17	12.1 µ sec	H
KUL 3-3	5.76	12.88e+6 psi	0.17	11.1 µ sec	H
KUL 3-4	5.8	12.91e+6 psi	0.17	11.1 µ sec	H
KUL 3-5	6.42	12.88e+6 psi	0.17	14.9 µ sec	H
KUL 4-1	5.5	12.92e+6 psi	0.17	11.3 µ sec	H
KUL 4-2	5.2	13.0e+6 psi	0.17	11 µ sec	H
KUL 4-3	5.96	13.1e+6 psi	0.17	11 µ sec	H
KUL 4-4	5.72	12.98e+6 psi	0.17	13.1 µ sec	H
KUL 4-5	5.5	13.13e+6 psi	0.17	11.4 µ sec	H
KUL 5-1	5.9	12.93e+6 psi	0.17	13 µ sec	H
KUL 5-2	4.89	13.12e+6 psi	0.17	11.1 µ sec	L
KUL 5-3	5.83	12.97e+6 psi	0.17	11.6 µ sec	H
KUL 5-4	5.97	12.94e+6 psi	0.17	12.2 µ sec	H
KUL 5-5	4.9	13.1e+6 psi	0.17	1.6 µ sec	L
KUL 6-1	5.58	13.34e+6 psi	0.17	12.3 µ sec	H
KUL 6-2	5.49	12.96e+6 psi	0.17	11.7 µ sec	H
KUL 6-3	5.45	12.98e+6 psi	0.17	10.3 µ sec	H
KUL 6-4	5.2	12.99e+6 psi	0.17	11.8 µ sec	H
KUL 6-5	5.16	12.66e+6 psi	0.17	12.8 µ sec	H
KUL Test_1	5.0	12.91e+6 psi	0.17	11.3 µ sec	H
KUL Test_2	5.0	12.96e+6 psi	0.17	12.1 µ sec	H
AVERAGE		***12.97 psi***	***0.17***		

Remarks: - For all measurements, instrument was set to 1 pulse per second

- The average *E* value was changed to Newton/m^2, yielding a value of 8.9425e+10 N/m^2 (*cf.* Hutchings 2011: table 1)